
Doctoral Dissertations

Student Theses and Dissertations

1971

On-line economic optimization of a chemical reactor

Jesse Daniel Bennett

Follow this and additional works at: https://scholarsmine.mst.edu/doctoral_dissertations



Part of the [Chemical Engineering Commons](#)

Department: **Chemical and Biochemical Engineering**

Recommended Citation

Bennett, Jesse Daniel, "On-line economic optimization of a chemical reactor" (1971). *Doctoral Dissertations*. 2230.

https://scholarsmine.mst.edu/doctoral_dissertations/2230

This thesis is brought to you by Scholars' Mine, a service of the Missouri S&T Library and Learning Resources. This work is protected by U. S. Copyright Law. Unauthorized use including reproduction for redistribution requires the permission of the copyright holder. For more information, please contact scholarsmine@mst.edu.

ON-LINE ECONOMIC OPTIMIZATION OF
A CHEMICAL REACTOR

by

JESSE DANIEL BENNETT, 1944-

A DISSERTATION

Presented to the Faculty of the Graduate School of the

UNIVERSITY OF MISSOURI-ROLLA

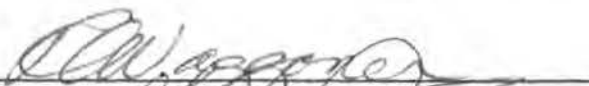
In Partial Fulfillment of the Requirements for the Degree

DOCTOR OF PHILOSOPHY

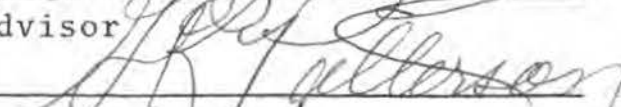
in

CHEMICAL ENGINEERING

1971

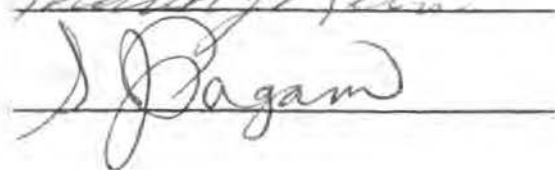


Advisor









ABSTRACT

An economic optimizing control system for a continuous flow stirred tank chemical reactor is designed, simulated, and installed on a pilot scale reactor.

The control scheme utilizes a reaction and reactor model to predict on-line the economic optimum of a reactant concentration. In this manner the control system manipulates the reactant flow rate to maintain the optimum concentration during changes in reaction-reactor parameters with time. Typical parameter changes include the decay of reaction catalyst activity. The optimizing controller will function in conjunction with various operating policies including control to maintain a specified production rate.

ACKNOWLEDGEMENT

The author wishes to acknowledge Dr. R.C. Waggoner, his advisor, and his advisory committee, Doctors V.J. Flanigan, F.J. Kern, S.J. Pagano. and G.K. Patterson for their assistance given throughout the duration of this research.

The author also wishes to express his gratitude to Dr. O.K. Crosser for his time and advice given on many occasions.

In addition the author would like to thank Dr. K.G. Mayhan for the use of the main reactor vessel, Mr. Robert Pahl for his assistance in obtaining an off-line chemical analysis and Mr. Myrlen Troutt for his assistance in the construction of the experimental system.

Finally the author would like to express his gratitude to his wife, Cheryl, for her encouragement and assistance in the preparation of this Dissertation.

TABLE OF CONTENTS

	Page
ABSTRACT.....	ii
ACKNOWLEDGEMENT.....	iii
LIST OF ILLUSTRATIONS.....	vii
LIST OF TABLES.....	xiv
I. INTRODUCTION.....	1
II. BACKGROUND.....	5
III. INVESTIGATION PLAN.....	15
A. On-Line Optimizing Control.....	15
B. Objective Function.....	16
C. Model.....	16
D. Analysis and Test Procedure.....	17
IV. DEVELOPMENT.....	18
A. System Description.....	18
B. Model.....	19
1. Stoichiometry.....	19
2. Reaction Rate Law.....	19
3. Reactor Characteristics.....	20
C. Objective Function.....	21
D. Application of the Model to the Objective Function.....	22
1. Bi-Molecular Reaction.....	23
2. Homogeneous Catalyst.....	25
3. Production Specified.....	26

Table of Contents (continued)	Page
E. Determination of the Economic Extremum Polynomial.....	28
1. Reactor Parameter Group.....	30
F. Solutions of the Economic Extremum Polynomial.....	31
1. First Order Rate Law with Respect to C.....	31
2. Second Order Rate Law with Respect to C.....	34
3. Income for Optimum Operation.....	38
4. Production for Optimum Operation.....	40
G. On-Line Measurement of the Reactor Parameter Group.....	42
H. Errors Introduced by Reaction Rate Law Approximation.....	45
V. IMPLEMENTATION.....	49
VI. EVALUATION TESTS AND RESULTS.....	53
A. Simulation Operation.....	53
1. Simulation Purpose.....	53
2. Simulation Equations.....	53
3. Continuous Analysis.....	54
4. Sampled Analysis.....	65
B. Experimental Operation.....	78
1. Experimental Purpose.....	78
2. Reaction.....	78
3. Reaction Parameters.....	80
4. Optimum Prediction Accuracy.....	81
5. Dynamic Tests.....	82

Table of Contents (continued)	Page
C. Discussion of Results.....	91
1. Simulation.....	91
2. Experimental.....	94
VII. CONCLUSIONS.....	95
BIBLIOGRAPHY.....	98
VITA.....	101
APPENDICES.....	102
A. List of Symbols.....	102
B. Simulation Development.....	104
1. Dynamic Equations.....	104
2. Time Scaling.....	106
3. Magnitude Scaling.....	106
4. Analog Program.....	107
a. Process.....	107
b. Non-Linear Calculations.....	111
c. Continuous Analysis Control Schemes.....	112
d. Sampled Analysis Control Schemes.....	121
C. Experimental System Construction.....	135
1. Reaction.....	135
2. Reactor Design.....	135
3. Process Description.....	137
4. Analog Program.....	148
D. Process - Analog Computer Interface.....	161
E. Chromatograph - Computer Interface.....	167
F. Pilot Scale Process Specifications.....	178

LIST OF ILLUSTRATIONS

Figures	Page
1. Extremum Curves of the Objective Function for $n = 1$	33
2. Zero Income Constraint for $n = 1$	35
3. Extremum Curves of the Objective Function for $n = 2$	37
4. Zero Income Constraint for $n = 2$	39
5. Income Index and Production Rate at Optimum Concentrations for $n = 1$	41
6. Income Index for an Incorrect Rate Law Assumption...	47
7. Income Loss for an Incorrect Rate Law Assumption....	48
8. Proposed Implementation Scheme for the Optimizing Controller.....	52
9. Simulation of a Step Down in the Feed of Reactant A, Open Loop.....	56
10. Simulation of a Step Down in the Feed of Reactant A, Continuous Analysis, $k_0 = 25.0$	57
11. Simulation of a Step Down in the Feed of Reactant A, Continuous Analysis, $k_0 = 2.5$, $T_0 = 0.1$ min.....	59

List of Illustrations (continued)

Figures	Page
12. Simulation of a Step Up in the Feed of Reactant A, Continuous Analysis, $k_o = 2.5$, $T_o = 0.1$ min.....	60
13. Simulation of a Step Down in the Reaction Rate Constant, Open Loop.....	61
14. Simulation of a Step Down in the Reaction Rate Constant, Continuous Analysis, $k_o = 25.0$, $T_o = 0.1$ min., $k_p = 10.0$, $T_p = 0.1$ min.....	63
15. Simulation of a Step Up in the Production Set Point, Continuous Analysis, $k_o = 25.0$, $T_o = 0.1$ min., $k_p = 10.0$, $T_p = 0.1$ min.....	64
16. Simulation of a Step Up in the Production Set Point, Continuous Analysis, $k_o = 25.0$, $T_o = 1.0$ min., $k_p = 10.0$, $T_p = 0.1$ min.....	66
17. Simulation of a Pulse in the Feed of Reactant A, Continuous Analysis, $k_o = 2.5$, $T_o = 0.1$ min.....	67
18. Simulation of a Step Up in the Feed of Reactant A, Sampled Analysis, $K_o = 0.25$	68
19. Simulation of a Step Up in the Feed of Reactant A, Sampled Analysis, $K_o = 0.5$	70
20. Simulation of a Step Up in the Feed of Reactant A, Sampled Analysis, $K_o = 1.25$	71

List of Illustrations (continued)

Figures	Page
21. Simulation of a Step Down in the Reaction Rate Constant, Sampled Analysis, $K_o = 0.5$, $K_p = 2.0$	72
22. Simulation of a Pulse in the Feed of Reactant A, Sampled Analysis, $K_o = 0.5$	74
23. Simulation of a Pulse in the Feed of Reactant A, Sampled Analysis, $K_o = 0.25$	75
24. Simulation of a Step Up in the Production Set Point, Sampled Analysis, $K_o = 0.5$, $K_p = 0.8$	76
25. Simulation of a Step Up in the Production Set Point, Sampled Analysis, $K_o = 0.5$, $K_p = 2.0$	77
26. Simulation of a Step Up in the Production Set Point, Sampled Analysis, $K_o = 0.25$, $K_p = 2.0$	79
27. Income Index in the Neighborhood of the Indicated Optimum Concentration for the Experimental Pilot Scale Reactor.....	83
28. Composition Response to a Step Up in the Feed of Hydrogen.....	84
29. Flow Rate Response to a Step Up in the Feed of Hydrogen.....	85
30. Composition Response to a Step Down in the Feed of Hydrogen.....	87

List of Illustrations (continued)

Figures	Page
31. Flow Rate Response to a Step Down in the Feed of Hydrogen.....	88
32. Composition Response to a Step Down in the Production Set Point.....	89
33. Flow Rate Response to a Step Down in the Production Set Point.....	90
34. Composition Response to a Step Up in the Production Set Point.....	92
35. Flow Rate Response to a Step Up in the Production Set Point.....	93
1B. Analog Program for Reactor Simulation.....	108
2B. Analog Program for Calculation of the Non-Linear Functions of Composition for use with the Simulation.....	113
3B. Continuous Analysis Optimizing Control Scheme.....	116
4B. Analog Program for Simulation of the Continuous Analysis Optimizing Control Scheme.....	116
5B. Optimum Curve for $n = 1$, Cost Ratio = 20.0, used in the Simulation and Experimental Test.....	118
6B. Continuous Analysis Production Control Scheme.....	120

List of Illustrations (continued)

Figures	Page
7B. Analog Program for Simulation of the Continuous Analysis Production Control Scheme.....	120
8B. Sampled Analysis Optimizing Control Scheme.....	125
9B. Sampled Analysis Optimizing Control Scheme for Simulation Purposes.....	125
10B. Analog Program for Simulation of the Sampled Analysis Optimizing Control Scheme.....	126
11B. Sampled Analysis Production Control Scheme.....	127
12B. Sampled Analysis Production Control Scheme for Simulation Purposes.....	127
13B. Analog Program for Simulation of Sampled Analysis Production Control Scheme.....	129
14B. Control Logic for Generation of Zero-Order Hold and Delay.....	132
15B. Action of Zero-Order Hold and Delay from One Track-Hold Pair.....	132
16B. Output of Track-Hold Pair Generating Both Zero-Order Hold and Delay for Ramp Input.....	134
1C. Reaction Chamber.....	136
2C. Main Reaction Chamber and Top Plate.....	138

List of Illustrations (continued)

Figures	Page
3C. Main Reactor in System.....	139
4C. Reactant Feed Control System.....	140
5C. Reactor - Chromatograph System.....	141
6C. Reactant Control Valves, dp Transmitters, and P/I Transducers.....	145
7C. Bubble Flow Meter, Exit Flow Control Equipment, and Pressure Indicators.....	149
8C. Analog Program for Pilot Scale Reactor Control....	150
9C. Analog Program for Calculation of Non-Linear Functions of Composition for use with the Experimental Reactor.....	157
10C. Logic Program for Activation of Sampled Data Control Sequence.....	159
1D. Current to Pressure Transducer Wiring.....	162
2D. Pressure to Current Transducer Wiring.....	163
3D. Transmitting Potentiometer Wiring.....	165
1E. Varian 90-P3 Gas Chromatograph.....	168
2E. Chromatograph Strip Chart Recorder.....	169

List of Illustrations (continued)

Figures	Page
3E. Analog Program for Calculation of Sample Composition from Chromatograph Output.....	171
4E. Logic Program and Cam Timer Settings for Controlling the Analog Computation of Sample Composition.....	173
5E. Wiring for the Control of the Cam Timer and Sampling Actuation Valve.....	176
6E. Cam Timer and Solenoid Valve.....	177
1F. Applied Dynamics 40, 24 Analog Computer.....	179
2F. Orifice Meter Specifications.....	181

LIST OF TABLES

Tables	Page
I. Simulation Variable Description.....	55
I-B. Component List for Reactor Simulation, Figure 1B.....	109
II-B. Component List for Simulation Non-Linear Calculations, Figure 2B.....	114
III-B. Component List for Simulation of the Continuous Analysis Controllers, Figures 4B and 7B.....	122
IV-B. Component List for Simulation of the Sampled Analysis Controllers, Figures 10B and 13B.....	130
I-C. Experimental Equipment List.....	143
II-C. Component List for Pilot Scale Reactor Control, Figure 8C.....	151
I-D. Process - Computer Interface Wiring.....	166
I-E. Chromatograph Timer Computer Wiring.....	174

I. INTRODUCTION

An optimizing control scheme is developed to maximize the operational income for a chemical process. It must be capable of implementation. If the process is a chemical reactor, it is mandatory to control the feed streams to produce the maximum profit. However, in many cases control points are chosen from tradition or the operator's intuition rather than from any systematic study of the process. An on-line control scheme to determine the best reactant concentration for a particular set of reaction parameters could greatly improve the economics of many chemical reactor facilities.

There are a number of terms which have been applied to various on-line schemes designed to find some type of optimum condition. Many authors distinguish between dynamic optimization and the economic or static optimization of a control point by reference to the first study as optimal control and the second as optimizing control. This distinction is followed in this work.

The performance criterion is a dependent variable to be maximized or minimized. The objective function is an expression defining the performance criterion in terms of dependent and independent variables of the system. The performance criterion used for this study defines the

economic performance of the reactor facility, income. The objective function defining that income is an economic balance around the reactor and is a function of measurable quantities.

Perturbation methods and peak-holding schemes continuously change the independent variable to be optimized so that the sensitivity of the performance criterion with respect to the optimized variable may be measured. The sensitivity is regulated so that its average is zero, the condition for an extremum point. The various schemes differ somewhat in the type of perturbation utilized and the sensitivity detection techniques applied.

One of the most confusing aspects of this field is the use of the term, adaptive. Aseltine, page 9, presents a survey of the work in "Adaptive Control Systems" to 1958. All the articles he classes as "Extremum Adaptation" seek static optimization of a control point and utilize some type of perturbation or peak-holding technique to achieve their goal. Gibson, page 10, states in his survey that adaptive control consists of three basic items:

1. A definition of an optimum condition or figure of merit.
2. Comparison of actual performance with the desired performance.
3. Adjustment of the system parameters to correct the actual performance toward the desired.

Truxal in his review of 1959, page 10, defines an adaptive system as "any physical system which has been designed with an adaptive viewpoint." The term adaptive is almost always

used to describe systems which are capable of accomplishing their task without detailed process information, i.e., by employing a perturbation, peak-holding or similar scheme. The description of adaptive elements given by Gibson above implies that adaptive control is tantamount to a perturbation or peak-holding scheme.

Gibson, page 10, contends that optimizing control is a subclass of adaptive control. However, optimizing control is defined in this dissertation as any control scheme designed to maintain an optimum control point with respect to some performance criterion.

A relationship is developed through the application of a reaction and reactor model to the objective function. This relationship predicts the best concentration of one reactant as a function of a group of reaction and reactor parameters which are indirectly measurable. Implementation of this scheme does not require measurement of the sensitivity, calculation of the performance criterion, or the use of any perturbation.

Although a great deal of work labeled adaptive control relates in some manner to this work, it is obvious from the various definitions of adaptive control that controversy would arise if this scheme were referred to as an adaptive control system. Therefore, the term adaptive is not used. The control scheme does however fit the definition of optimizing control given above.

The optimizing scheme is developed from the objective function, tested on an analog computer simulation of a reactor and investigated in conjunction with a pilot scale reactor.

II. BACKGROUND

In order to achieve a static optimum, i.e., to maximize or minimize some function, called the objective function, a number of approaches have been followed. The great bulk of these involve the application of some type of perturbation of the system in order to generate correlations used to drive the controlled variable to the optimum point.

The first use of the principle was made by C. S. Draper and Y. T. Li (1) in an application for the optimization of an internal combustion engine. The performance criterion was the power output of the engine and the variable optimized was the fuel to air ratio. In later articles Li (2) proposes three types of controllers in which a perturbation is introduced and the output measured. The sensitivity of a system can be represented by the ratio of the output rate to the input rate. If the objective function is simply the output, i.e., if it is wished to maximize the output of the system, the optimum point would be the point at which the sensitivity becomes zero. For a unimodal system the sensitivity would go to zero at only one point in the operating range of the output. Li therefore proposes to drive the input toward the optimum until the sensitivity changes sign. This direction is continued until a stabilization limit is reached

at which time the direction is reversed. In this manner the input continuously oscillates around the optimum. The stabilization zone is incorporated around the optimum and made sufficiently large that noise does not interfere with the decisions of the controller.

Li further proposes a continuous sinusoidal test signal to be imposed on the input. The corresponding output variation corrected for phase shift is then correlated with the input variation. He states that the sensitivity of a system is proportional to the average of the product of the sinusoidal input test signal and the corresponding output signal. This average is then used to control the direction the input should be driven.

In this article Li (2, page 191) also discusses what he calls an "output-sampling optimizing-controller." This type of controller operates in a manner similar to the first one proposed. It differs in that the sensitivity is found by taking the difference between the output at successive sampling periods. This sensitivity is then used to determine the input drive direction.

Li also discusses a peak-holding controller in which the input is driven in the direction which increases the output until the output begins to decrease. The control signal is proportional to the difference between present output and the largest value the system has had in the past. Again a stabilization zone is incorporated to overcome the influence of noise.

The quarie optimal controller discussed by White (3) is said to be the first commercial embodiment of optimal control. White states that an optimal controller is simply one that uses the slope of the output with respect to input as the signal to be controlled rather than just the output. In order to obtain this slope a unit disturbance is imposed on the process, the response analyzed and a control action taken. White states that the continuous hunting about the control point is eliminated by lowering the disturbance to zero when the desired slope is reached. No further change is imposed on the system until the output being controlled changes in value. If the output does change, the controller begins its action again. The quarie controller still relies on an imposed disturbance and numerical differentiation techniques to determine the slope.

Tsien and Serdengecti (4) studied the dynamics of a peak-holding controller applied to a system characterized by a first order linear delay. They were able to construct design charts for peak-holding systems using characteristic parameters, the time constant of the system and the critical difference, Li's stabilization limit.

Genthe (5) applied a peak-holding control scheme to a cruise control for jet aircraft. The performance criterion was the aircraft range. Genthe refers to other methods used to attempt to maximize range by controlling speed. A cruise data computer (6,7) was developed for the Air Force B-52

long range bomber. The computer measured various ambient conditions and through non-linear relationships generated a continuous indication of the best altitude for present mach number or best mach number for present altitude. The only inputs required were gross aircraft weight, present altitude, and fuel weight. However, as Genthe points out, any changes in these functions due to airframe or engine aging, uncertainties introduced by aircraft production tolerances, or icing during flight can cause optimum conditions predicted by the computer to be incorrect. The cruise data computer is however, the only example of the optimum point predicted directly even though the relationships were obtained empirically.

Farber (8) designed a peak finding mechanism for analog computers. His system used a friction switch to determine the sign of the slope of the objective function and relays to generate the logic. If the input is increasing and the output increasing there is no change; if the input is increasing and the output is decreasing the input is reversed; etc. Basically Farber's system operated in the same way as other optimizing systems utilizing the slope of the objective function.

Young (9) describes a system in which the control element is scanned through its entire range of adjustment and returned to the position resulting in the desired optimum. This procedure does eliminate the problem of a multi-peak function

but since the adaptive feature does not function during normal operation, Young's system would not be applicable to chemical process optimization.

Whitaker, Yamron, and Kezer (10) reported using small variations occurring in normal operation in their correlation to generate the slope of the performance curve.

Aseltine (11) presents a survey of the work in "Adaptive Control Systems" to 1958. In his article he groups adaptive control into five classifications (11, page 102):

1. Passive adaptation: Systems which achieve adaptation without system parameter changes, but rather through design for operation over wide variations in environment.
2. Input signal adaptation: Systems which adjust their parameters in accordance with input signal characteristics.
3. Extremum adaptation: Systems which self-adjust for maximum or minimum of some system variable.
4. System-variable adaptation: Systems which base self-adjustment on measurements of system variables.
5. System-characteristic adaptation: Systems which make self-adjustments based on measurement of transfer characteristics.

Stromer (12) followed in 1959 with a very comprehensive bibliography of articles published in adaptive control.

Gibson states in his survey (13, page 113) that "the principle of adaptive control attempts to overcome those control system limitations brought about by changes in environment." He defines adaptive control in the following way:

An adaptive control system provides a means of continuously monitoring the system's performance in relation to a given figure of merit or

optimum condition and a means of automatically modifying the system's parameters, by closed-loop action, to approach this optimum.

He further states that adaptive control consists of three basic items:

1. A definition of an optimum operating condition or figure of merit.
2. Comparison of actual performance with the desired performance.
3. Adjustment of the system parameters to correct the actual performance toward the desired.

Gibson contends that optimizing or extremum control is a subclass of adaptive control: "The extremum controller is a one dimensional adaptive control in which the index of performance (figure of merit) is directly measurable."

In a later review (14) Gibson discusses seven approaches to adaptive control, all utilizing some type of perturbation.

Truxal (15, page 4) defines an adaptive system as "any physical system which has been designed with an adaptive viewpoint."

Hurley (16) investigated parameter perturbation optimizing control systems in general. His work involved a digital simulation in which the stability of continuous and sampled data systems was studied.

Deem (17) applied a sinusoidal perturbation extremum-seeking control scheme to control the air and gas flow rates into a natural gas combustion process. The combustion process dynamics were obtained by the application of pulse testing techniques. These dynamics are necessary for the phase correction used in these systems. Optimal values of

the sinusoidal perturbation amplitude and frequency and feedback loop gain were determined on the furnace and an analog simulation.

Schindler (18) applied a method of optimization he calls "Questing Control" to continuous flow stirred tank reactors in a simulation study. Schindler uses this method to maximize the reaction rate in a reaction system involving two continuous flow stirred tank reactors in series by adjusting the temperatures in the two reactors. He also uses the method to adjust the temperature and phase proportions in a two phase reactor and the feed temperature and rate in a single reactor.

His method, "Questing Control" is an input perturbation scheme in which the product of the performance criterion and the input corrected for phase shift is integrated continuously. The resulting integral, which Schindler calls the "performance integral," guides the controlled variable in the direction of an extremum. In this respect Schindler's work is similar to the original work of Li since the integration is an averaging technique.

Schindler did investigate the case in which random measurement errors are present in the evaluation of the performance criterion.

Wiley (19) applied the Maximum Principle to a batch reaction-distillation system. His results gave a unique distillate rate profile to maximize yield for a particular

set of initial reactant concentrations, reaction rates, total number of plates, relative volatilities, and equilibrium constants. In this work Wiley studied particular cases with emphasis on the parameters that influenced yield the greatest.

Wiley was not interested in the control of his system, he was interested only in predicting the optimum distillate profile given the values of all the applicable system parameters. This was essentially a design problem.

Hoyer (20) contrasted sinusoidal perturbation optimizing control with conventional control to manipulate the temperature and methane flow rate in a methane oxidation reaction system. The reaction catalyst slowly deactivated and the optimizer followed the moving optimum. Along with Deem, Hoyer's presentation is one of the few in which the proposed optimizing scheme was applied to an actual process.

Chao (21) used a pseudo-optimum search method for the solution of multi-stage optimization problems. He used his search method in the design of a tubular chemical reactor, to determine the optimal temperature policy in tubular reactors and in the control of an adsorption tower. The last application was a dynamic optimization problem. Like Wiley, Chao did not apply his procedure on-line but used it as a calculation and design tool.

Foley (22) studied extremum seeking systems which used input perturbations for optimizing a unimodal non-linear

objective function. He discusses both the univariable and dual variable configurations and presents a stability analysis of the dual variable system. In his work he utilized analog and hybrid simulation for verification of his predicted transient and stability behavior. Foley also presents a complete design and stability analysis of a gas-fired furnace application for an input perturbation extremum seeking system.

Newberger (23) conducted a theoretical and experimental study to determine the optimal steady state operation of a jacketed tubular reactor in which two, consecutive, second order, homogeneous, liquid phase reactions occurred. The objective function maximized was the yield of the middle product. The Maximum Principle was employed to determine temperature and heat flux profiles which were optimal.

Newberger modeled his reactor, obtained the optimum conditions and verified them in the experimental system. His work was specific to one set of operating conditions. He did not study changes which might occur due to environmental conditions, aging or the use of new operating policies. There was therefore no emphasis on the maintenance of an optimum profile in the presence of such changes.

White (24) applied an input perturbation optimizing scheme to systems with time delay. A stability analysis is made and hybrid simulation employed to verify the analysis. Although some difficulties associated with the practical

implementation on actual processes are considered, no experimental work was done.

Price and Rippin (25) used sinusoidal perturbation in an optimizing controller for a laboratory scale water gas shift reactor. The objective function used in this experimental investigation was an economic balance and included terms from both the input and the output of the process. Two variables, temperature and steam flow, were optimized. In a simulation study the best performance expressed as loss due to not being permanently at the optimum were 1.26 percent for the temperature and 31 percent for the steam flow optimization.

Barrett and Alford (26) optimized the set points for the coolant temperatures of the two cooling jackets on a tubular type reactor in a computer simulation. The objective function was the yield of the intermediate product in a consecutive reaction. Barrett and Alford do not specify their optimization procedure, described as a hill climbing technique apparently similar to Li's first approach.

III. INVESTIGATION PLAN

A. On-Line Optimizing Control

The objective of this investigation is to design an optimizing control scheme which will maximize the operational income of a chemical reactor and which may be implemented on-line in a real situation. The optimized variable is the concentration of one reactant and the manipulated variable is the feed rate of that reactant.

The optimizing control scheme is to be applied to an existing reactor; therefore, the only costs that are applicable are those that are a function of the operational variables. Capital costs, fixed costs and labor costs which do not change appreciably with changes in the process control points are irrelevant.

The scheme must be capable of implementation in a real situation. Perturbation schemes are capable of controlling a variable so that it remains in the vicinity of an extremum point of the objective function. However, these schemes are rejected because of the objectionable disturbances caused by the perturbations. In addition to these disturbances an average error from the true optimum must be tolerated if the perturbation schemes are employed, page 14. The authors of the perturbation and peak-holding schemes state that essentially the only information necessary to employ their

procedures is the knowledge that an optimum condition exists. In many cases much is known about a process but the existing control equipment is not capable of taking advantage of the knowledge. It is true that the perturbation schemes have a more general application but they also ignore valuable information that may be available.

The approach followed here is to derive a relationship capable of on-line implementation which predicts the control point as a function of a group of reactor parameters. This optimum predicting relationship is derived through the application of a model to the objective function.

B. Objective Function

The performance criterion used is the operational income of the reactor. The objective function which defines the income is an economic balance around the reactor and uses a credit/mole for product and costs/mole for reactants fed. The form is applicable when fixed costs and utilities are not functions of reactor conditions and can be used with a wide variety of reactor operating policies as long as the various cost terms are known.

C. Model

In order to obtain an optimum predicting relationship which allows on-line implementation without the use of perturbation techniques a model must be available. The elements required for construction of the model are the stoichiometry of the reaction, the reaction rate law and the reactor characteristics.

D. Analysis and Test Procedure

The optimizing control scheme was investigated for the following operating policies:

1. One reactant flow held constant and the second reactant flow optimized.
2. The rate of production controlled and one reactant flow optimized.

These two policies were studied for both continuous and sampled analyzers in a simulation utilizing an electronic analog computer. The sampled analyzer system was also investigated in a pilot scale reactor setup. The simulation was used to test the stability and operational characteristics of the control scheme in an ideal situation. The application of the scheme to the pilot scale reactor demonstrated its operation and implementation in a particular real situation and provides an insight into the accuracy of the optimum prediction.

IV. DEVELOPMENT

A. System Description

The system can be adequately described as a continuous stirred tank reactor with at least two feed streams. The optimizing control scheme is used to manipulate one of the two feed streams to maximize the operational income as defined by an objective function.

If the reaction rate is slow, the reactor cost high and the reaction rate directly dependent on the concentration of reactants it becomes advantageous to operate with high concentrations of reactants. This high concentration acts as a driving force, speeding the reaction. Operation at low conversion minimizes subsequent reaction to unwanted by-products. Operation usually requires the use of separation equipment to extract the product from the unused reactants and/or catalysts. In these cases where the product must be recovered a small additional expenditure on separation equipment might allow the unused reactants and/or catalysts to be recycled and a much smaller reactor to be used.

Typical examples of applicable reactions include unimolecular or decomposition reactions requiring a homogeneous catalyst, dimerization reactions requiring a homogeneous

catalyst and any homogeneous bimolecular reaction.

B. Model

1. Stoichiometry: The following stoichiometric relation was chosen to represent a typical reaction.



This reaction form is irreversible and involves a change in molar flow due to reaction.

2. Reaction Rate Law: Chemical reactions are generally characterized by a rate law, an expression which relates the reaction rate as a function of the reactant and product concentrations. The reaction rate law chosen is written:

$$-r_A = kx_Ax_C^n \quad 2.$$

where:

$$-r_A = \text{reaction rate of component A; (moles}_A\text{) / (time, volume)}$$

$$k = \text{reaction rate constant; (moles}_A\text{) / (time, volume, mole fraction A, mole fraction C}^n\text{)}$$

$$x_C = \text{concentration of C; mole fraction C}$$

$$x_A = \text{concentration of A; mole fraction A}$$

$$n = \text{order of the reaction with respect to C; unitless}$$

The rate constant, k , is a function of temperature, catalyst activity and reactant conditions. It will therefore change from time to time as reaction conditions, feed stocks and catalyst activity change. Even though k varies, once the basic rate law is established it reproduces the

reaction rate if the rate constant is known at the time.

The value of n , the order of the reaction rate law with respect to reactant C, is actually a parameter used to obtain a correlation between the reaction rate and reactant compositions. However, its value is governed somewhat by the molecularity of the reaction and can be predicted if the mechanism of the reaction is known. The order of a reaction determined from experimental data may be used to verify a particular mechanism.

3. Reactor Characteristics: The reactor is described as a continuous flow stirred tank (backmix) reactor. Perfect mixing in a reactor is never achieved but there are many industrial situations which differ from perfect mixing only slightly. These situations occur at times when a tank is agitated violently and the tank time constant is low. These conditions may exist in a tank which employs a stirring device or in a tank with a recycle line which contains a high volume pump. In many cases the tank is simply a pipe around a pump and the recycle rate is kept high with respect to the through-put. The backmix model is especially applicable to the recycle reactor.

The combination of the material balances from the stoichiometric relation, the reaction rate law and the specification of perfect mixing provides a relationship between the production rate and the reactant concentrations.

$$F_B = Fx_B = kVx_A x_C^n \quad 3.$$

where:

F_B = molar flow of product out of the reactor;
(moles_B)/(time)

F = total molar flow out of the reactor;
(moles)/(time)

x_B = concentration of B; mole fraction B

V = reactor volume; volume units

Equation 3 is then the model of the reaction in the continuous flow stirred tank reactor.

C. Objective Function

The economic objective function to be maximized is total income around the reactor written as cost of reactants used and credit for product. It can be written as:

$$G = F_B C_B - F_{Ain} C_A - F_{Cin} C_C \quad 4.$$

where:

F_{Ain} , F_{Cin} = molar flows of reactants into the reactor; (moles)/(time)

C_A , C_C , C_B = molar costs and credits;
(monetary units)/(mole)

G = performance index (income);
(monetary units)/(time)

If separation equipment is not involved the various costs could be intra-company credits or market values. If separation equipment is used, the costs of the reactants and the products reflect the purchase costs of the reactants and the separation costs but the objective function does not change.

Any objective function requires weighting factors, molar costs in this case, and these factors must be available or derivable. In this case the weighting factors, molar costs, must also be constant or changing very little over a long period of time.

D. Application of the Model to the Objective Function

The standard routine to find a maximum is applied to the objective function. The objective function is differentiated with respect to the variable to be optimized, the first derivative equated to zero, and the resulting equation solved for its roots. The solutions of the first derivative set equal to zero can then be tested by introduction into the second derivative. This operation indicates whether the solutions are maximum, minimum, or inflection points. The roots might also be tested by calculation of the objective function in the neighborhood of the root.

A formal proof of the validity of this routine is given by Olmsted (27).

In order to apply the routine described above, the objective function must be differentiated with respect to the independent variable to be optimized. If other independent variables are present then a partial differential equation results. In order to obtain the solution of this resulting partial differential equation the partials of the other variables must be evaluated. This can be done if expressions are available which relate that particular

variable to the optimized variable. A model provides these expressions. The procedure followed here was to solve the objective function and the model simultaneously to obtain a function of one variable, the one to be optimized, and a number of terms held constant. The concentration of reactant C is chosen as the optimized variable. The objective function resulting from application of the model is expressed in terms of the concentration of reactant C, and other terms which are held constant including the feed rate of reactant A, the reaction rate constant and the cost terms.

The following development describes the reduction of the objective function to this function of one variable.

1. Bimolecular Reaction: Equations which relate the steady state reactant flow rates, compositions and production rates are obtained directly from the reaction stoichiometry. For the reaction chosen:



the following relationships are written.

Component Material Balances:

$$F_{Ain} - Fx_A = F_B = Fx_B \quad 5.$$

$$F_{Cin} - Fx_C = F_B = Fx_B \quad 6.$$

For Ternary Systems:

$$x_A + x_C + x_B = 1.0 \quad 7.$$

Solution of these equations simultaneously with the objective function and the model, equations 3 and 4 generates an expression of one variable, the composition of reactant C.

Equations 5 and 7 are solved simultaneously to obtain a function for F , the total molar flow out of the reactor.

$$F = F_{Ain}/(1 - x_C) \quad 8.$$

The production rate can then be written as:

$$F_B = Fx_B = F_{Ain}x_B/(1 - x_C) \quad 9.$$

$$F_B = F_{Ain}(1 - x_A - x_C)/(1 - x_C) \quad 9.$$

Equation 9 is then equated to the model, equation 3.

$$F_{Ain}(1 - x_A - x_C)/(1 - x_C) = kVx_Ax_C^n \quad 10.$$

Equation 10 is then solved for x_A , the concentration of reactant A.

$$x_A = F_{Ain}(1 - x_C)/(F_{Ain} + kVx_C^n(1 - x_C)) \quad 11.$$

Thus an expression for the concentration of A in terms of the concentration of C, the reaction parameters and the flow rate of reactant A is obtained.

The objective function, equation 4, page 21, can now be solved simultaneously with the above equations to obtain an expression of one variable, x_C , the reaction parameters and the flow of reactant A.

Replacing F_{Cin} in the objective function, equation 4, with the solution of equation 6 gives the following:

$$G = F_B(C_B - C_C) - Fx_C C_C - F_{Ain} C_A \quad 12.$$

Equation 8, can be used to provide a function for the total exit molar flow, F , reducing the objective function further.

$$G = F_B(C_B - C_C) - F_{Ain}((x_C C_C)/(1 - x_C) + C_A)$$

The model, equation 3, is used to provide an expression for

the production, F_B .

$$G = kVx_A x_C^n (C_B - C_C) - F_{Ain} ((x_C C_C / (1 - x_C)) + C_A)$$

Equation 11, is now used to eliminate the concentration of reactant A from the objective function.

$$G = (kVx_C^n (1 - x_C) F_{Ain}) (C_B - C_C) / (F_{Ain} + kVx_C^n (1 - x_C)) - F_{Ain} (x_C C_C / (1 - x_C) + C_A) \quad 13.$$

2. Homogeneous Catalysis: For different stoichiometry, a different form of this equation is obtained. If reactant C is actually a homogeneous catalyst the component balances become:

$$F_{Ain} - Fx_A = F_B \quad 5.$$

$$F_{Cin} = Fx_C \quad 14.$$

that is, the component C is not destroyed. In this case equation 14 is used to eliminate F_{Cin} . The objective function then becomes:

$$G = (kVx_C^n (1 - x_C) F_{Ain}) C_B / (F_{Ain} + kVx_C^n (1 - x_C)) - F_{Ain} (x_C C_C / (1 - x_C) + C_A) \quad 15.$$

Therefore, the only effect of the change in stoichiometry is to replace the cost group $C_B - C_C$ by C_B .

Two operating policies are investigated:

- (1) The molar feed of reactant A held constant and the molar feed of reactant C manipulated to optimize the concentration of reactant C.

- (2) The rate of production controlled and the molar feed of reactant C manipulated to optimize the concentration of reactant C.

The first policy would be employed if a plant with little or no storage capacity was required to accept a raw material from upstream. In this case the plant must accept whatever quantity of reactant A it receives and process it or dispose of it in some manner--an unpopular and unprofitable alternative. Since equation 13 is written in terms of the feed rate of reactant A it is tailored for use with this first policy in which the feed rate of reactant A is held constant.

The second policy investigated would be employed to meet production quotas or prior sales commitments. The application of this policy can use the same reduced objective function, equation 13, developed for the first policy. However, because the production is not independent of the concentration of reactant C interaction occurs between the production controller and the optimizing controller.

The objective function may be written in terms of any other independent variable instead of the feed rate of reactant A but it will be shown that some interaction will always occur when the second policy is followed.

3. Production Specified: The objective function can be written in terms of the production rate, F_B . Equation 5, page 23, is solved for F_{Ain} .

$$F_{Ain} = Fx_A + F_B \quad 5.$$

Equation 3, page 20, is solved for x_A .

$$x_A = F_B / kVx_C^n \quad 3.$$

Equation 3 and 5 are then solved simultaneously to generate a function of F_{Ain} in terms of the mole fraction of reactant C, the reaction parameters, and the production rate, F_B .

$$F_{Ain} = F_B kVx_C^n (1 - x_C) / (kVx_C^n (1 - x_C) - F_B) \quad 16.$$

In a similar manner equation 6, page 23, can be solved for F_{Cin} .

$$F_{Cin} = Fx_C + F_B \quad 6.$$

Equation 3 and 6 can then be solved simultaneously to generate a function of F_{Cin} in terms of the mole fraction of reactant C, the reaction parameters, and the production of B, F_B .

$$F_{Cin} = (F_B kVx_C^n - F_B^2) / (kVx_C^n (1 - x_C) - F_B) \quad 17.$$

Substitution of equations 16 and 17 into the objective function, equation 4, page 21, provides equation 18, an objective function in terms of the mole fraction of C, the reaction parameters and the production rate, F_B .

$$G = (F_B kVx_C^n (1 - x_C) (C_B - C_A) - F_B^2 (C_B - C_C) - F_B kVx_C^n C_C) / (kVx_C^n (1 - x_C) - F_B) \quad 18.$$

Equation 18 could be used to derive the optimum concentration of reactant C for a particular set of production rate and reaction parameters.

The output variables of the reactor are dependent on the reaction parameters and the input variables. Any change in a parameter or input variable can change the value of an output variable. Any change in the flow of reactant C manipulated by the optimizing controller can potentially change the production thereby upsetting the production controller. If it is desired to control an output variable, one of the input variables must be manipulated. In this case the feed rate of reactant A is manipulated to control production. Any change in the production set point will affect the feed rate of reactant A which will change the concentration of reactant C thereby upsetting the optimizing controller. In this manner interaction between an optimizing controller and a production controller always occurs.

Since the interaction is always present equation 13 was used for both operation policies.

E. Determination of the Economic Extremum Polynomial

An expression relating the performance criterion, income, to the concentration of reactant C, the feed rate of reactant A and the reaction parameters has been developed in equation 13, page 25. The maximum determination procedure described on page 22, can now be applied to equation 13. The flow rate of reactant A is independent of the concentration of reactant C; therefore, equation 13 may be differentiated with respect to the mole fraction of reactant C, x_C . The result is the following ordinary differential equation:

$$\begin{aligned}
 dG/dx_C = & ((C_B - C_C)(1 - x_C)^2 \\
 & (F_{Ain}^2 kV(n x_C^{n-1} - (n + 1)x_C^n)) \\
 & - F_{Ain} C_C (F_{Ain} + kV(1 - x_C)x_C^n)^2) / \\
 & (F_{Ain} + kV(1 - x_C)x_C^n)^2 (1 - x_C)^2 \quad 19.
 \end{aligned}$$

Since the cost of reactant A is constant with respect to the concentration of reactant C, dC_A/dx_C becomes zero.

The solutions of this equation when the derivative is set equal to zero are the extrema of the objective function according to the maximum determination procedure, page 22. When equation 19 is set to zero the non-zero denominators may be deleted; therefore, since the quantities $(F_{Ain} + kV(1 - x_C)x_C^n)^2$ and $(1 - x_C)^2$ will be zero only at a boundary point, when $x_C = 1.0$, i.e., when there is no flow of reactant A, a condition not encountered, the denominators may be deleted.

The derivative, equation 19, is set equal to zero, the denominator is dropped out, and the terms of equal powers of x_C are grouped. The coefficient of the highest order term is then divided into the equation to obtain the following arithmetical expression:

$$\begin{aligned}
 & x_C^{2n+2} - 2x_C^{2n+1} + x_C^{2n} \\
 & + x_C^{n+2} ((n + 1)(C_B - C_C)/C_C) F_{Ain}/kV \\
 & - x_C^{n+1} ((3n + 2)(C_B - C_C)/C_C + 2) F_{Ain}/kV \\
 & + x_C^n ((3n + 1)(C_B - C_C)/C_C + 2) F_{Ain}/kV \\
 & - x_C^{n-1} ((C_B - C_C)/C_C) n F_{Ain}/kV \\
 & + (F_{Ain}/kV)^2 = 0 \quad 20.
 \end{aligned}$$

It should be pointed out that the only cost information necessary is the group, $(C_B - C_C)/C_C$, which can be written, $(C_B/C_C - 1)$, for the bimolecular reaction. If the stoichiometry specified was for the homogeneous catalysis this term would be replaced by C_B/C_C ; therefore, in both cases a ratio of credit for product to the cost of reactant C would suffice and absolute cost data would not be required.

The derivative of the objective function set equal to zero, equation 20, is a polynomial when the order of the rate law with respect to x_C , n , is an integer. For $n = 1$, equation 20 becomes a fourth order polynomial.

$$\begin{aligned} & x_C^4 - x_C^3(2 + 2(F_{Ain}/kV)(C_B/C_C - 1)) \\ & - x_C^2(-1 + 2(F_{Ain}/kV) + 5(F_{Ain}/kV)(C_B/C_C - 1)) \\ & + x_C(-2(F_{Ain}/kV) - 4(F_{Ain}/kV)(C_B/C_C - 1)) \\ & + (F_{Ain}/kV)^2 - (F_{Ain}/kV)(C_B/C_C - 1) = 0 \end{aligned}$$

1. Reactor Parameter Group: Since cost terms will rarely change the only parameter is the group, F_{Ain}/kV . All feasible optimum points may be determined for the concentration of C, x_C , if equation 20 is solved as a function of F_{Ain}/kV for particular values of the order of the rate law with respect to x_C , n , and the cost ratios. For particular values of the order of the rate law and the cost ratios, specification of F_{Ain}/kV fixes the position of the optimum concentration of reactant C; therefore, the group, F_{Ain}/kV , is called the reactor parameter.

F. Solutions of the Economic Extremum Polynomial

1. First Order Rate Law with Respect to C: Equation 20 was solved for $n = 1$, i.e., first order rate law with respect to x_C and five cost ratios for 100 values of the reactor parameter, F_{Ain}/kV . Since for the first order case equation 20 becomes the fourth order polynomial, equation 21, a standard library subroutine, IBM's POLRT, was used to determine the roots. One set of complex roots and two real roots were obtained for the range of F_{Ain}/kV chosen; however, only one of the real roots fell in the feasible range. At least one of the real roots was always negative--a meaningless solution in terms of mole fraction. Therefore, this objective function with the first order rate law with respect to each reactant is effectively unimodal. The range of F_{Ain}/kV for feasible solutions always extends from zero to the value of the cost ratio minus one, i.e., $C_B/C_C - 1$. This characteristic is demonstrated graphically in figure 1, page 33. At the point, $F_{Ain}/kV = C_B/C_C - 1$, the feasible solution becomes zero. Both of the real solutions of the polynomial become negative when F_{Ain}/kV is increased above $C_B/C_C - 1$. This characteristic is verified by substitution of $F_{Ain}/kV = C_B/C_C - 1$, into equation 21 which eliminates the zero power term of x_C . Elimination of this term forces at least one root of equation 21 to be $x_C = 0$. Should the reaction rate ever drop low enough to generate this result the operator would probably elect to regenerate the catalyst,

change feed stocks, shut down or run for good will.

Figure 1, page 33, is a plot of the solutions of equation 21, extremum concentration of reactant C vs. the reactor parameter group, F_{Ain}/kV , for cost ratios, C_B/C_C , of 2.0, 3.0, 5.0, 10.0, and 20.0. Investigation of the performance criterion in the neighborhood of these extremum points verifies that they are all maxima. Therefore, figure 1 is a plot of the optimum concentration of reactant C vs. the reactor parameter group, F_{Ain}/kV .

The objective function describes an "incremental operation" situation. It alone cannot predict the practical limit of operation for F_{Ain}/kV in a "book cost" situation since it does not consider fixed costs such as utilities and labor or capital charges. The objective function can however give an indication of the very maximum limit possible if certain basic assumptions are made. The maximum range would occur when all fixed costs were considered zero and the cost of reactant A was considered zero. The limiting values of F_{Ain}/kV can then be found by solving the equation obtained from setting the performance criterion, income, equal to zero and the cost of reactant A, C_A , equal to zero. At this point the plant ceases to be profitable regardless of fixed costs or cost of reactant A.

$$G = \frac{(kVx_C^n(1 - x_C)F_{Ain})(C_B - C_C)}{(F_{Ain} + kVx_C^n(1 - x_C))} - F_{Ain}(x_C C_C / (1 - x_C)) = 0 \quad 22.$$

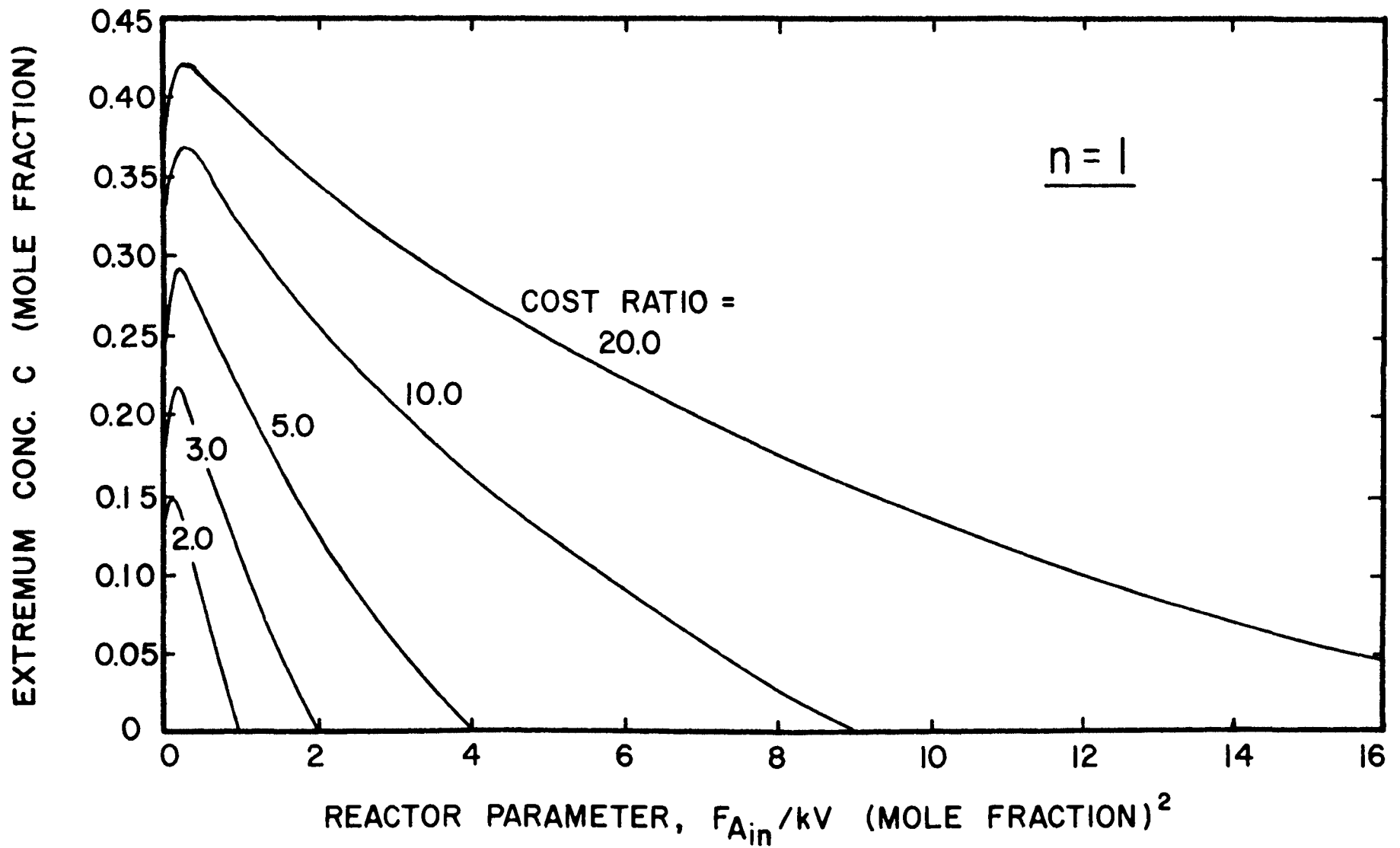


Figure 1. Extremum Curves of the Objective Function for $n = 1$.

Dividing equation 22 by the reaction rate constant, the reactor volume and the cost of reactant C yields equation 23.

$$\begin{aligned} G/kVC_C &= (F_{Ain}/kV)(1 - x_C)x_C^n(C_B/C_C - 1)/ \\ & (F_{Ain}/kV + (1 - x_C)x_C^n) \\ & - (F_{Ain}/kV)(x_C/(1 - x_C)) = 0 \end{aligned} \quad 23.$$

Rearrangement of equation 23, gives a function for F_{Ain}/kV in terms of x_C and the cost ratio for particular values of the order of the reaction rate law with respect to reactant C.

$$\begin{aligned} F_{Ain}/kV &= x_C^{n-1}(C_B/C_C - 1) \\ & x_C^n(-2C_B/C_C + 1) + x_C^{n+1}(C_B/C_C) \end{aligned} \quad 24.$$

Equation 24 is then a function which describes the limiting value of F_{Ain}/kV which can be tolerated in a reaction process and continue to produce profit. It is therefore a constraint on the optimum solutions.

Figure 2, page 35, is a plot of the optimum mole fraction of reactant C vs. F_{Ain}/kV for a first order reaction rate law with respect to reactant C and a cost ratio, C_B/C_C of 3.0. This plot, figure 2, is taken from figure 1, page 33. The dashed line on figure 2 is the locus of points representing equation 24 for the parameters used. It can be seen that in this case the constraint always lies above the optimum curve and does not interfere with the function.

2. Second Order Rate Law with Respect to C: The solutions to equation 20 for a second order rate law with

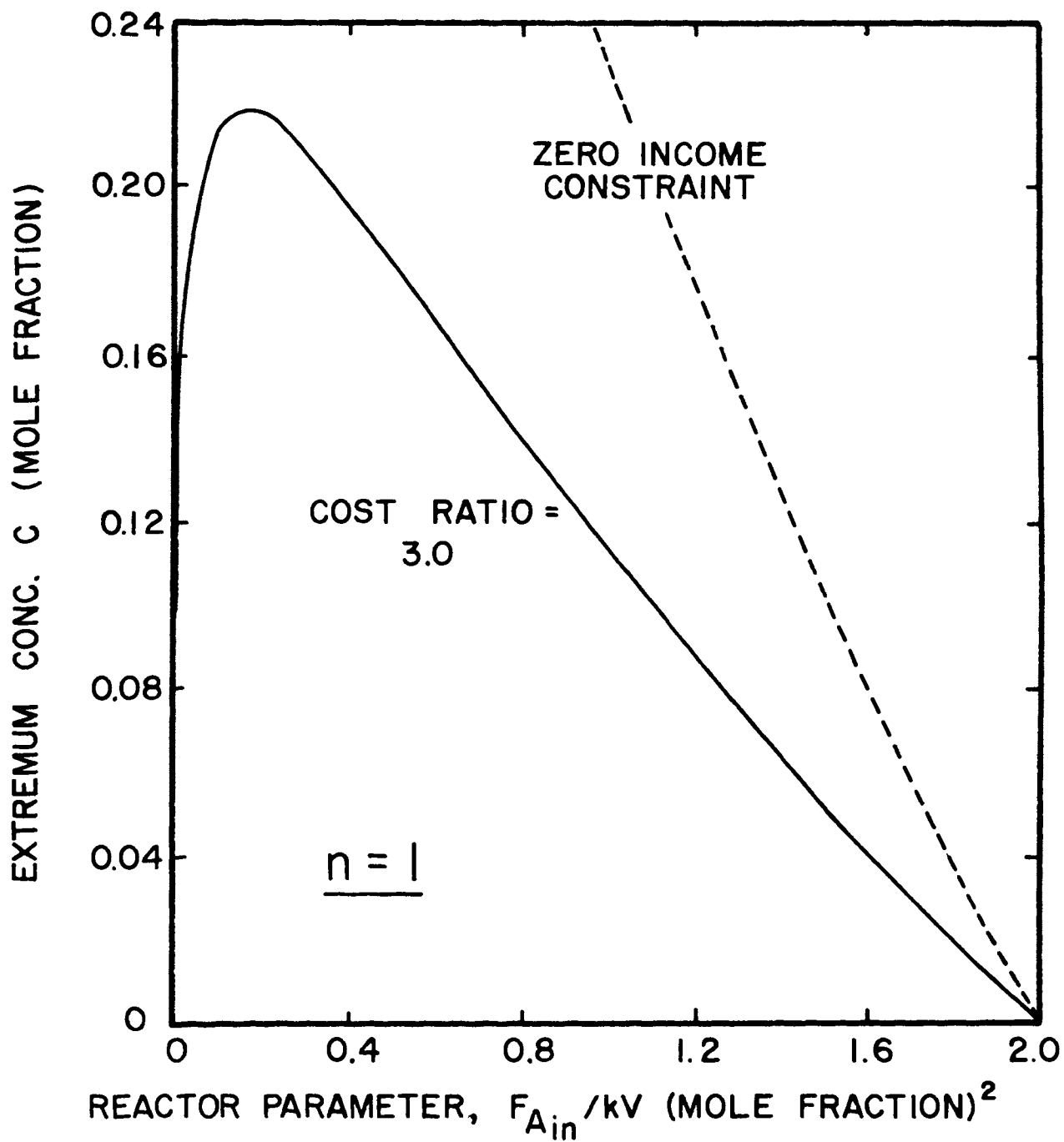


Figure 2. Zero Income Constraint for $n = 1$.

respect to reactant C were investigated. For the second order rate law, equation 20 becomes a sixth order polynomial.

$$\begin{aligned}
 & x_C^6 - 2x_C^5 + x_C^4(1 + 3(F_{Ain}/kV)(C_B/C_C - 1)) \\
 & + x_C^3(-8(F_{Ain}/kV)(C_B/C_C - 1) - 2(F_{Ain}/kV)) \\
 & + x_C^2(7(F_{Ain}/kV)(C_B/C_C - 1) + 2(F_{Ain}/kV)) \\
 & + x_C(-2(F_{Ain}/kV)(C_B/C_C - 1)) \\
 & + (F_{Ain}/kV)^2 = 0
 \end{aligned} \tag{25}$$

Two positive real solutions exist for each value of F_{Ain}/kV . One set of these feasible solutions represents a maximum condition of the objective function and the other set defines a minimum condition of the objective function. The two solutions approach each other as the parameter group, F_{Ain}/kV , is increased until a point is reached at which the two sets converge at an inflection point of the objective function. Once the inflection point is passed there are no feasible solutions to equation 25. The solutions take the form of three sets of complex roots. Figure 3, page 37, is a plot of the solutions of equation 25 vs. F_{Ain}/kV for cost ratios of 5.0, 10.0, and 20.0. Figure 3, graphically demonstrates the characteristics described above.

The application of the limiting profit constraint, equation 24, for the second order rate law can now be made. For the second order rate law this constraint completely eliminates the minimum solutions of equation 25 from practical consideration.

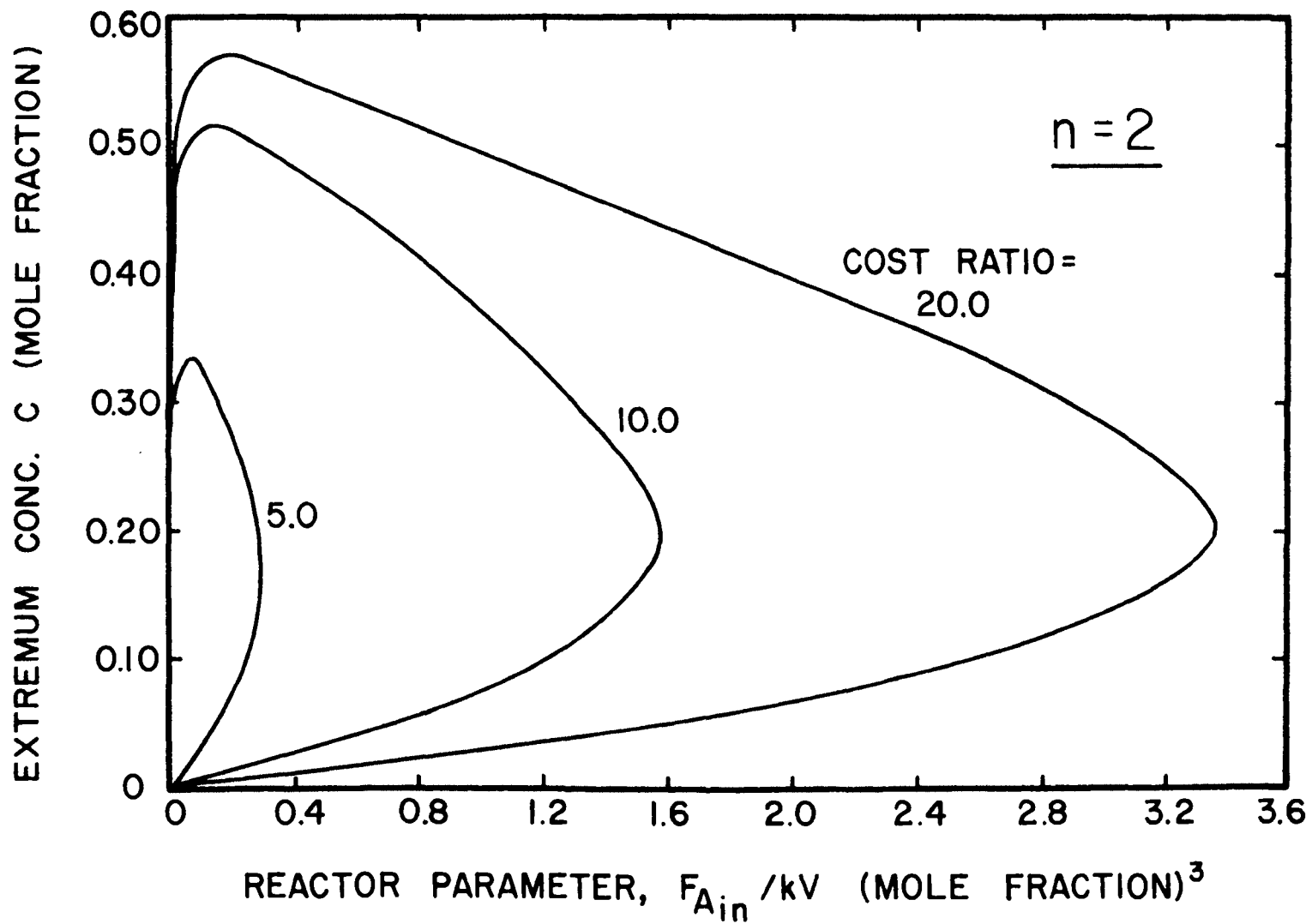


Figure 3. Extremum Curves of the Objective Function for $n = 2$.

Figure 4, page 39, is a plot of the solutions to equation 25, with the cost ratio equal to 10.0. The dashed line of figure 4 is the locus of the solutions of equation 24, the profit constraint for the second order rate law. Figure 4 then graphically demonstrates the action of the profit constraint described above.

These plots may now be used to predict the optimum concentration of reactant C anytime the parameter group, F_{Ain}/kV can be determined.

3. Income for Optimum Operation: The solutions of equation 20, page 29, for a particular value of n are optimum points for any particular value of F_{Ain}/kV . However, if the molar flow of reactant A, F_{Ain} , can be selected at random, the solutions of equation 20 must be considered local optimum points. The absolute income varies with changes in the parameter, F_{Ain}/kV . One particular value of F_{Ain}/kV and corresponding optimum mole fraction of reactant C will produce the greatest income, i.e., be the global optimum.

This subject is not treated in detail here but the global optimum may be found mathematically by defining equation 19, page 29, a partial differential equation for constant F_{Ain} . Another partial differential equation, the partial of G with respect to F_{Ain} , for constant x_C is obtained. Setting both partials equal to zero and solving simultaneously will generate the conditions, x_C and F_{Ain}/kV

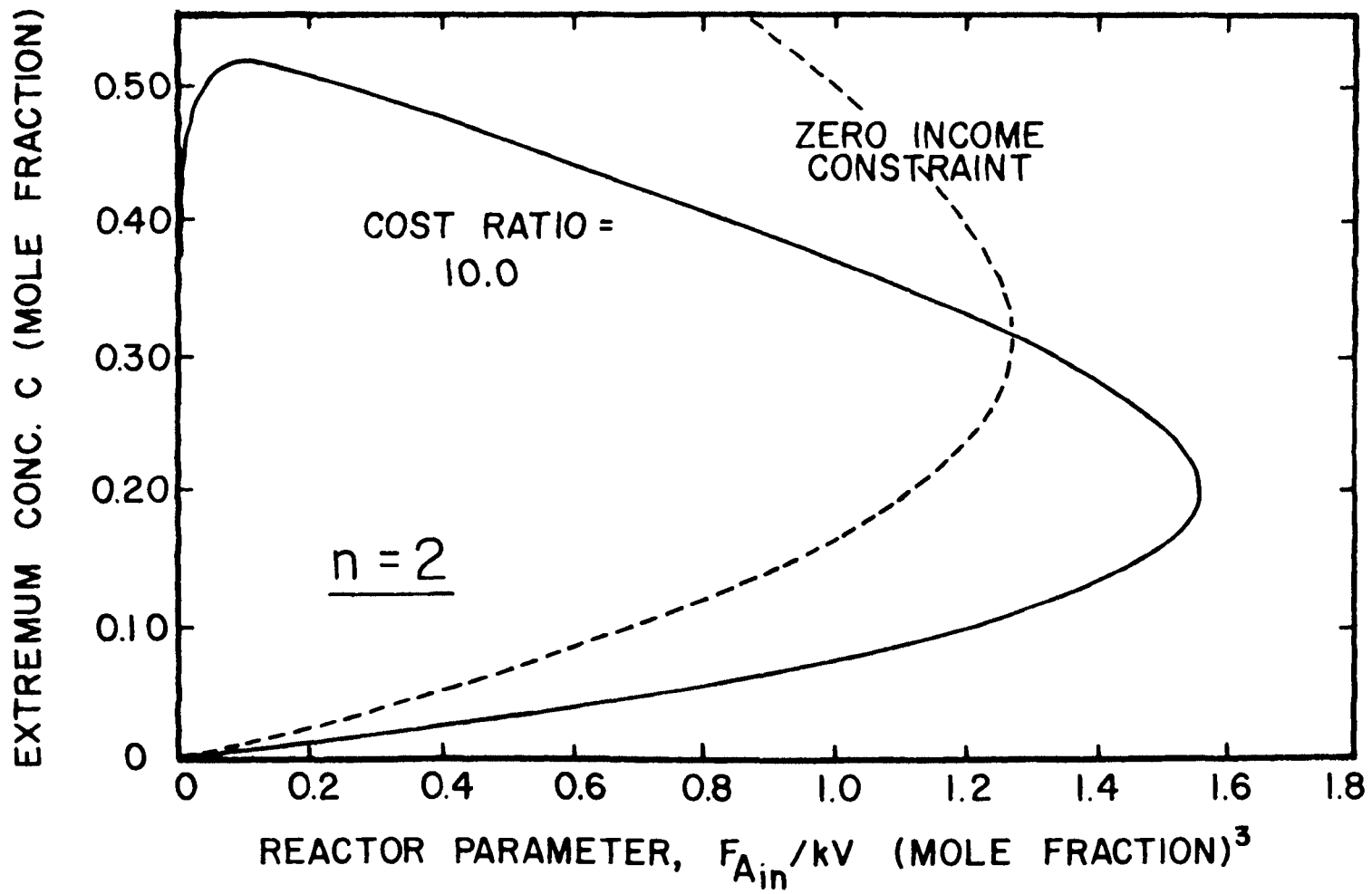


Figure 4. Zero Income Constraint for $n = 2$.

for the global optimum. These values could then be placed as set points controlling the molar flow of reactant C and reactant A respectively. Any change in the reaction rate constant due to catalyst decay, temperature changes or other environmental affects would be detected and a new set of molar feed rates would be found which would maintain the derived set points for the global optimum.

To demonstrate the position of the global optimum graphically the objective function, equation 13, is divided by kV and C_C and solved for various solutions of equation 20 for $n = 1$ and C_B/C_C of 10.0. The position of the global optimum also depends on the cost ratio of A to C, C_A/C_C . For the demonstration, C_A/C_C was set to zero. Figure 5, page 41, is a plot of the solutions of equation 20, page 29, for $n = 1$ and $C_B/C_C = 10.0$ and includes a plot of the objective function, income, divided by kV and C_C for these solutions of equation 20.

4. Production for Optimum Operation: Also included in figure 5, page 41, is a plot of the molar production divided by kV and C_C , F_B/kVC_C , for the solutions of equation 20 presented. It can be seen that the production goes through a maximum. These two curves, the absolute income along the optimum curve and the production along the optimum curve effectively limit the operation range. There are conceivable instances in which the reactor parameter would become very large due to external policies but there would

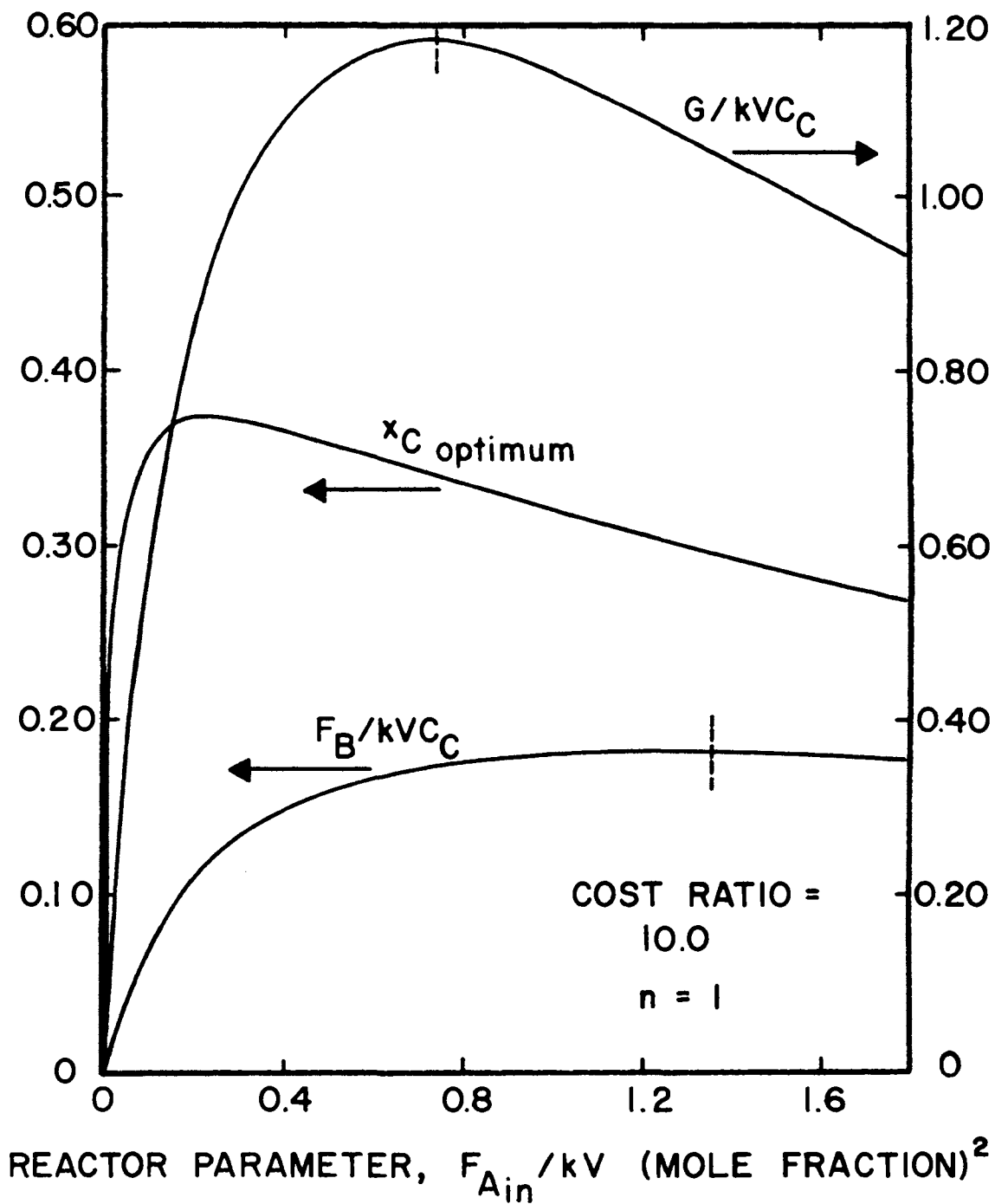


Figure 5. Income Index and Production Rate at Optimum Concentrations for $n = 1$.

never be a conscious decision to increase F_{Ain}/kV past the point which generates the maximum production because there is nothing to be gained--both income and production decrease.

G. On-Line Measurement of the Reactor Parameter Group

It has been shown that the optimum mole fraction of one component, C, may be determined given the reactor parameter, F_{Ain}/kV , and the cost terms. Then if the optimizing scheme is to be employed on-line this reactor parameter must be measurable on-line.

The reactor parameter might be determined by measuring the feed rate of reactant A, the reaction rate constant and the volume of the reactor. The feed rate of reactant A could be measured accurately and the reaction rate constant could be correlated with the temperature and pressure of the reaction (measurable quantities) but properties such as catalyst poisoning or changes in the feed stocks would not be easily measured. An estimate of the reactor parameter is therefore more reliable if the parameter can be obtained directly from measurement of the composition of the product stream. Chemical analyzers would have to be employed in any type of optimization scheme whether it depended on perturbations or a model; therefore, the use of chemical analysis does not complicate the operation.

The dynamic behavior of a backmix reactor at constant temperature and pressure can be described by the following ordinary differential equation obtained from a component

material balance:

$$VD_m dx_A/dt = -kVx_Ax_C^n - Fx_A + F_{Ain} \quad 26.$$

where:

$$D_m = \text{molar density in the reactor;} \\ \text{(moles)/(volume)}$$

Equation 8, page 24, is valid during dynamic changes provided incompressible flow is maintained.

$$F = F_{Ain}/(1 - x_C) \quad 8.$$

Substitution of equation 8 and equation 7 into equation 26 provides the following ordinary differential equation:

$$VD_m dx_A/dt = -kVx_Ax_C^n + F_{Ain}x_B/(1 - x_C) \quad 27.$$

Both sides of equation 27 are then divided by the reaction rate constant and the reactor volume to give the following expression:

$$(VD_m/kV)dx_A/dt = -x_Ax_C^n \\ + (F_{Ain}/kV)x_B/(1 - x_C) \quad 28.$$

Solution of equation 28 for the reactor parameter group gives the following expression for F_{Ain}/kV .

$$F_{Ain}/kV = ((D_m/k)dx_A/dt + x_Ax_C^n) \\ (1 - x_C)/x_B \quad 29.$$

At steady state the derivative, dx_A/dt , becomes zero and the following expression is obtained for the group,

F_{Ain}/kV :

$$F_{Ain}/kV = (x_Ax_C^n)(1 - x_C)/x_B \quad 30.$$

When the reactor is not at a steady state condition the error in the approximation of F_{Ain}/kV is the group which

contains the derivative, $((D_m/k)dx_A/dt)(1 - x_C)/x_B$.

Equation 30 may be applied as an approximation of F_{Ain}/kV , correct at steady state; therefore, only the concentrations of the exit stream are required to obtain a measure of the reactor parameter. If the temperature, pressure, catalyst activity or feed stock quality change, the effect on F_{Ain}/kV will be detected in the analysis.

H. Errors Introduced by Reaction Rate Law Approximation

It is desired to obtain an insight into the magnitude of the errors incurred due to the failure of the assumed rate law to reproduce the actual reactor characteristics. The effect on the objective function, income, was calculated for cases in which very large errors were intentionally introduced. The cost ratio of reactant A to reactant C is specified zero.

The two rate laws investigated in this dissertation, first order with respect to each reactant and first order with respect to A--second order with respect to C, are used as models to demonstrate the effect of rate law approximation. A cost ratio, C_B/C_C , of 10.0 is employed. The first order law with respect to each reactant was employed when in fact a second order correlation with respect to reactant C would be correct. A test procedure is specified.

1. Select a value of F_{Ain}/kV for $n = 1$, the incorrect rate law.
2. Using figure 1, page 33, determine the indicated optimum x_C for the value of F_{Ain}/kV selected for $n = 1$.
3. Determine the correct value of F_{Ain}/kV , $n = 2$, by application of equation 30, page 43, for each value of F_{Ain}/kV , $n = 1$, selected.
4. Determine the true optimum x_C from figure 3, page 37, for the correct values of F_{Ain}/kV found in 3, above.

5. Determine the income for the indicated optimum x_C and for the true optimum x_C from equation 23, page 34.

Figure 6, page 47, is a plot of both the income at the true optimum and the indicated optimum when the incorrect rate law is assumed. Figure 7, page 48, is a plot of the percent loss in income created by the incorrect rate law assumption. As demonstrated, this loss becomes very great for high values of F_{Ain}/kV .

As demonstrated in figure 5, page 41, the production and income both begin to decrease at a particular value of F_{Ain}/kV . It can be seen from figure 5, also valid for $C_B/C_C = 10.0$, that the production begins to decrease at an F_{Ain}/kV of approximately 1.35. This corresponds to F_{Ain}/kV for $n = 2$ of approximately 0.40, if the second order rate law was correct. From figure 7, page 48, the percent loss in income from the optimum is approximately 31.5 percent for the specified F_{Ain}/kV of 0.40. Therefore, if operation is restricted to a region of increasing production with an increase in F_{Ain} , the maximum loss in income to be expected from such a gross error in the rate law would be less than 32.0 percent.

This magnitude of loss is of course intolerable and indicates the strong need for a thorough investigation of the reaction kinetics and an accurate representation of the rate law.

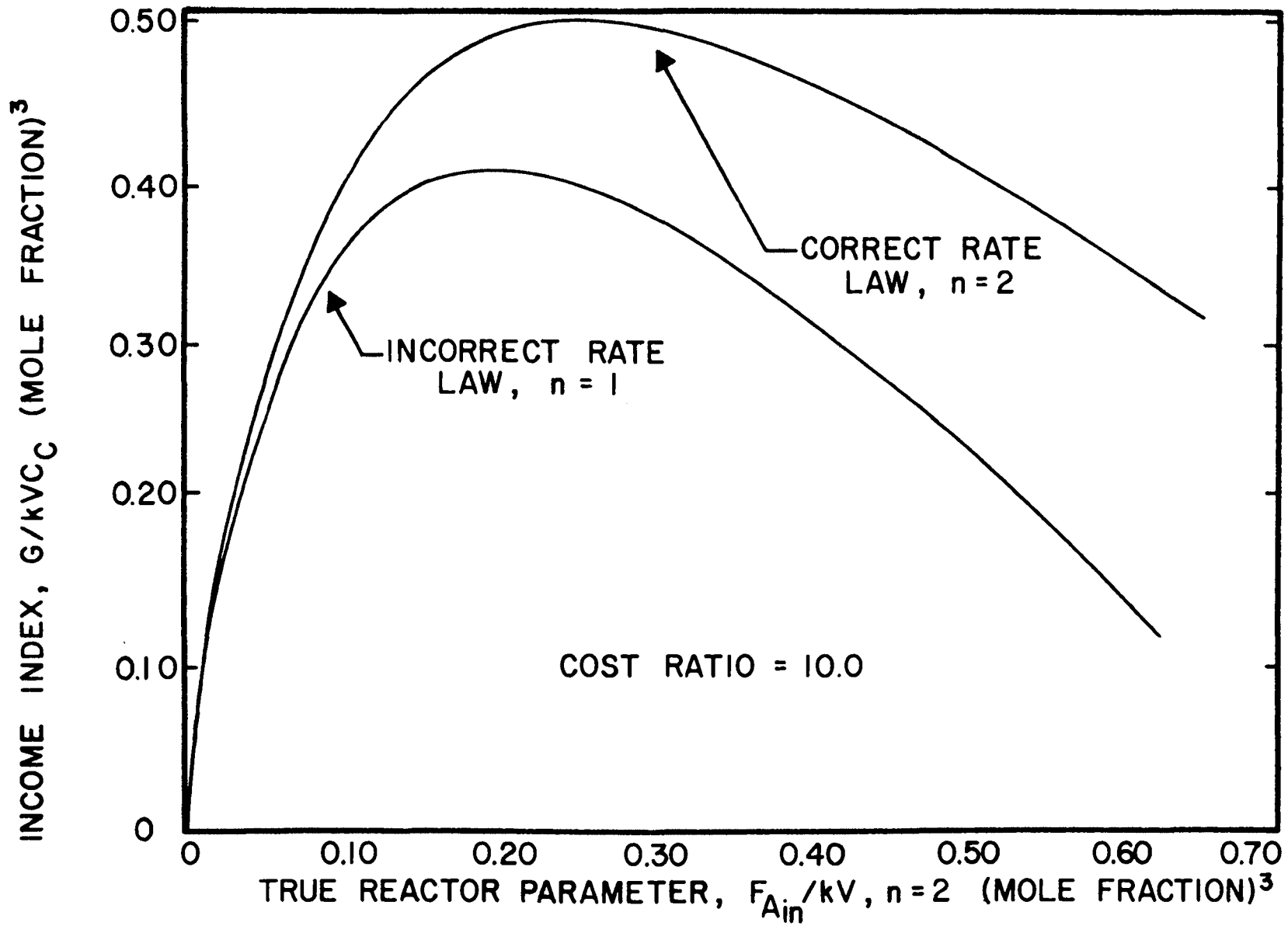


Figure 6. Income Index for an Incorrect Rate Law Assumption.

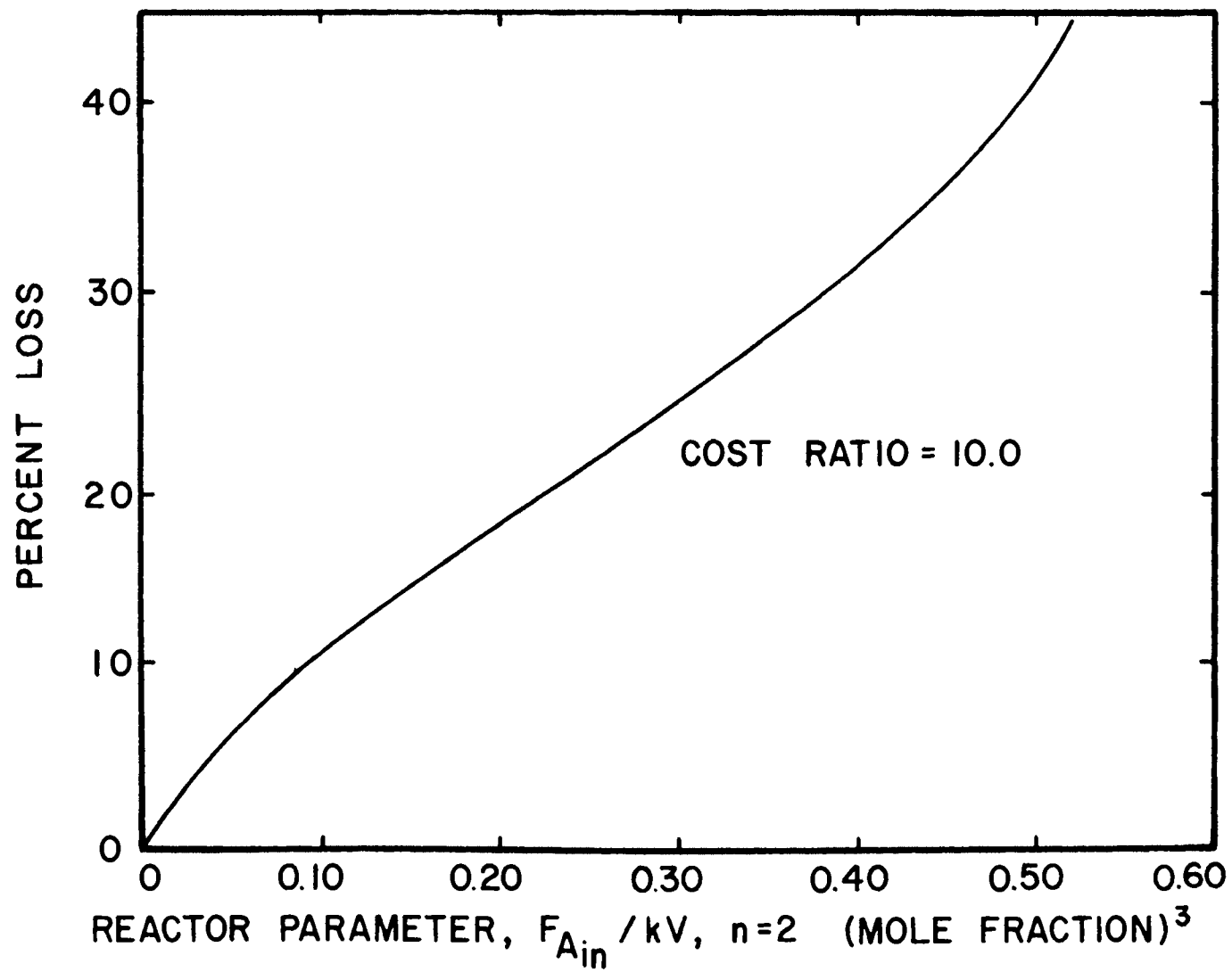


Figure 7. Income Loss for an Incorrect Rate Law Assumption.

V. IMPLEMENTATION

In order to implement the proposed optimizing scheme the reactor parameter, F_{Ain}/kV , must be measured and on-line hardware used to provide the optimum concentration of reactant C. The value of the reactor parameter, F_{Ain}/kV , is determined from equation 30 which requires a complete chemical analysis of the exit stream.

To obtain a complete analysis of a ternary system at least two compositions must be determined. If continuous analysis is desired, instruments such as densitometers, continuous titrators, light absorption devices, or boiling point analyzers may be employed. Continuous on-line analysis application is investigated in the simulation section, page 54.

In recent years the gas-liquid chromatograph has found wide application in the chemical process industry. Although its output is sampled and delayed it is a valuable tool because of the quantity of information obtainable and the basic simplicity of its operation. With one GLC installation all the components amenable to partition chromatography may be analyzed accurately. However, in many cases the chromatograph is operated only as another "handle" of the plant and not employed in closed loop control. The use of the gas chromatograph is investigated in the simulation

section and it is the method of analysis used in the experimental operation.

Once the composition of the product stream has been determined the mole fractions are combined in equation 30, derived earlier for F_{Ain}/kV . The calculation of this group is done most accurately with the use of a digital mini-computer or in a subroutine of an on-line digital control computer. This same digital computer may be used to sample the output of the chromatograph. However if the digital computer is not available, analog components may be used to perform the multiplications and divisions necessary.

A small general purpose electronic analog computer was used to interface with the chromatograph and perform the necessary computations.

When the reactor parameter group, F_{Ain}/kV , is known a plot such as figure 2 may be used to obtain the optimum x_C . An operator may adjust the set-point on a composition controller which manipulates the flow of reactant C. In order to close the loop the plot may be transferred to a variable diode function generator (VDFG) in analog equipment or a polynomial correlation stored in a digital subroutine. If analog equipment is to be used the input to the VDFG would be the value of F_{Ain}/kV obtained from computations described by equation 30, page 43. The output of the VDFG would be the optimum mole fraction of reactant C. This output is then used as the set point for a

composition controller manipulating the feed of reactant C. The measured variable for this controller, x_C , is also obtained from the chromatograph. A block diagram of such a system is illustrated in figure 8.

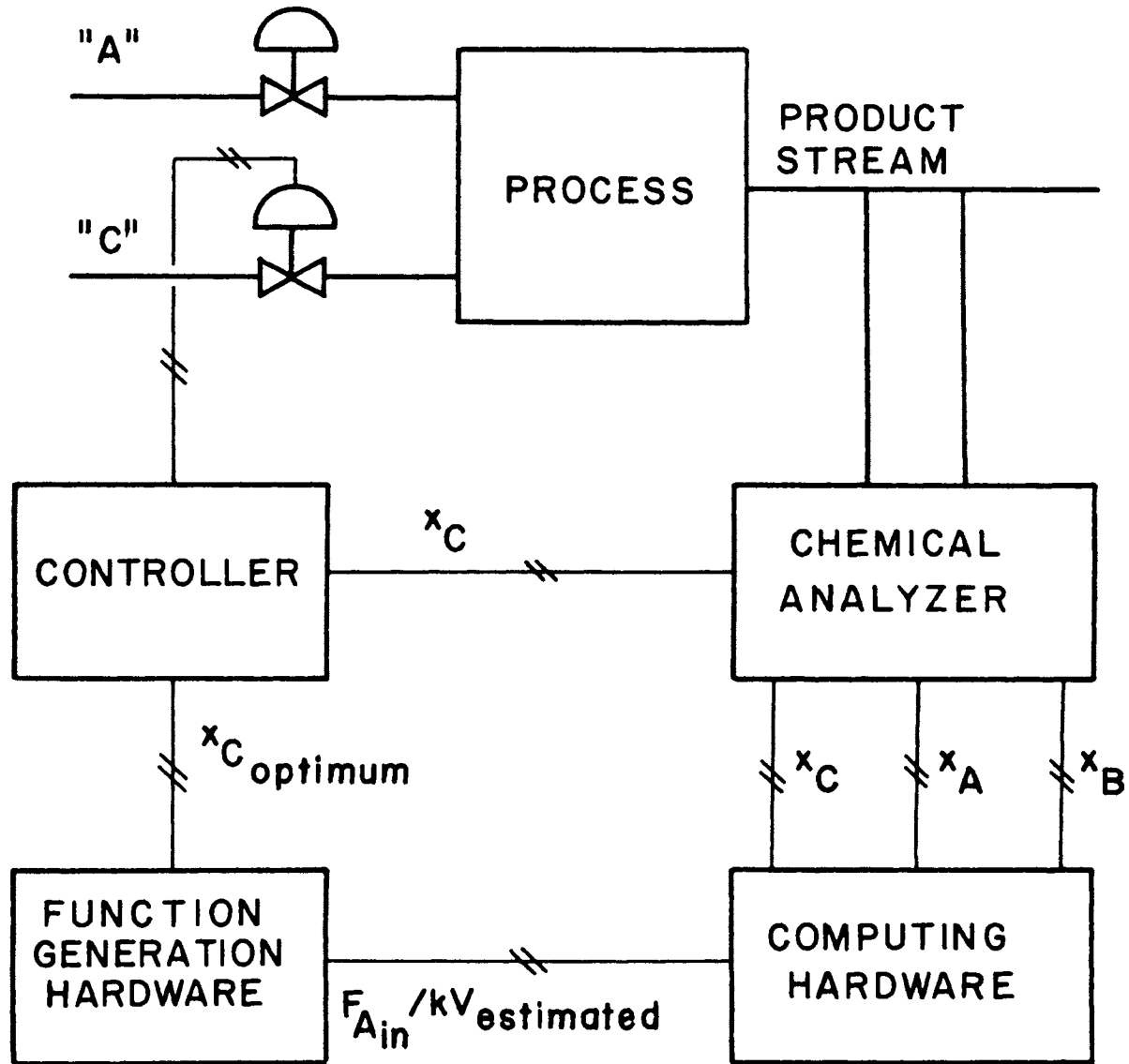


Figure 8. Proposed Implementation Scheme for the Optimizing Controller.

VI. EVALUATION TESTS AND RESULTS

A. Simulation Operation

1. Simulation Purpose: The purpose of constructing a simulation of the proposed optimizing control scheme is to insure that such a scheme will function, i.e., drive the process to a steady state optimum of the particular objective function under ideal conditions in which all assumptions made in developing the scheme are absolutely correct. An additional purpose is to study the dynamic characteristics of the optimized reactor.

2. Simulation Equations: The development of the simulation equations and programs is presented in Appendix B, page 104. The system simulated is a bimolecular reaction with a reaction rate law which is first order with respect to each reactant. This reaction takes place in a continuous flow stirred tank reactor and is limited to reaction systems which may be approximated by incompressible flow.

The simulation equations are derived in Appendix B and are restated here.

$$\begin{aligned} dx_A/dt = & -(k/D_m)x_Ax_C - (F/VD_m)x_A \\ & + F_{Ain}/VD_m \end{aligned} \quad 6B.$$

$$\begin{aligned} dx_C/dt = & -(k/D_m)x_Ax_C - (F/VD_m)x_C \\ & + F_{Cin}/VD_m \end{aligned} \quad 7B.$$

$$F/VD_m = F_{Ain}/VD_m + F_{Cin}/VD_m - (k/D_m)x_Ax_C \quad 8B.$$

$$F_{Ain}/kV = x_A^2x_C/x_B + x_Ax_C \quad 9B.$$

$$F_B = F_{Ain}(x_B/(1 - x_C)) \quad 10B.$$

The variables used in these equations and on the simulation plots are groups of variables which have been previously encountered. A list of these groups and their physical significance is presented in Table I.

Step and pulse type upsets were imposed on the reaction rate constant and the molar flow rate of reactant A with the optimizing controller functioning. Upsets on the rate constant were imposed with both the optimizing controller and production controller functioning.

The cost ratio, C_B/C_C , used in the simulation is 20.0. The optimum relationship for this cost ratio is presented in figure 5B, page 118.

3. Continuous Analysis: The first simulation run presented, figure 9, is the open loop response to a step down in the feed rate of reactant A from F_{Ain}/VD_m of 0.8 to 0.2 minutes⁻¹. The initial conditions are those which represent an optimum x_C at F_{Ain}/VD_m of 0.8 minutes⁻¹. The upper plot of the simulation runs provides the error from the optimum and the error from the production set point.

Conventional P-I controllers were employed for the continuous analysis investigation. Figure 10, page 57, demonstrates the use of the optimizing controller with the

TABLE I
SIMULATION VARIABLE DESCRIPTION

Variable Group	Description	Units
F_{Ain}/VD_m	The reciprocal time constant of the reactor with respect to feed of reactant A alone	Minute ⁻¹
F_{Cin}/VD_m	The reciprocal time constant of the reactor with respect to feed of reactant C alone	Minute ⁻¹
F_B/VD_m	The reciprocal time constant of the reactor with respect to production alone	Minute ⁻¹
F/VD_m	The reciprocal time constant of the reactor based on exit flow	Minute ⁻¹

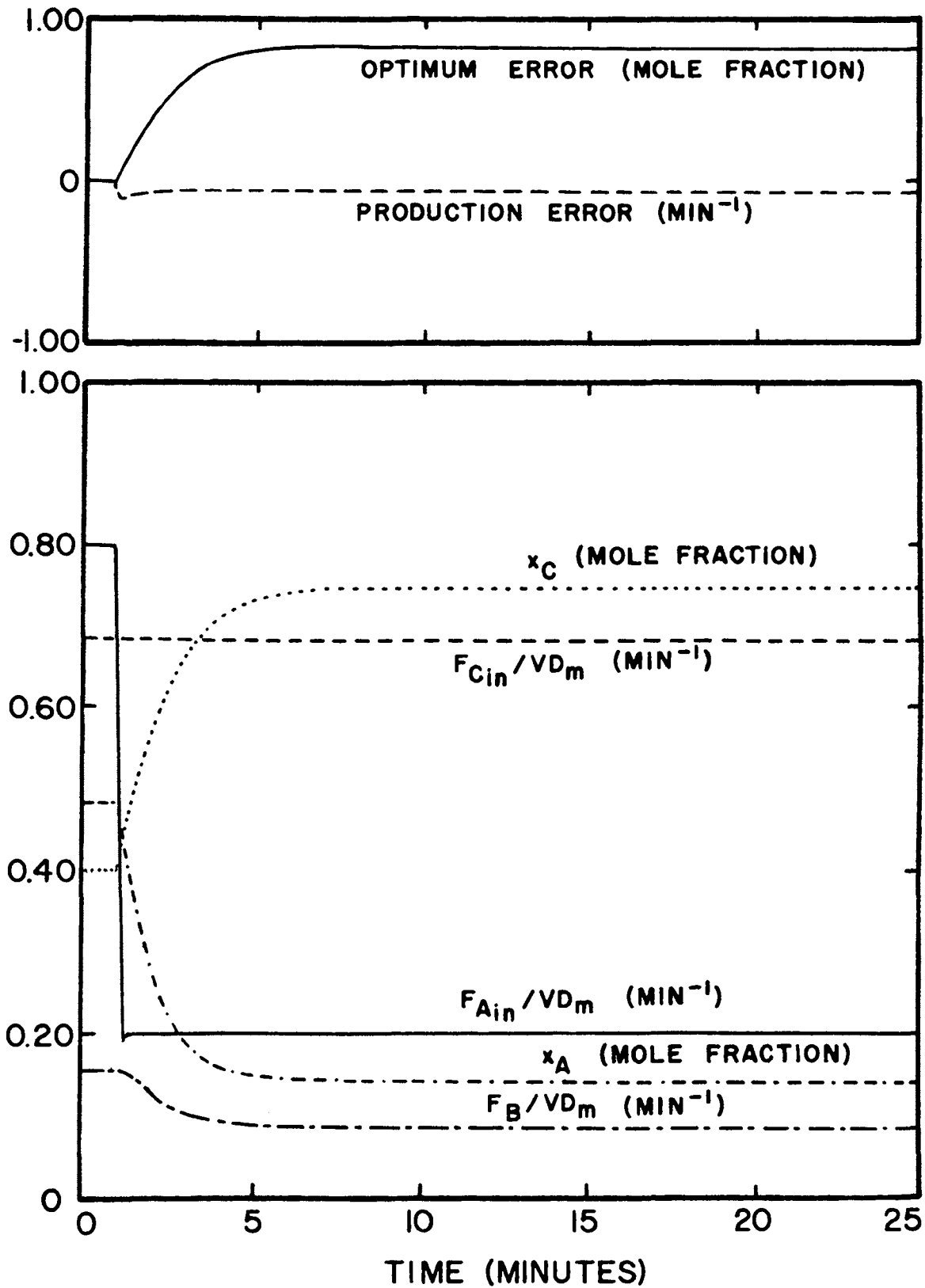


Figure 9. Simulation of a Step Down in the Feed of Reactant A, Open Loop.

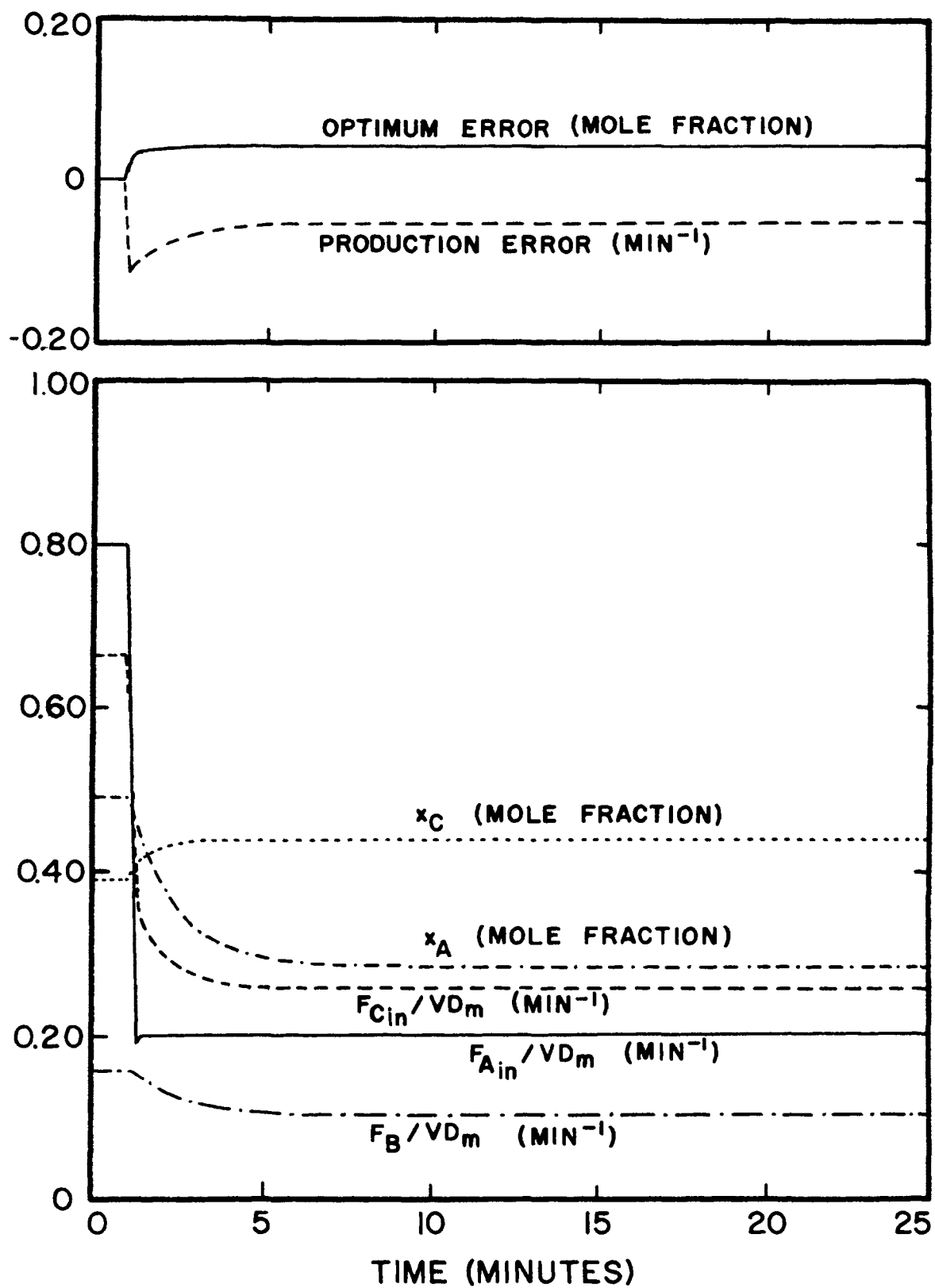


Figure 10. Simulation of a Step Down in the Feed of Reactant A, Continuous Analysis, $k_0 = 25.0$.

proportional control mode only. The proportional gain for figure 10 is $25.0 \text{ (minute}^{-1} \text{ C)}/(\text{mole fraction C})$, a proportional band of 4. The system is very well behaved for this gain and exhibits no under-damped tendency.

A more realistic case is presented in figure 11, page 59. For this simulation run reset was employed with a proportional gain of $2.5 \text{ (minute}^{-1} \text{ C)}/(\text{mole fraction C})$ and an integral time constant of 0.1 minutes. These controller settings are realistic and bring the system back to the optimum very quickly.

For the step down in F_{Ain}/VD_m presented in figures 9, 10, and 11 the initial time constant for the reactor is 0.76 minutes and the final time constant after steady state is reached at the new optimum is 2.9 minutes; therefore, the reactor response is considerably slower after the step. To investigate the effect of a fast response, steps up in F_{Ain}/VD_m were made. Figure 12, page 60, is a simulation run for a step up in the flow of reactant A from F_{Ain}/VD_m of 0.2 to 0.8 minutes^{-1} . The optimizing controller settings are a proportional gain of $2.5 \text{ (minute}^{-1} \text{ C)}/(\text{mole fraction C})$ and an integral time constant of 0.1 minutes. This response is well behaved and responds very quickly to the step change

Figure 13, page 61, is the open loop response to a step down in the reaction rate constant group, k/D_m , from 0.8 to $0.5 \text{ (mole fraction}^2, \text{ minutes)}^{-1}$. For this upset both the optimizing and production control schemes were employed.

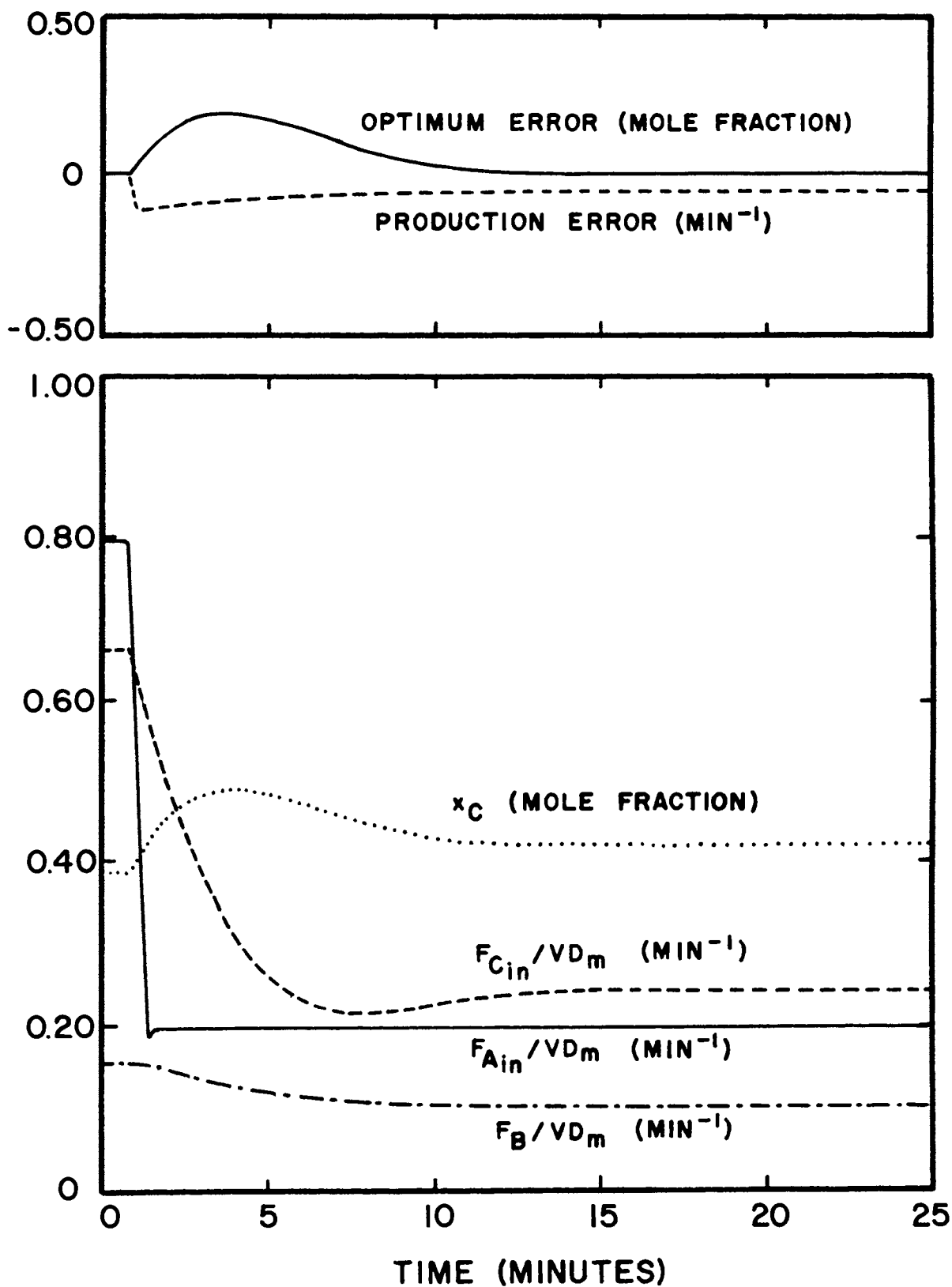


Figure 11. Simulation of a Step Down in the Feed of Reactant A, Continuous Analysis, $k_0 = 2.5$, $T_0 = 0.1$ min.

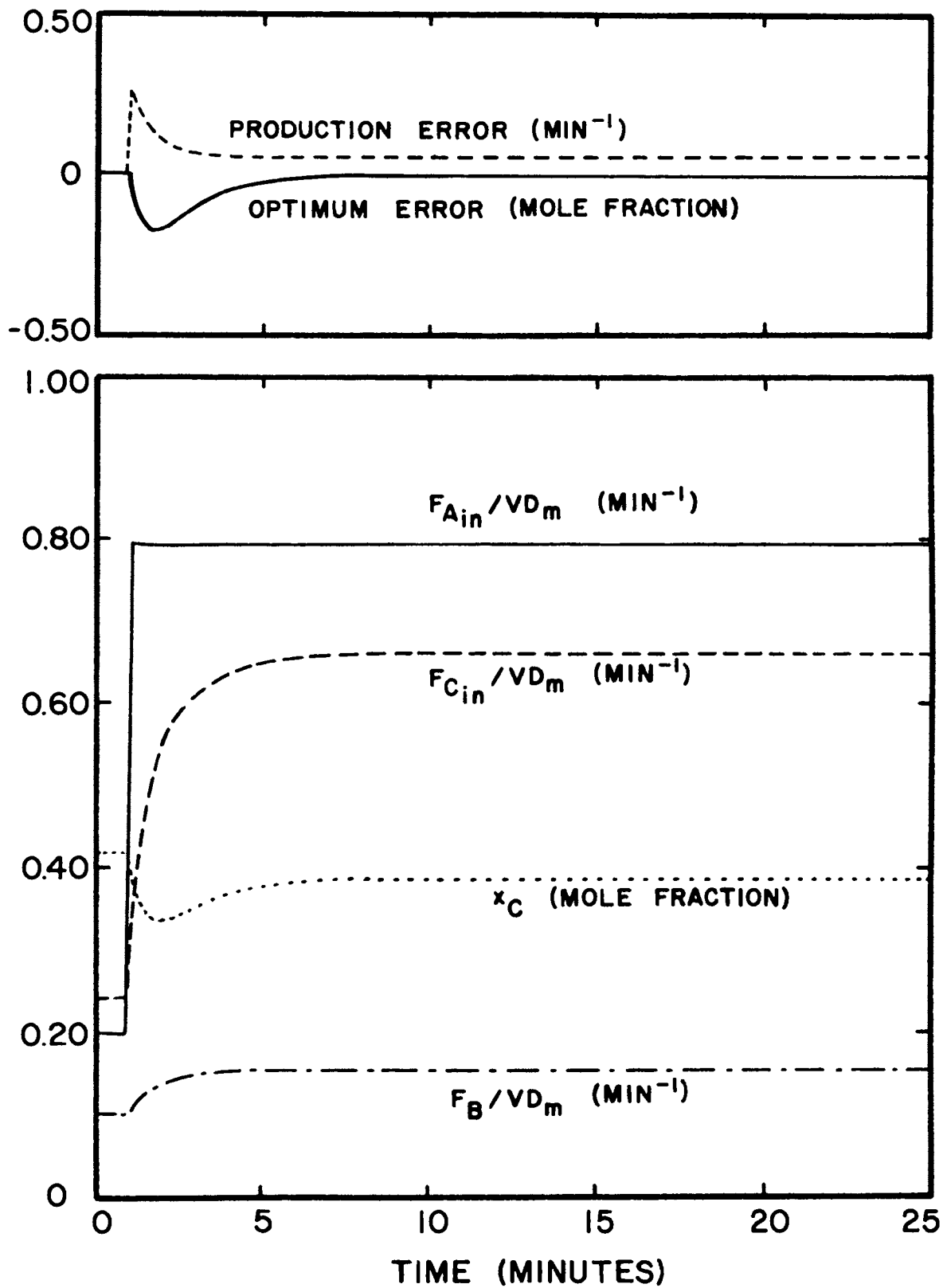


Figure 12. Simulation of a Step Up in the Feed of Reactant A, Continuous Analysis, $k_0 = 2.5$, $T_0 = 0.1$ min.

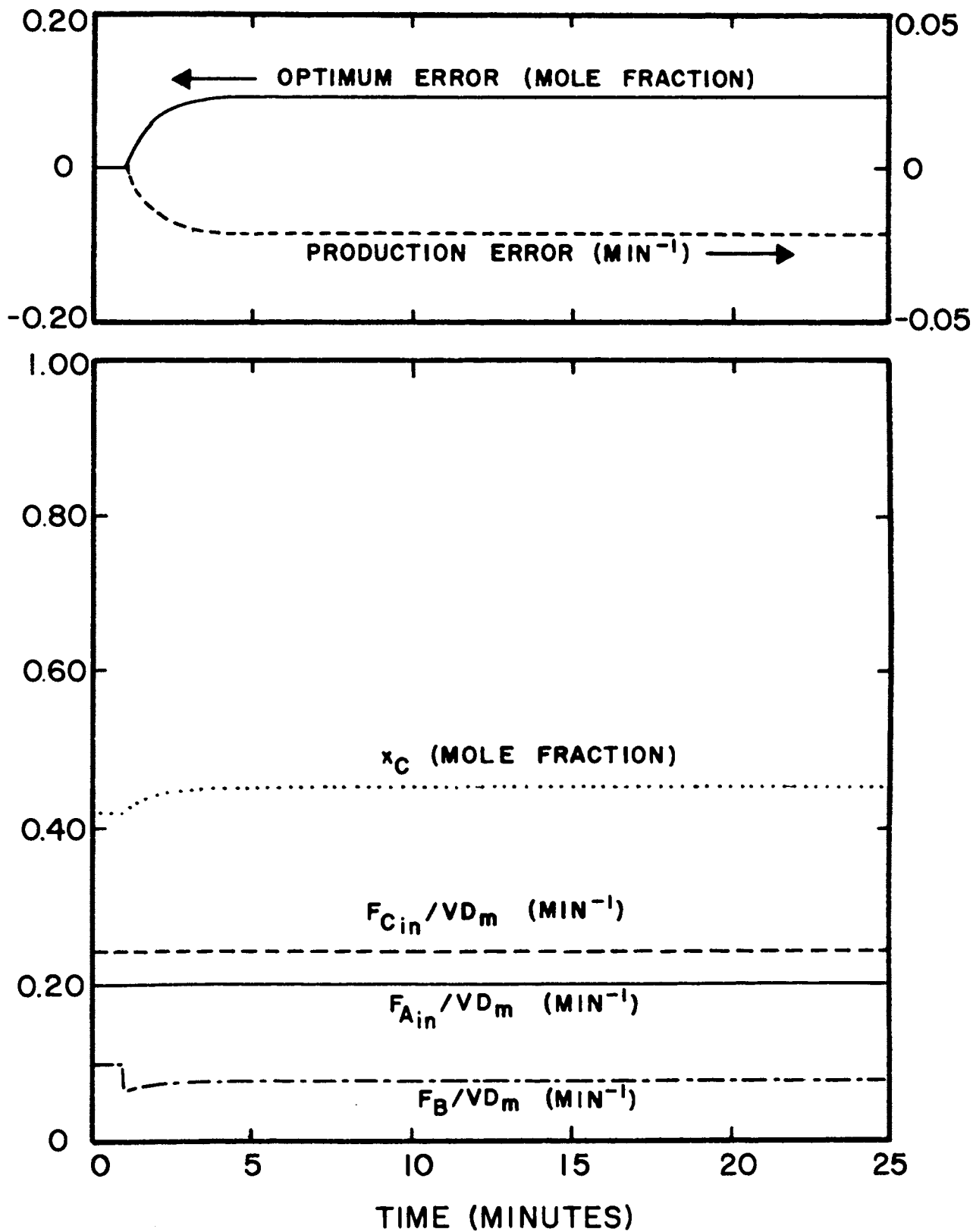


Figure 13. Simulation of a Step Down in the Reaction Rate Constant, Open Loop.

It is desired to maintain the same production; therefore, the set point is placed at the production rate prior to the step. Figure 14, page 63, is a simulation run with the optimizing proportional gain, k_o , set to 25.0 (minute⁻¹ C)/(mole fraction C) and the integral time constant, T_o , set to 0.1 minutes. The production proportional gain, k_p , is set to 10 (minute⁻¹ A)/(minute⁻¹ B) and the production controller integral time constant, T_p , also set to 0.1 minutes. The flow rate of reactant A, manipulated by the production controller must be raised by almost a factor of 3 in order to maintain the production rate at its specified value.

Figure 15, page 64, is the response of the system to a step change in the set point for production control. The requested production, F_B/VD_m , is 0.1563 minutes⁻¹ which is fairly close to the maximum for this cost ratio and reaction rate constant, 0.1630 minutes⁻¹. As indicated earlier, operation close to the production maximum requires care since if the production maximum is passed the sensitivity changes sign and the production controller will be unstable due to positive feedback. Fine controller tuning becomes significant. The response recorded in figure 15 uses the same controller constants as presented in figure 14, k_o of 25.0 (minute⁻¹ C)/(mole fraction C), T_o of 0.1 minutes, k_p of 10 (minute⁻¹ A)/(minute⁻¹ B) and T_p of 0.1 minutes. The optimizing controller must "keep up" with the changes in

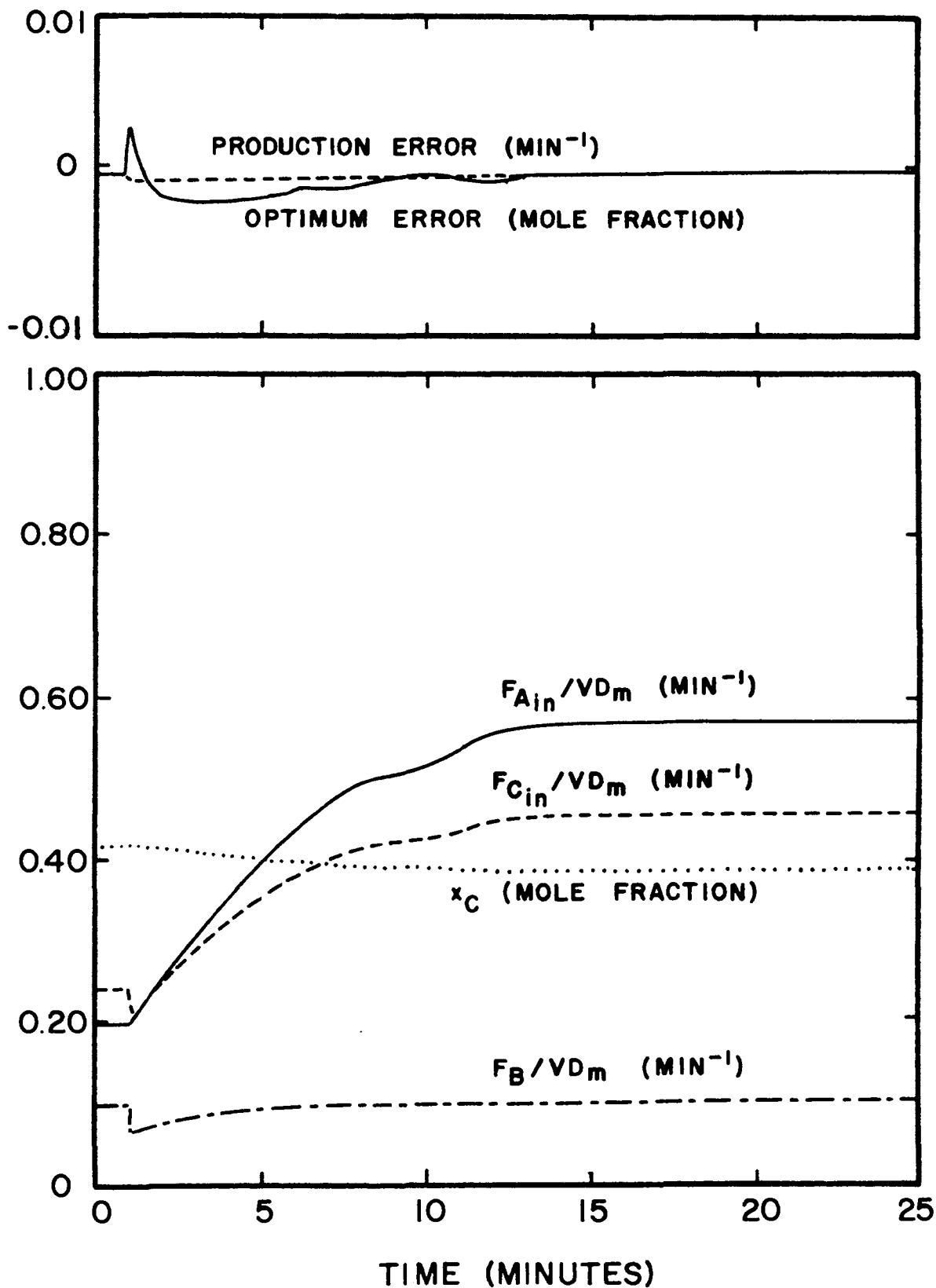


Figure 14. Simulation of a Step Down in the Reaction Rate Constant, Continuous Analysis, $k_o = 25.0$, $T_o = 0.1$ min., $k_p = 10.0$, $T_p = 0.1$ min.

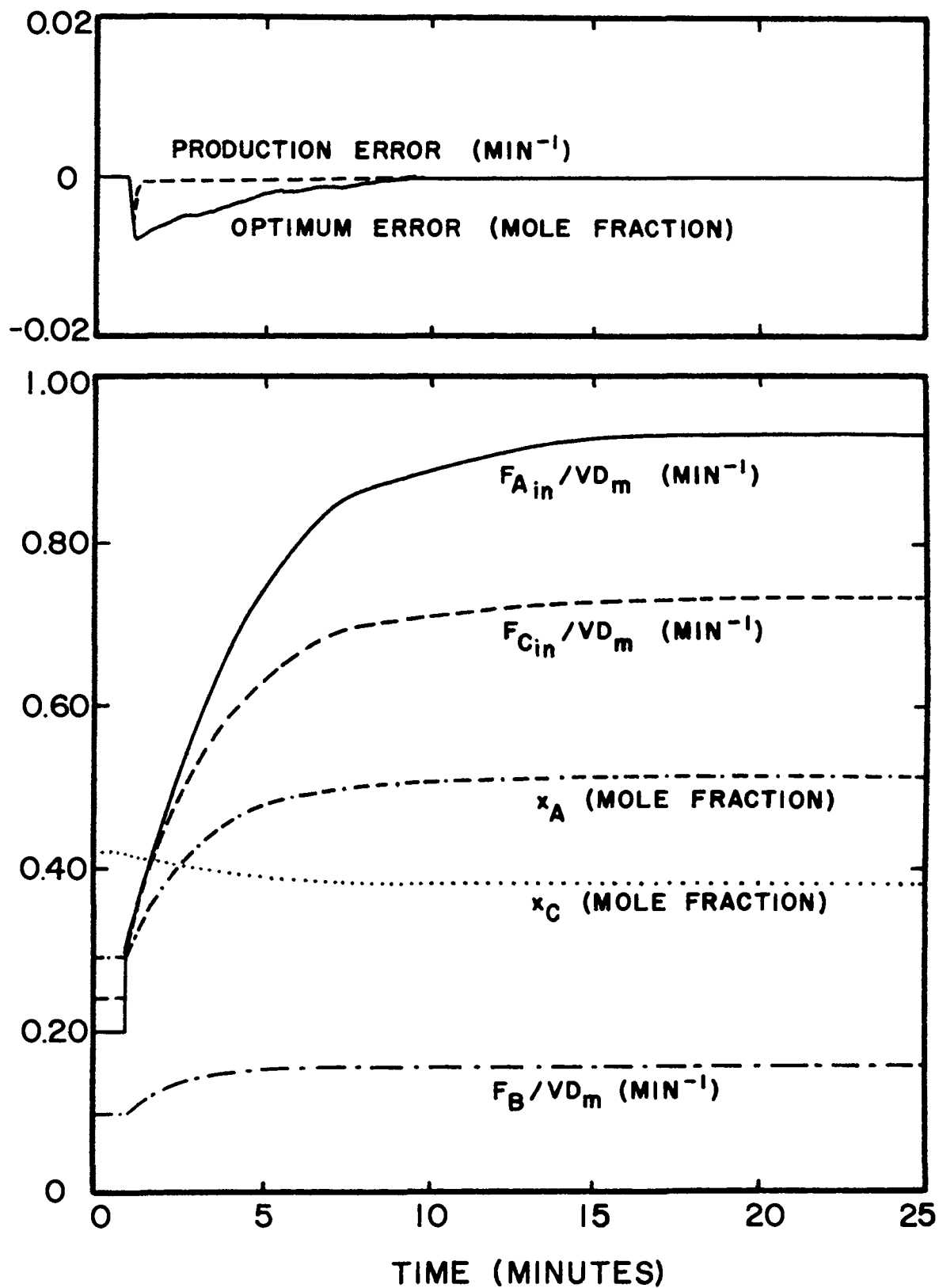


Figure 15. Simulation of a Step Up in the Production Set Point, Continuous Analysis, $k_o = 25.0$, $T_o = 0.1$ min., $k_p = 10.0$, $T_p = 0.1$ min.

F_{Ain}/VD_m created by the production controller. This requirement is demonstrated in figure 16, page 66, in which the optimizing integral time constant, T_o , is raised to 1.0 minute. The flow of reactant A is increased at a higher rate because of the lag in the concentration of reactant C and subsequent lower production. When the concentration of reactant C does level off because of the action of the optimizing controller, the flow of reactant A is higher than necessary, the production goes past the maximum and the system becomes unstable.

The response of the system to pulse type upsets was also investigated. Figure 17, page 67, is the response of the system to a pulse in the flow rate of reactant A. For this simulation run the optimizing proportional gain, k_o , was $2.5 \text{ (minute}^{-1} \text{ C)}/(\text{mole fraction C})$ and the integral time constant was 0.1 minutes. The production control loop was open.

4. Sampled Analysis: The equations describing the controller action for sampled analysis are presented in Appendix B, pages 124 and 128.

The first simulation run based on sampled analysis, figure 18, is the response of the system to the upset presented in figure 12, page 60, of the continuous analysis section, i.e., a step up in the feed of reactant A, F_{Ain}/VD_m from 0.2 to 0.8 minutes^{-1} . Figure 18 is the response for an optimizing loop gain of $0.25 \text{ (minute}^{-1} \text{ C)}/(\text{mole fraction C})$. The response is well behaved and appears to be just

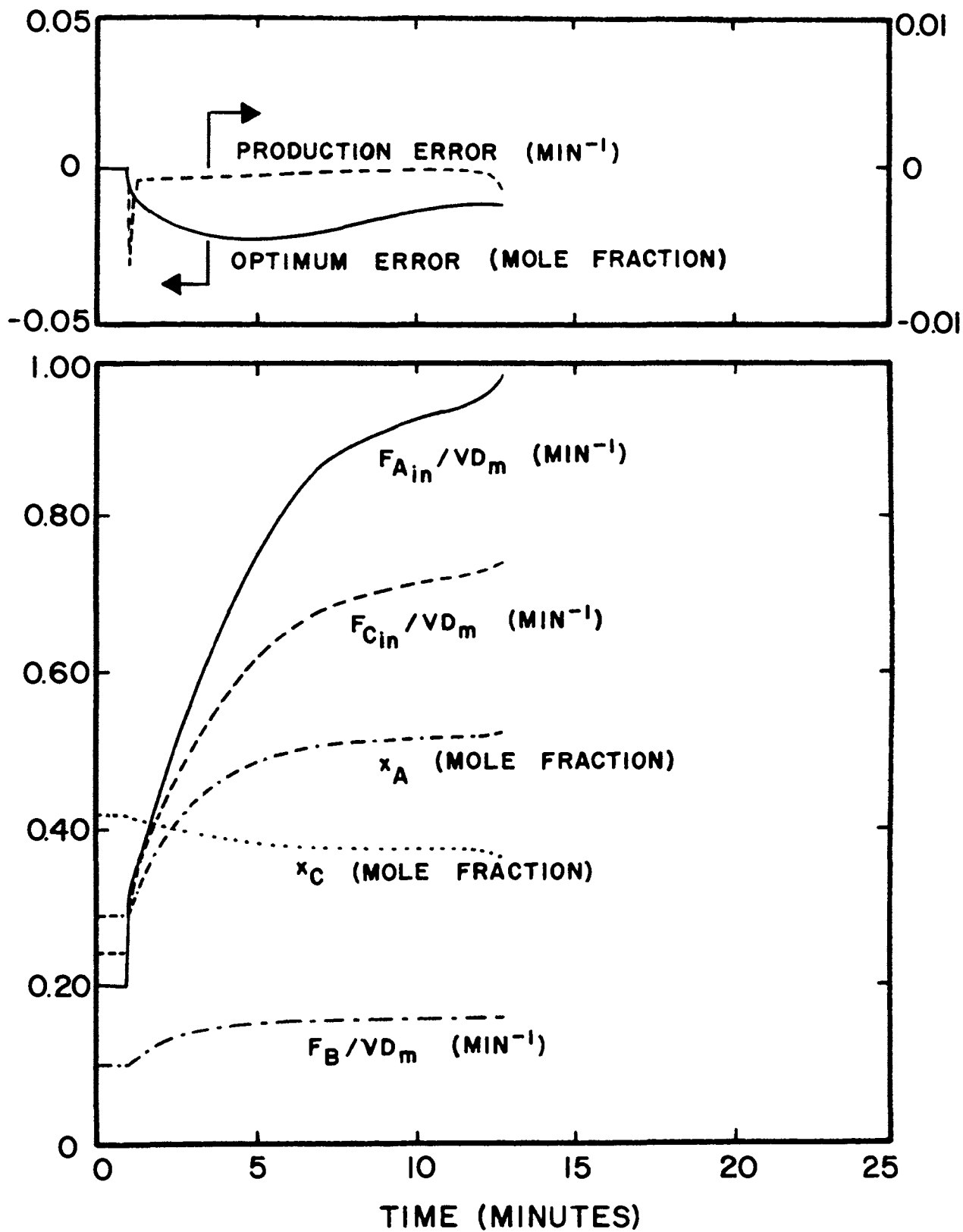


Figure 16. Simulation of a Step Up in the Production Set Point, Continuous Analysis, $k_o = 25.0$, $T_o = 1.0$ min., $k_p = 10.0$, $T_p = 0.1$ min.

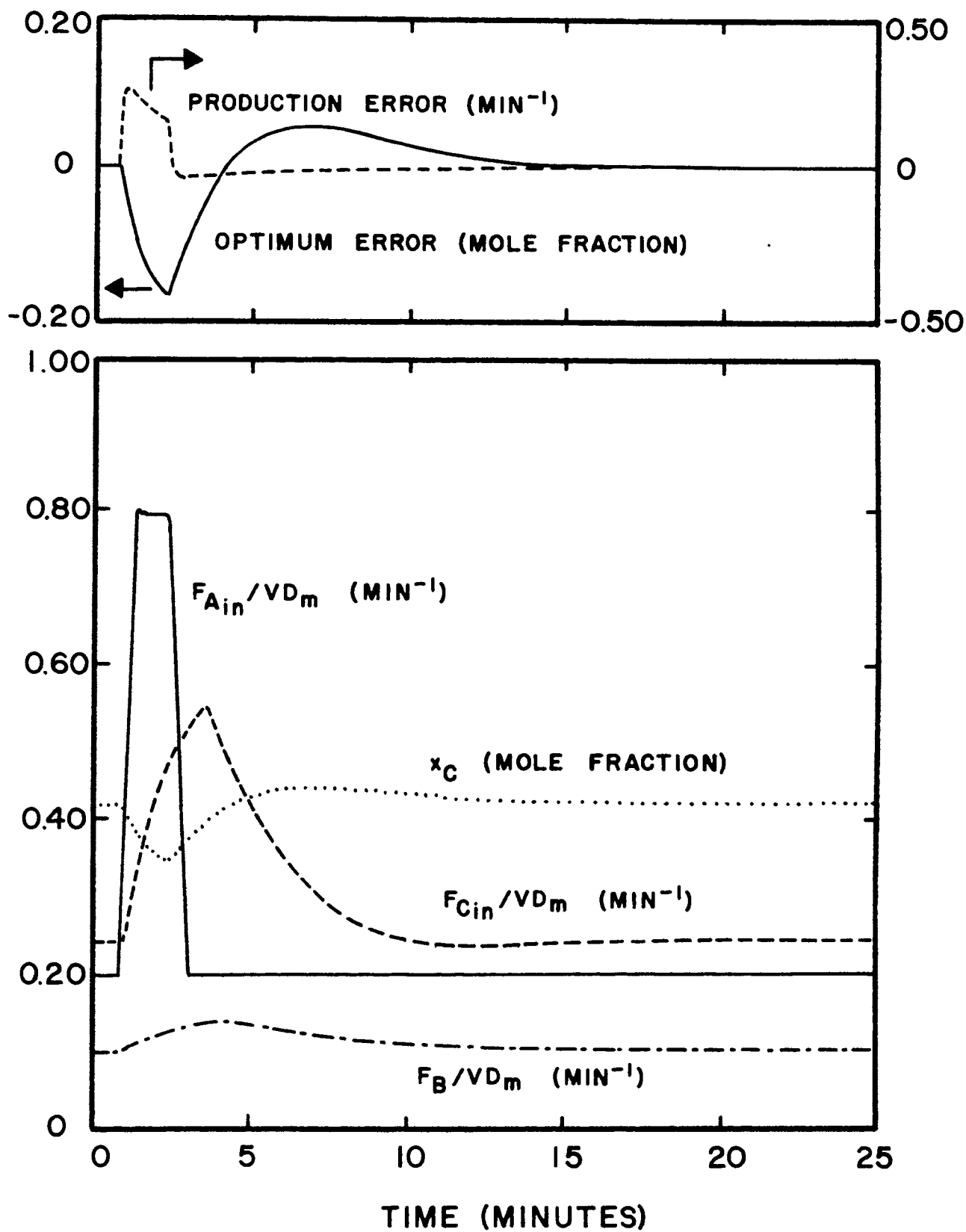


Figure 17. Simulation of a Pulse in the Feed of Reactant A, Continuous Analysis, $k_0 = 2.5$, $T_0 = 0.1$ min.

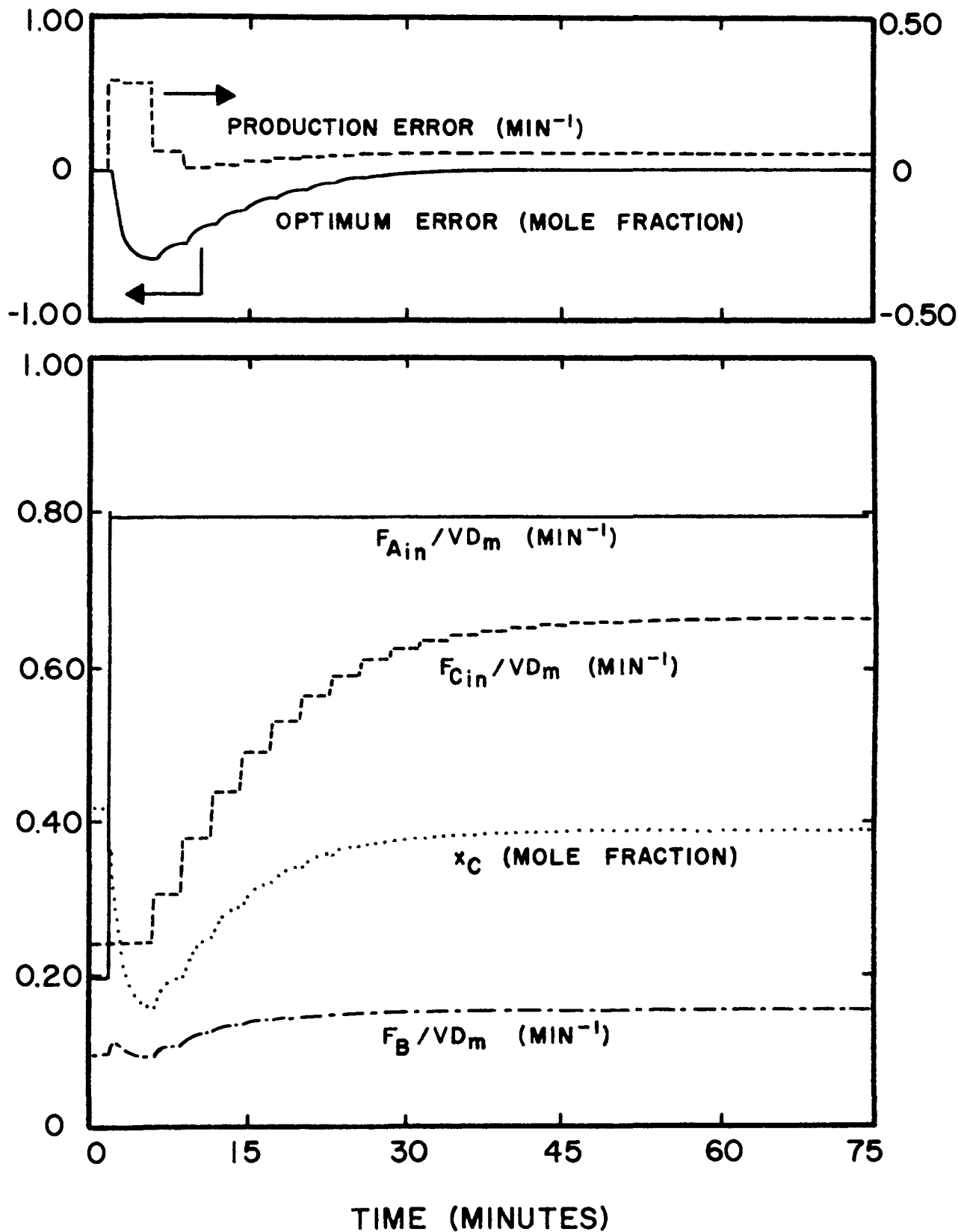


Figure 18. Simulation of a Step Up in the Feed of Reactant A, Sampled Analysis, $K_0 = 0.25$.

over-damped.

Figure 19, page 70, is the response of the system to the same upset for an optimizing loop gain of $0.5 \text{ (minute}^{-1} \text{ C)}/\text{(mole fraction C)}$. This gain creates a slightly under-damped response which settles quickly.

Figure 20, page 71, is the response of the system to the same upset for an optimizing loop gain of $1.25 \text{ (minute}^{-1} \text{ C)}/\text{(mole fraction C)}$. This gain creates an under-damped response not at all acceptable.

Figure 21, page 72, is the response of the system to the upset presented in figure 13, page 61, of the continuous analysis section, i.e., a step down in the reaction rate constant from a value of k/D_m of 0.8 to 0.5 $\text{(mole fraction}^2, \text{ minute)}^{-1}$. As in the continuous analysis the production controller maintains production at the rate prior to the step. The optimizing loop gain employed for figure 21 is $0.5 \text{ (minutes}^{-1} \text{ C)}/\text{(mole fraction C)}$ and the production loop gain employed was $2.0 \text{ (minute}^{-1} \text{ A)}/\text{(minute}^{-1} \text{ B)}$. The error used by the production controller recorded in the upper plot is actually the magnitude of the spike.

It was shown in figure 19 that an optimizing loop gain of 0.5 generated a slightly under-damped response for a step up in the flow of reactant A. As discussed in the continuous simulation section, the time constant of the reactor is much smaller after this step has occurred, 0.76 minutes for F_{Ain}/VD_m of 0.8 minutes^{-1} and 2.9 minutes for

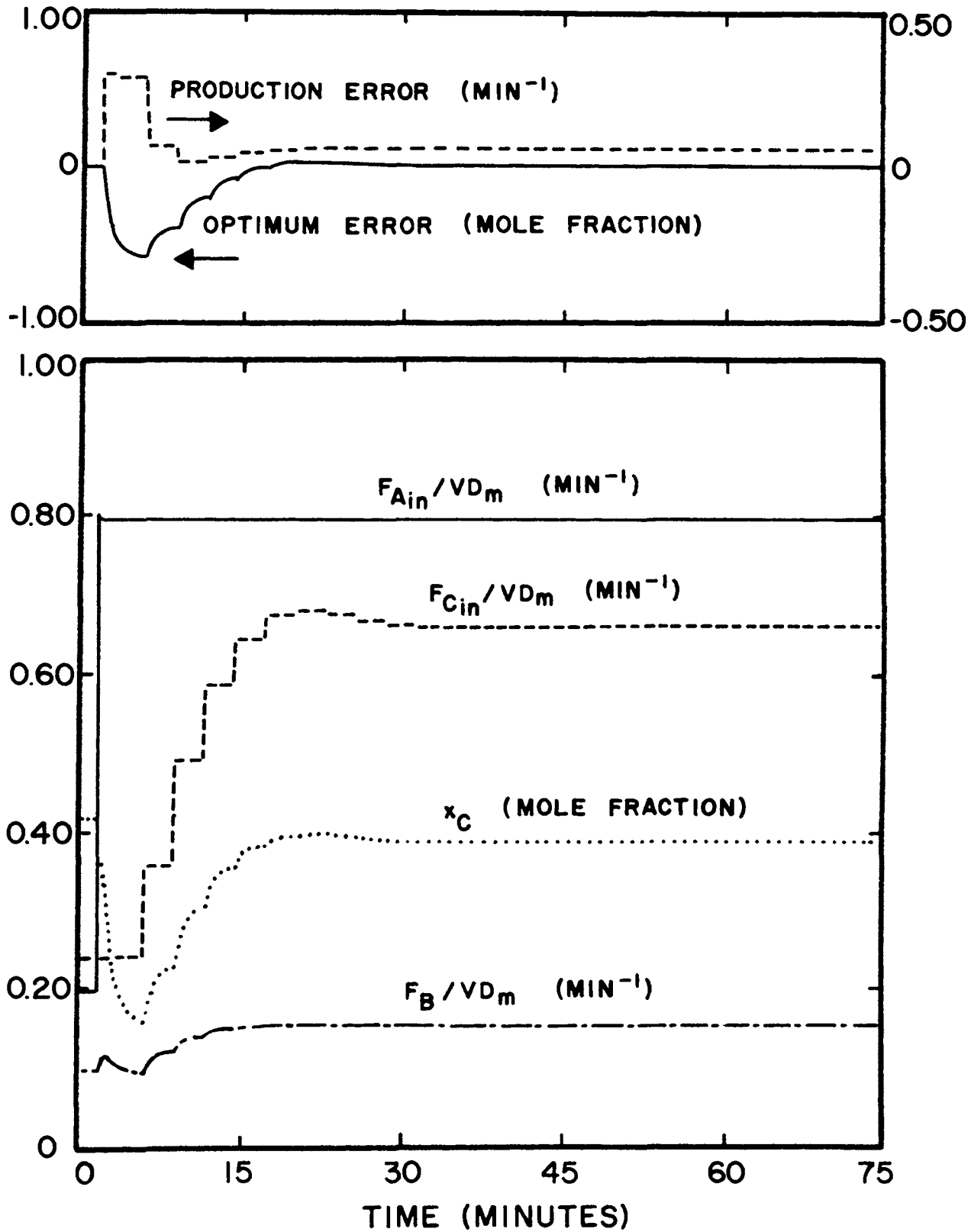


Figure 19. Simulation of a Step Up in the Feed of Reactant A, Sampled Analysis, $K_0 = 0.5$.

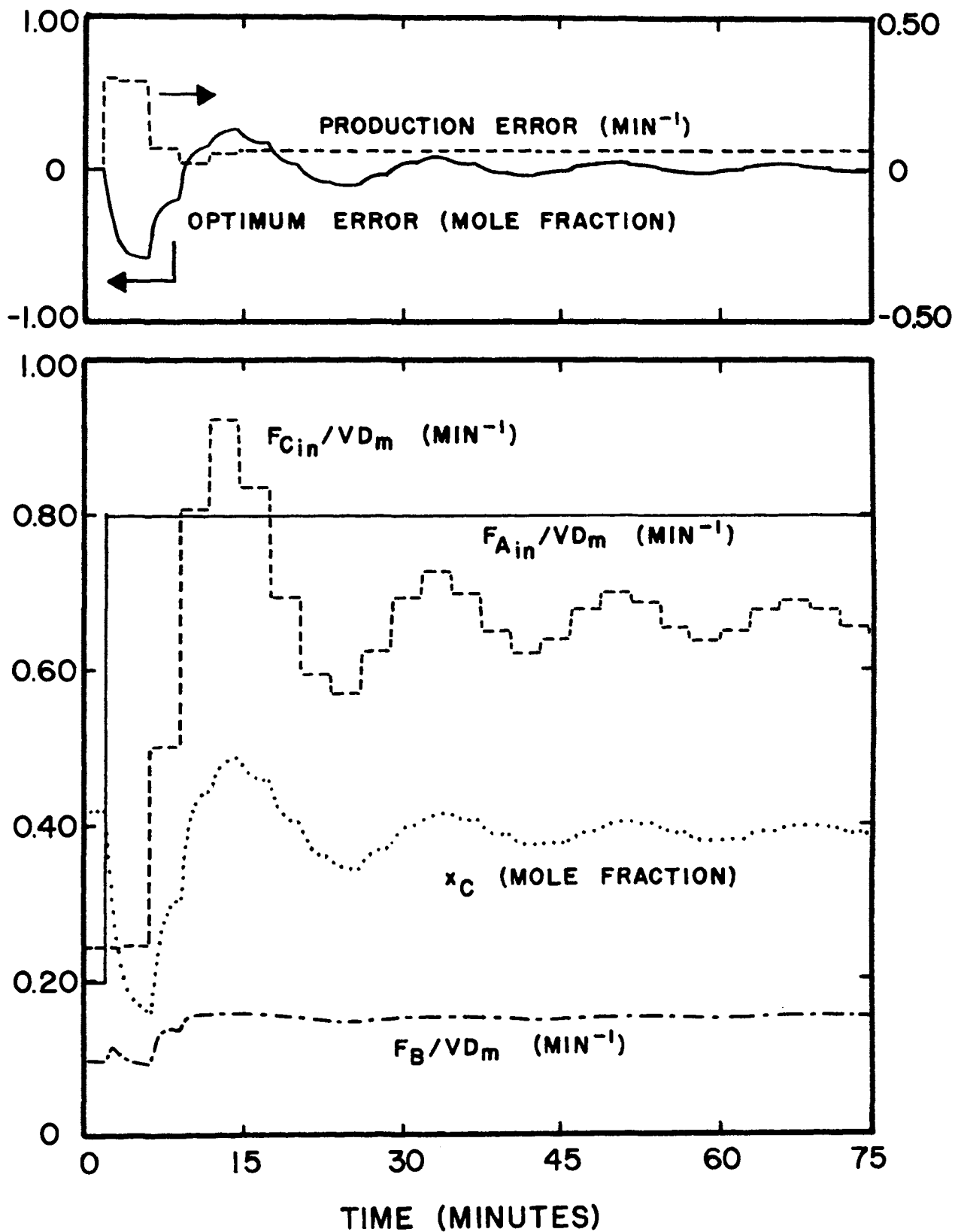


Figure 20. Simulation of a Step Up in the Feed of Reactant A, Sampled Analysis, $K_0 = 1.25$.

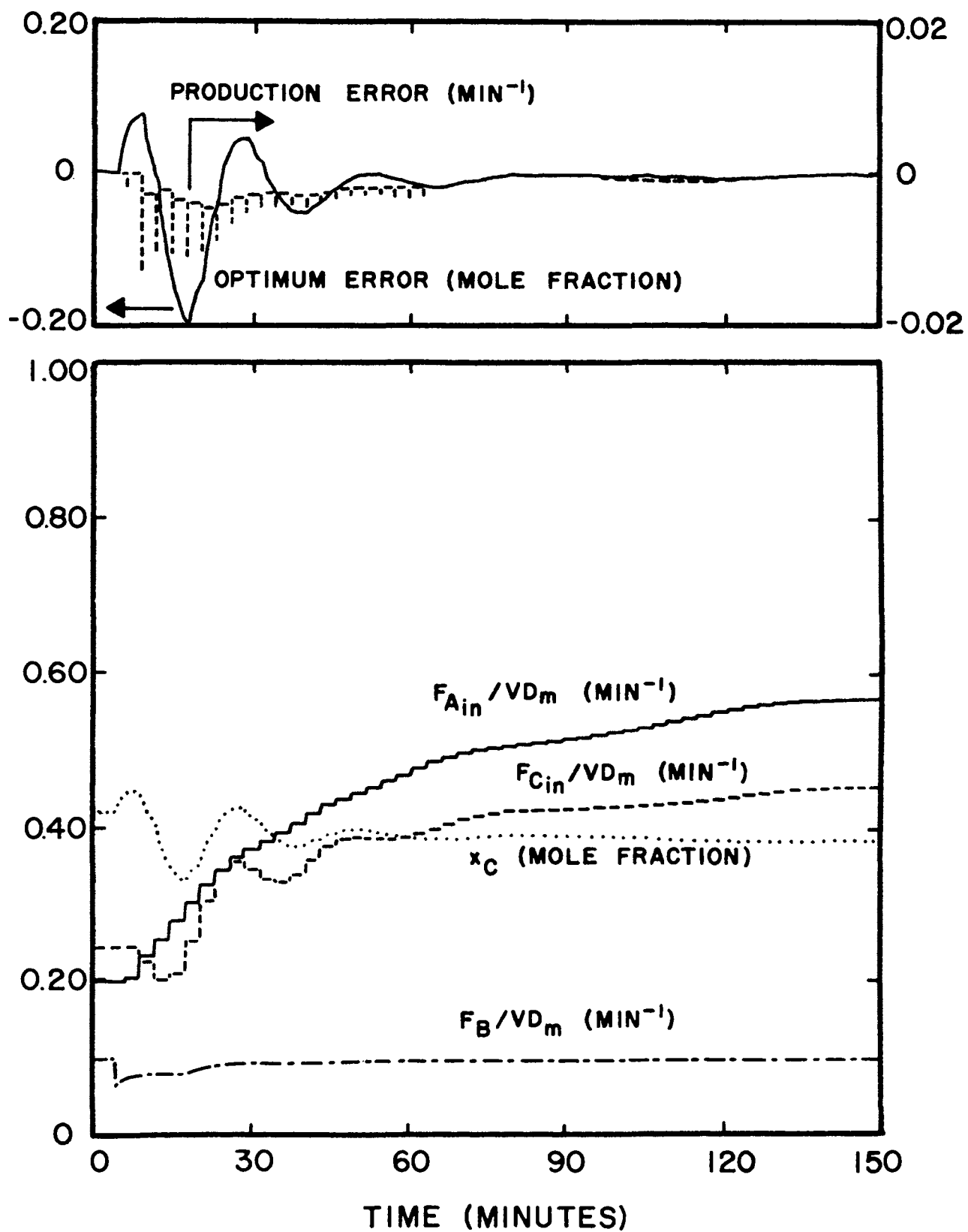


Figure 21. Simulation of a Step Down in the Reaction Rate Constant, Sampled Analysis, $K_o = 0.5$, $K_p = 2.0$.

F_{Ain}/VD_m of 0.2 minutes^{-1} . Figure 22 is the response of the system to a pulse in the flow of reactant A to 0.8 minutes^{-1} with an optimizing loop gain of $0.5 \text{ (minute}^{-1} \text{ C)}/\text{(mole fraction C)}$. The response is highly oscillatory for this longer time constant. If the flow rate is low a lower optimizing loop gain should be employed. Figure 23, page 75, is the response of the same pulse in the flow of reactant A with an optimizing loop gain of $0.25 \text{ (minute}^{-1} \text{ C)}/\text{(mole fraction C)}$. This gain generates a response which is just slightly under-damped.

The response of the system to a step change in the production set point, F_B/VD_m , is given in figure 24, page 76, for an optimizing loop gain of $0.5 \text{ (minute}^{-1} \text{ C)}/\text{(mole fraction C)}$ and a production loop gain of $0.8 \text{ (minute}^{-1} \text{ A)}/\text{(minute}^{-1} \text{ B)}$. Although this response is adequate it is very slow, after 50 samples the production controller has not settled at all. The response of the system to the step up in production set point with a production loop gain of $2.0 \text{ (minute}^{-1} \text{ A)}/\text{(minute}^{-1} \text{ B)}$ is given in figure 25, page 77. This response is much faster.

If it is desired to use a lower optimizing loop gain because of the oscillatory problem exhibited in figure 22 the same difficulty experienced in the continuous analysis section with positive feedback, page 65, may be encountered. If a lower optimizing loop gain is utilized the optimizing loop may not be able to keep up with the changes in the flow

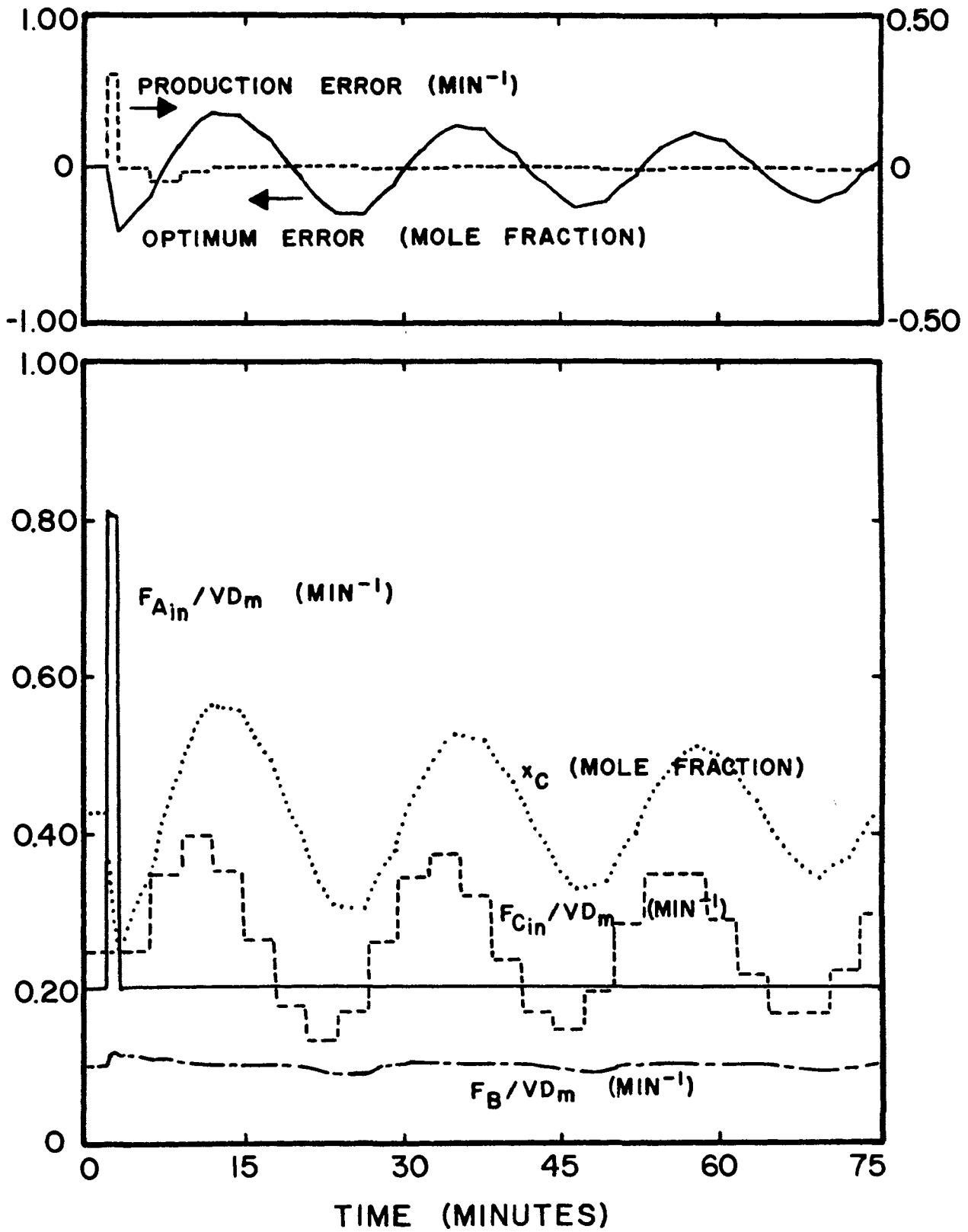


Figure 22. Simulation of a Pulse in the Feed of Reactant A, Sampled Analysis, $K_o = 0.5$.

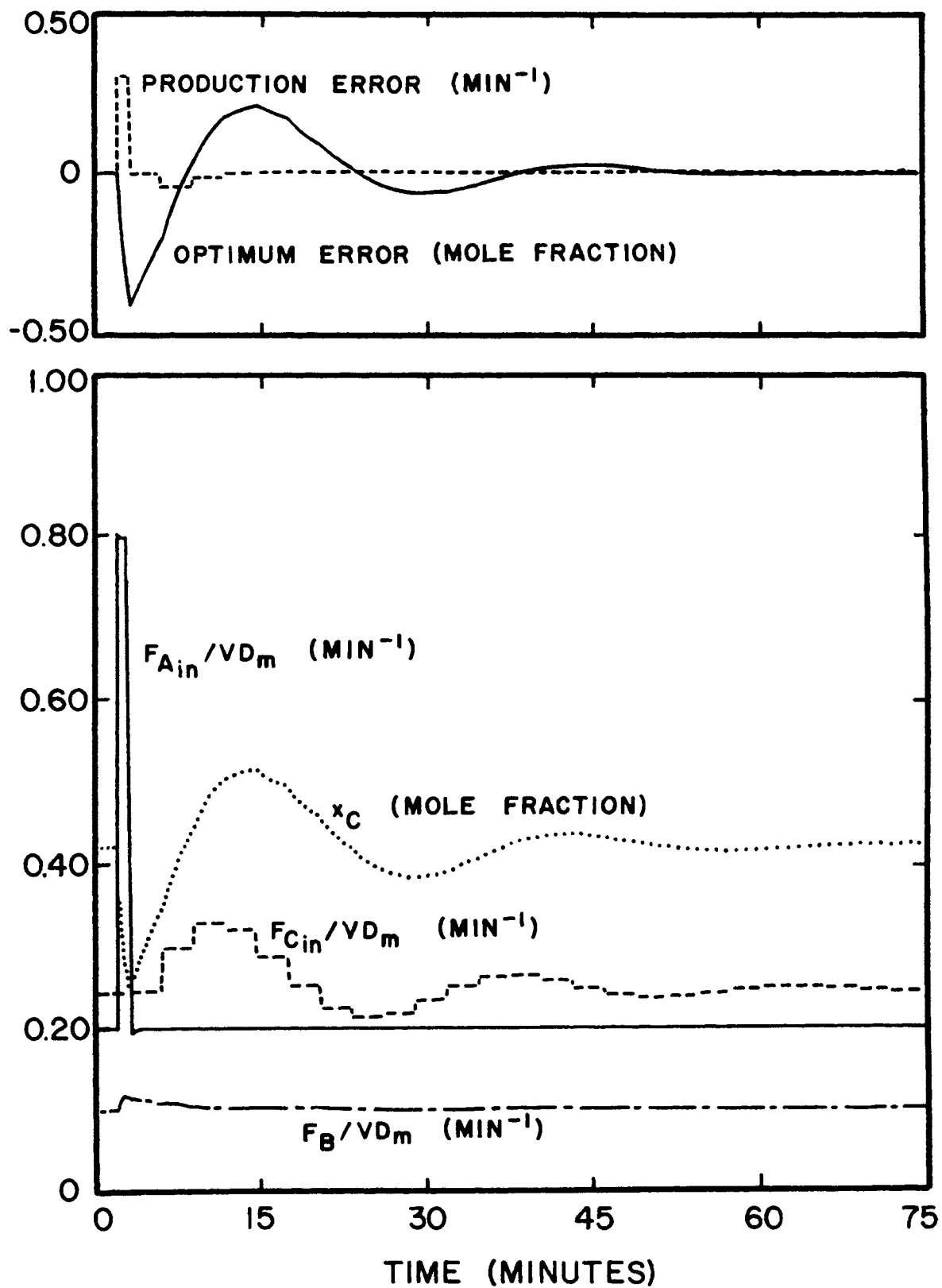


Figure 23. Simulation of a Pulse in the Feed of Reactant A, Sampled Analysis, $K_0 = 0.25$.

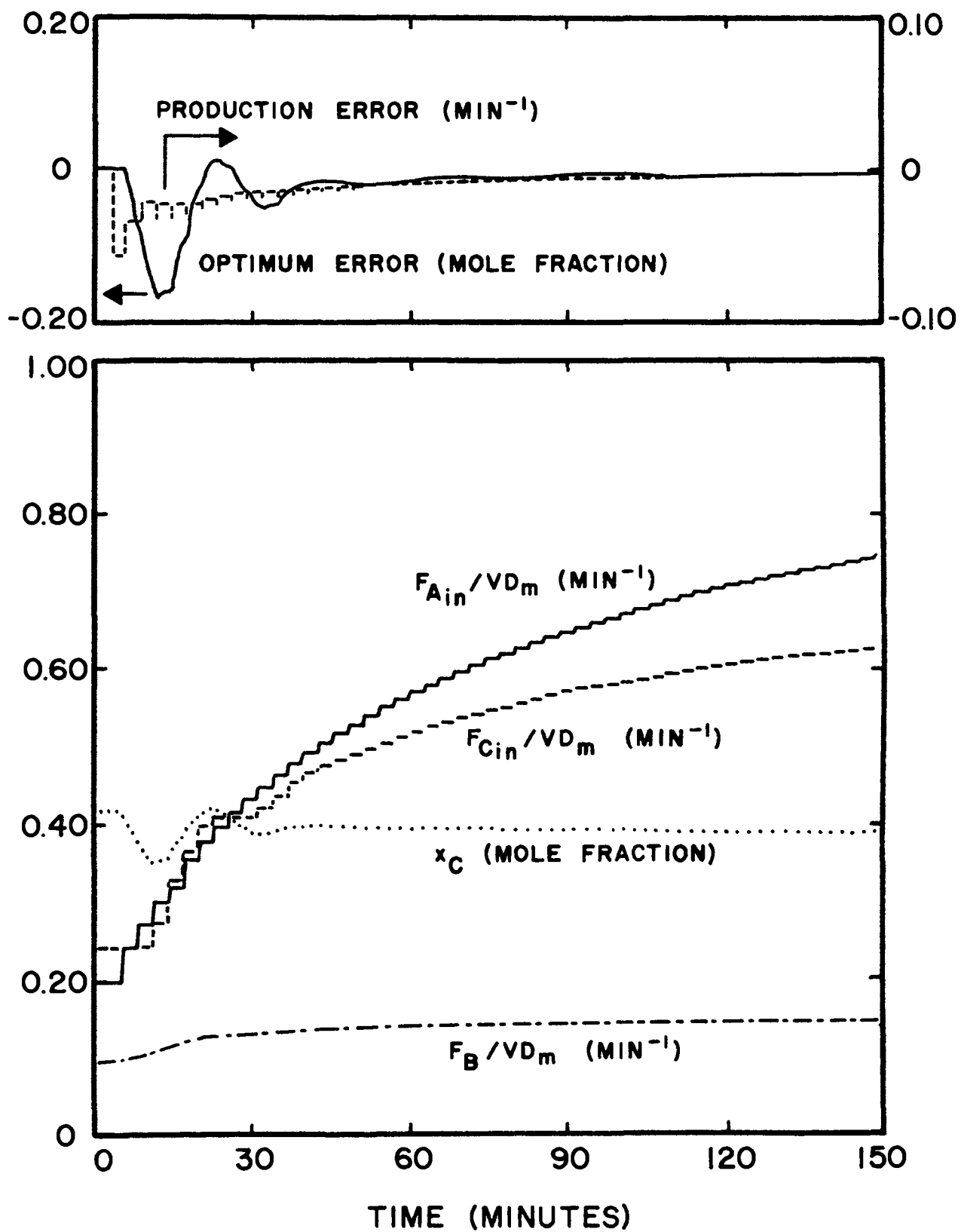


Figure 24. Simulation of a Step Up in the Production Set Point, Sampled Analysis, $K_o = 0.5$, $K_p = 0.8$.

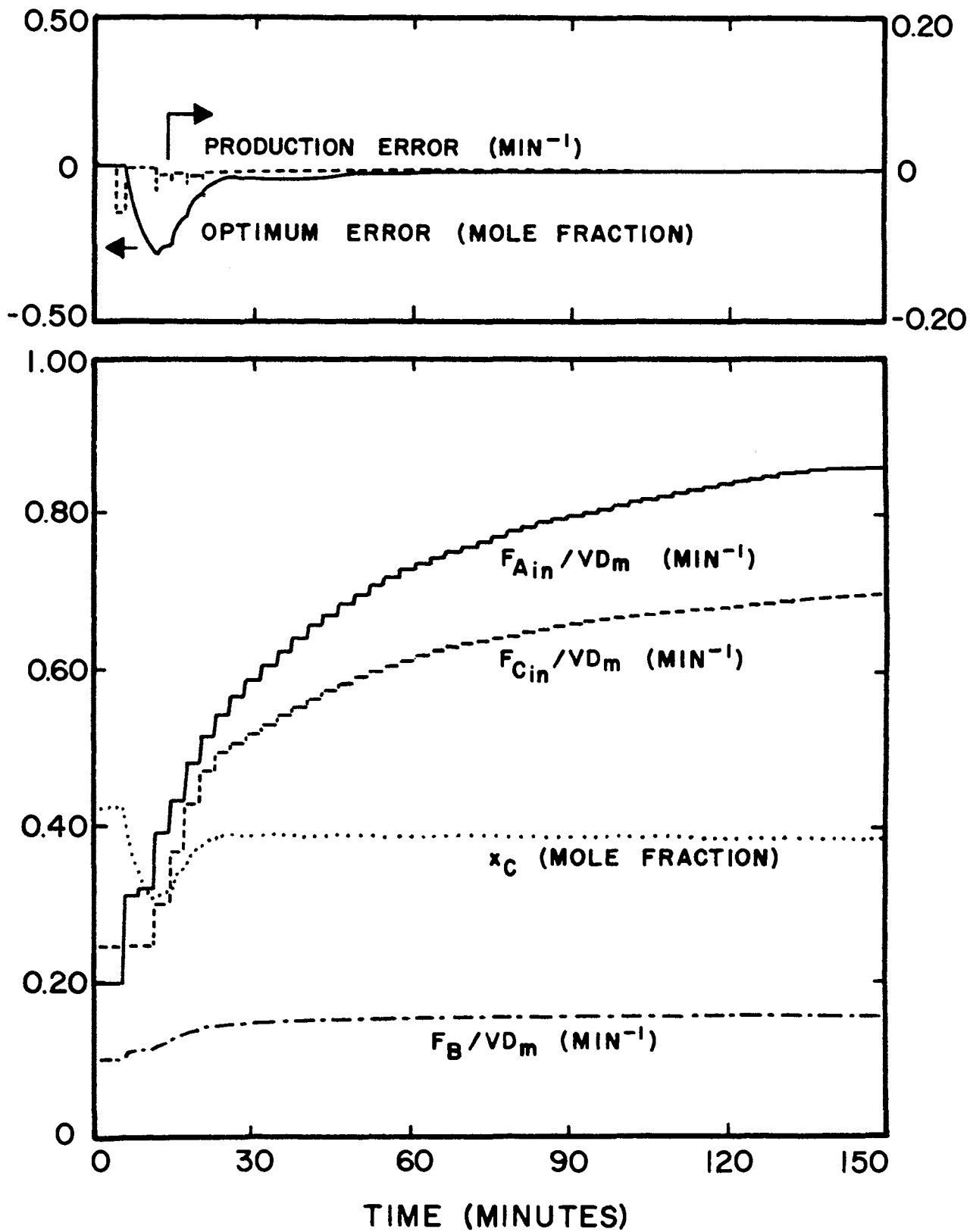


Figure 25. Simulation of a Step Up in the Production Set Point, Sampled Analysis, $K_o = 0.5$, $K_p = 2.0$.

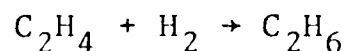
of reactant A during step changes approaching the maximum production and the system could move past the maximum creating positive feedback. This difficulty is demonstrated in figure 26, page 79, which is the response of the system to the same step change in the production set point with an optimizing loop gain of $0.25 \text{ (minute}^{-1} \text{ C)}/\text{(mole fraction C)}$.

B. Experimental Operation

1. Experimental Purpose: The purpose of conducting an experimental test of the proposed optimizing scheme is to check the validity of the optimum prediction method and to demonstrate that it can be implemented with commercially available equipment.

The construction and operation of the experimental reactor system is presented in Appendix C, page 135.

2. Reaction: The reaction chosen for this experimental test was the hydrogenation of ethylene to ethane on a nickel catalyst. This reaction is not economically sound but was chosen because of its convenient characteristics. It has a molecularity of two, the stoichiometry being as follows:



The reaction has been studied by many investigators and substantial kinetic data are available. The reaction proceeds without any side reactions and the hydrogenation does not occur to a measurable degree in the absence of a catalyst.

The reaction is unaffected by the presence of ethane (26, 27) which satisfies the assumption of essential

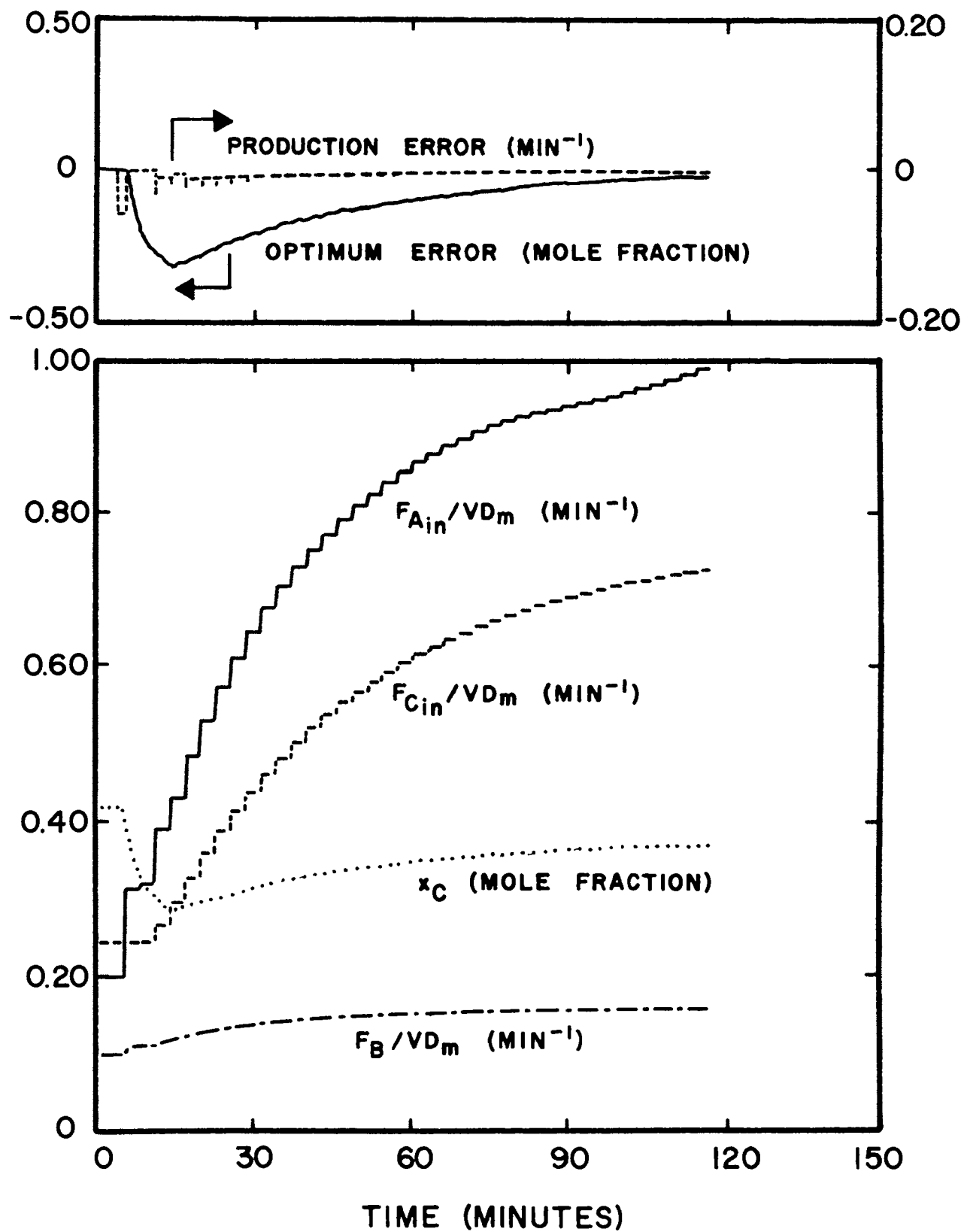


Figure 26. Simulation of a Step Up in the Production Set Point, Sampled Analysis, $K_o = 0.25$, $K_p = 2.0$.

irreversibility, page 19. The reaction mechanism at temperatures above 150° C is generally correlated as first order with respect to each reactant concentration (28). The optimizing scheme for this correlation was developed in Chapter IV, used in the simulation and retained for the experimental investigation.

Since a gas chromatograph is used to accomplish the chemical analysis necessary and since on-line sampling is to be employed, another major advantage of this reaction is the absence of any condensables at ambient temperature in the product stream. This allows convenient use of a gas sampling valve.

3. Reaction Parameters: The reactor was always operated at $150 \pm 1^\circ \text{C}$ and 168 ± 2 inches water gauge. The nickel catalyst was in the form of eight 1/8 inch by 1/8 inch cylindrical pellets. This catalyst was in a prereduced and stabilized form, type G-65RS, supplied by the Chemtron Corporation.

The cost ratio, $C_{\text{C}_2\text{H}_6} / C_{\text{C}_2\text{H}_4}$, used in the experimental test is 20.0. The optimum relationship for this cost ratio is presented in figure 5B, page 118.

The optimizing loop gain used throughout the experimental section is $50.0 (\% \text{ maximum } F_{\text{C}_2\text{H}_4 \text{ in}}) / (\text{mole fraction } \text{C}_2\text{H}_4)$. The units of the gain used in the simulation section are $(\text{minute}^{-1} \text{ C}) / (\text{mole fraction C})$. The reciprocal time, $\text{minute}^{-1} \text{ C}$, refers to the time constant of the system with respect to ethylene feed only. In order to compare the two

gains the volume of the reactor and the maximum flow rate of ethylene must be considered. The maximum flow rate of ethylene is 13.2 (cc)/(second) and the reactor volume is approximately 1400 cc. The optimizing loop gain in terms of the units used in the simulation is calculated to be $0.282 \text{ (minute}^{-1} \text{ C}_2\text{H}_4\text{)}/\text{(mole fraction C}_2\text{H}_4\text{)}$.

The best optimizing loop gains for the flow rates used in the simulation were found between 0.25 and 0.50 ($\text{minute}^{-1} \text{ C)}/\text{(mole fraction C)}$). The best gain is of course dependent on the time constant of the reactor.

The production loop gain used throughout the experimental section is $2.0 \text{ (% maximum } F_{\text{H}_2\text{in}}\text{)}/\text{(production in % maximum } F_{\text{H}_2\text{in}}\text{)}$. Since both the numerator and denominator are expressed in the same units, percent hydrogen feed, there is no change in the magnitude of the gain when the units are changed to those used in the simulation, ($\text{minute}^{-1} \text{ A)}/\text{(minute}^{-1} \text{ B)}$). This gain of 2.0 is the same production loop gain employed widely in the simulation section.

4. Optimum Prediction Accuracy: One of the goals of operating an experimental system in conjunction with the optimizing scheme is to determine the deviation between the predicted optimum and the true optimum. In order to accomplish this goal the optimizing loop was closed and the feed of hydrogen held constant. The system was allowed to settle at the indicated optimum and then various offsets were intentionally introduced to the optimizing controller. The

actual income was then calculated at each point.

Figure 27 is a plot of the performance criterion divided by the cost of ethylene and the hydrogen feed for various offsets from the indicated optimum mole fraction of ethylene. The feed rate of hydrogen is held constant at 11.3 (cc)/(second) and the temperature controller set point placed at 150^o C. The full span of the y-axis of figure 27 is only about 3 percent of the full range of this income index. The possible range of the calculated income index indicated at each point is based on analysis precision of ± 0.1 percent of the composition.

From figure 27 it can be concluded that the true optimum concentration of ethylene is at least within ± 0.02 mole fraction of the indicated optimum. When the optimizing loop is closed at steady state, the greatest loss in income from the maximum possible is less than 1.0 percent of the maximum income.

5. Dynamic Tests: Dynamic tests of the system are made to investigate the response of the system to step type upsets in the reactor parameter and the production set point.

Figure 28, page 84, is a plot of the composition response to a step up in the feed of hydrogen from 3.84 (cc)/(second) to 15.4 (cc)/(second). Figure 29, page 85, is the flow rate response from the same experimental run.

The reactor time constant prior to the step is calculated to be 3.76 minutes. The reactor time constant after

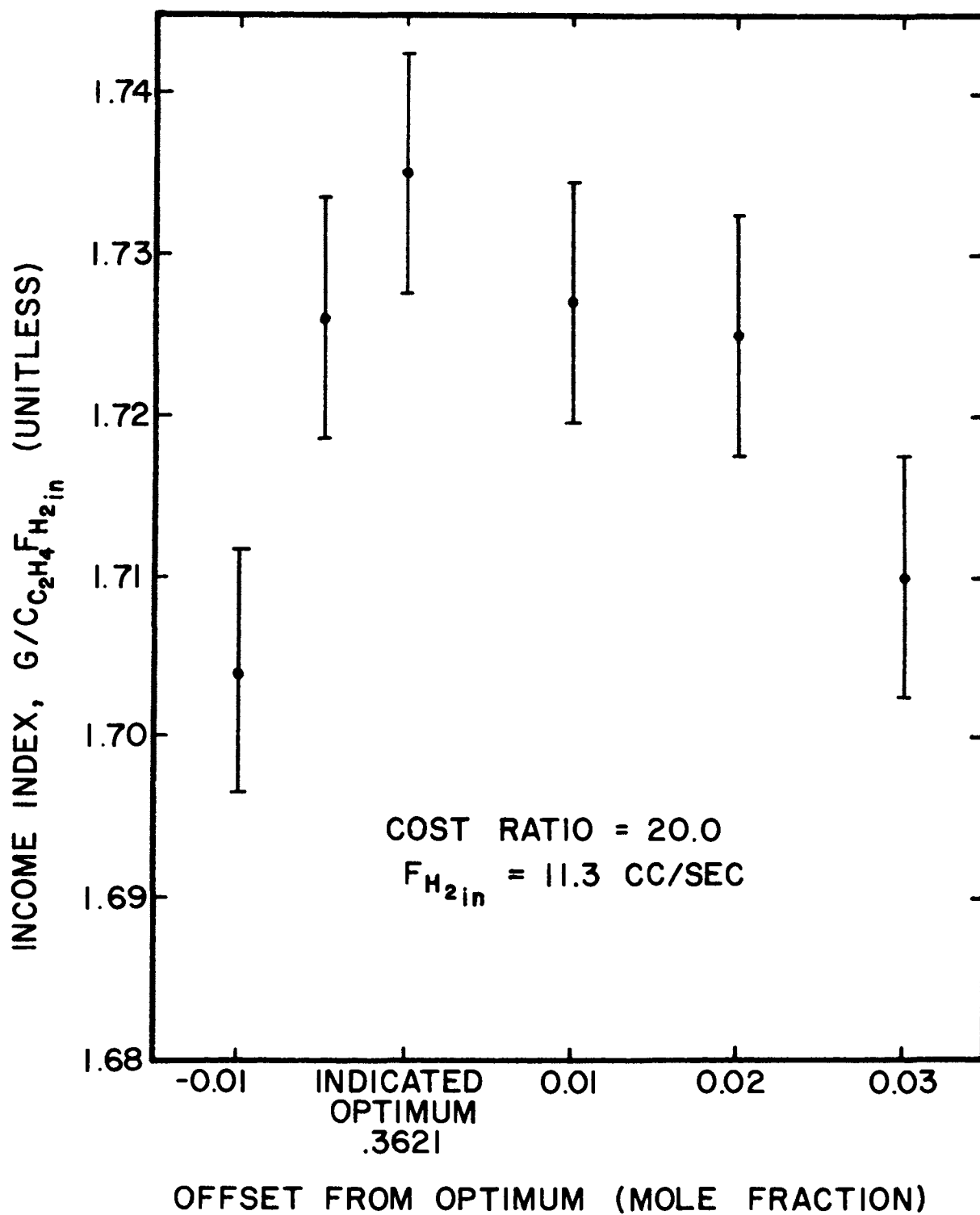


Figure 27. Income Index in the Neighborhood of the Indicated Optimum Concentration for the Experimental Pilot Scale Reactor.

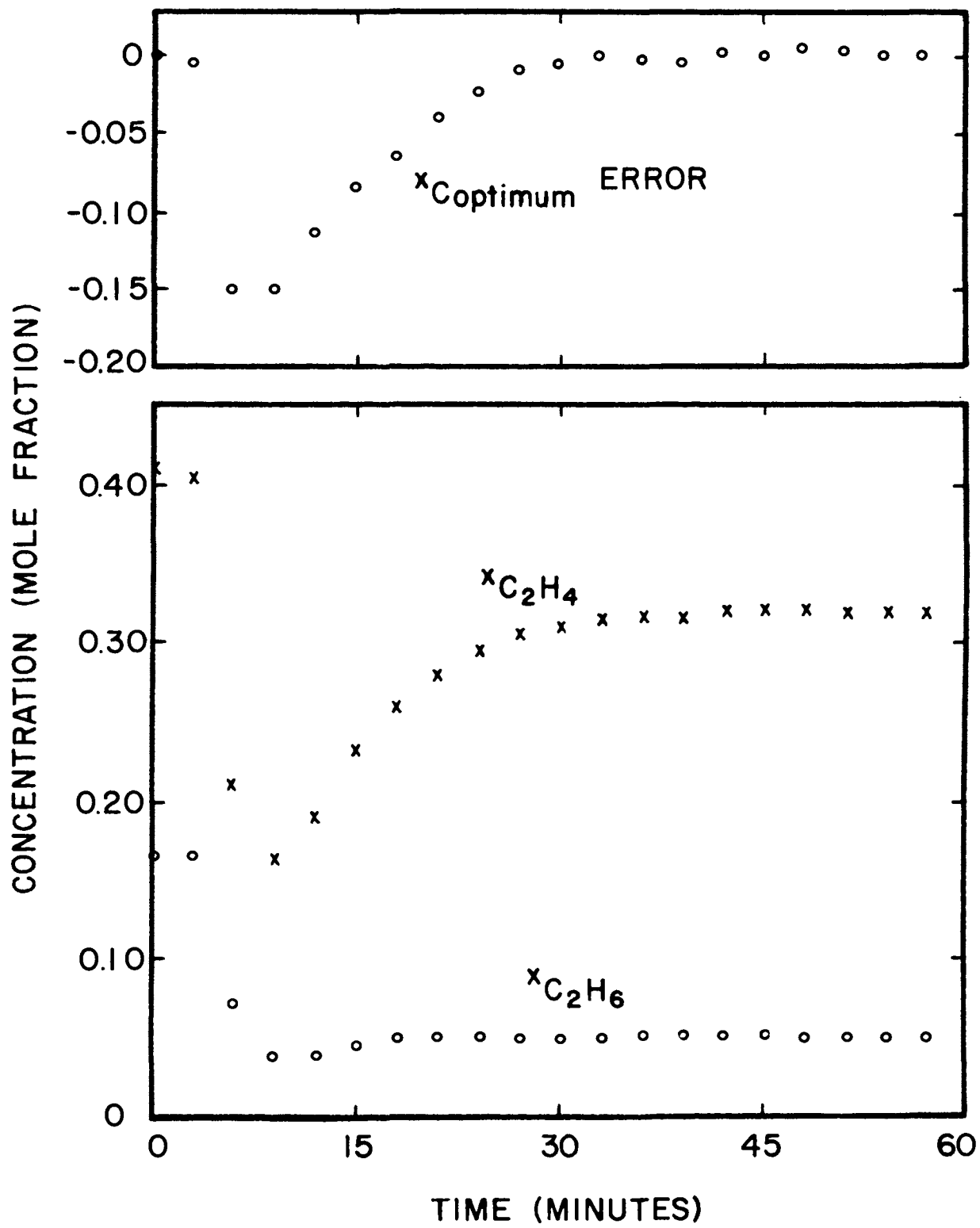


Figure 28. Composition Response to a Step Up in the Feed of Hydrogen.

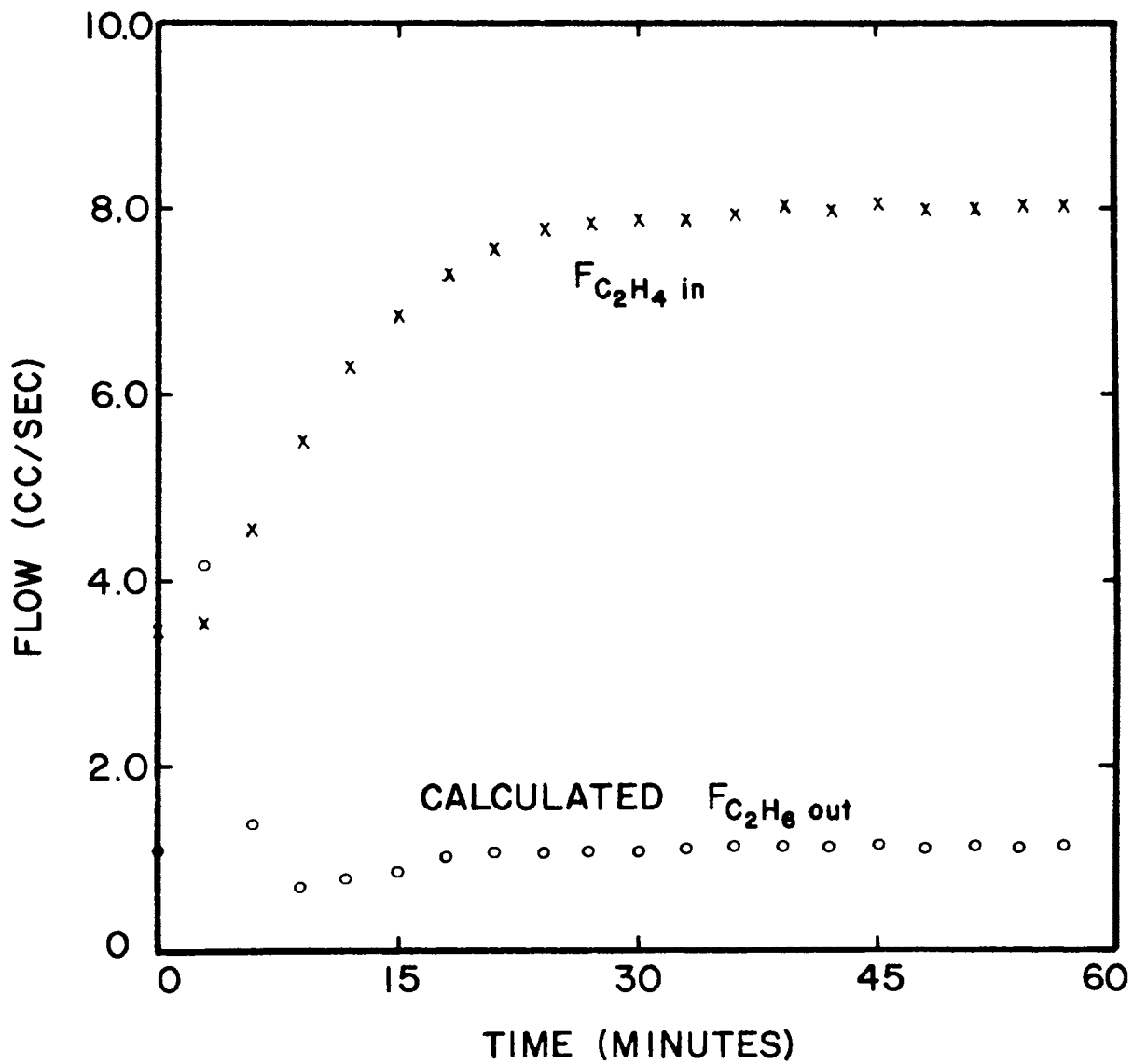


Figure 29. Flow Rate Response to a Step Up in the Feed of Hydrogen.

settling is found to be 1.05 minutes. This response can be compared to figure 18, page 68, in which a simulation is presented of a step up in the feed rate of reactant A, hydrogen in this case, of approximately the same magnitude with a similar optimizing loop gain, $0.25 \text{ (minute}^{-1} \text{ C) / (mole fraction C)}$.

Figure 30 is the composition response to a step down in the feed rate of hydrogen from 15.4 (cc)/(second) to 3.84 (cc)/(second) with the optimizing loop gain unchanged. Figure 31, page 88, is the flow rate response of the same experimental run. The reactor time constant in this run becomes much longer after the step and the response becomes highly oscillatory. A lower optimizing loop gain would probably be more appropriate for this low flow rate but would not be acceptable for the higher flow rates.

Figure 32, page 89, is the composition response to a step down in the production set point from 1.28 (cc)/(second) to 1.07 (cc)/(second) ethane. The sensitivity of the upper plot of figure 32 which shows the optimizing and production errors is much higher than the previous experimental plots. Figure 33, page 90, is a recording of the flow rate responses of the same experimental run. For the optimizing loop to function a change in the flow rate of hydrogen must be detected through analysis. The lag in the optimizing loop can be detected in error and flow rate plots of figures 32 and 33.

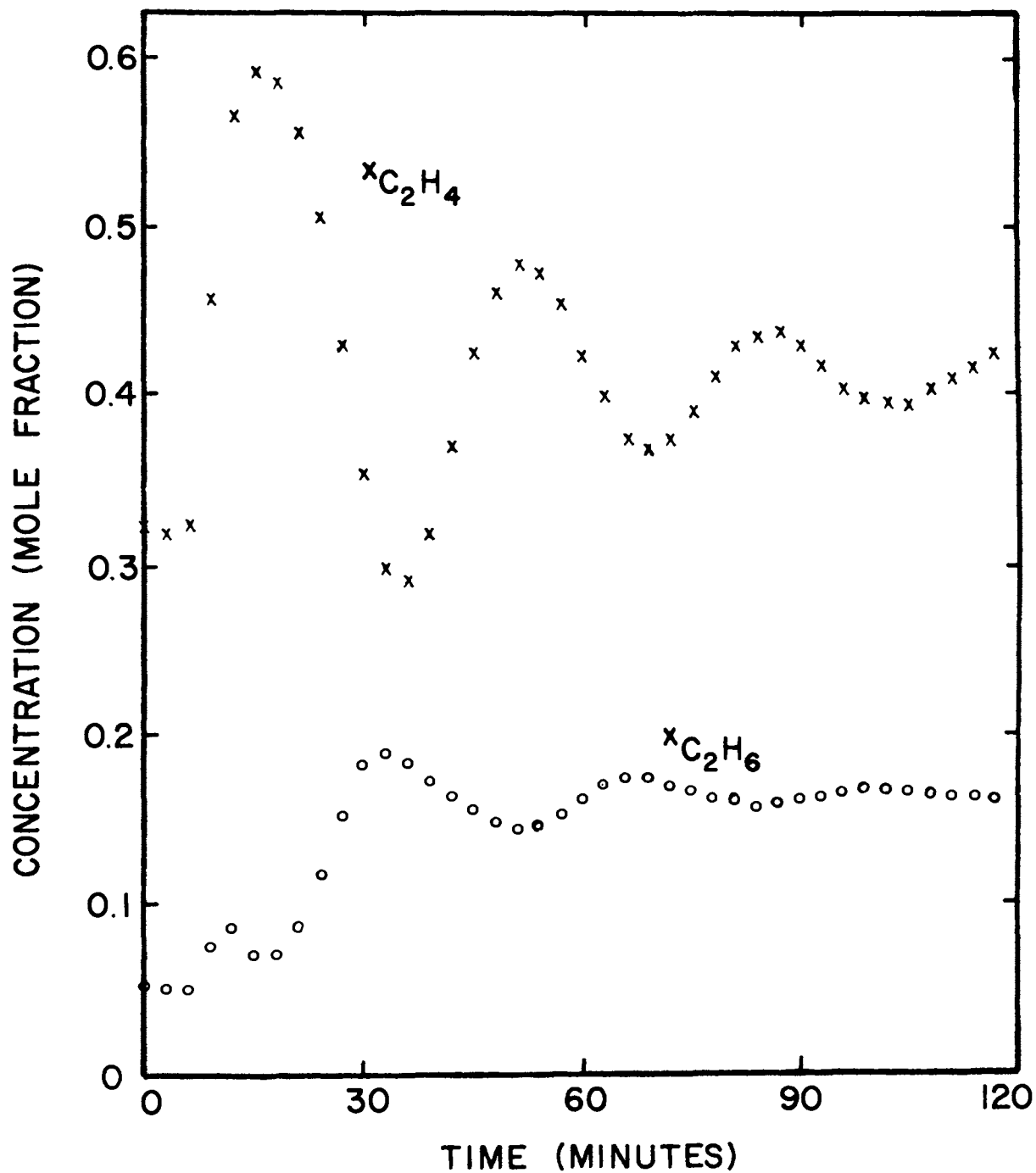


Figure 30. Composition Response to a Step Down in the Feed of Hydrogen.

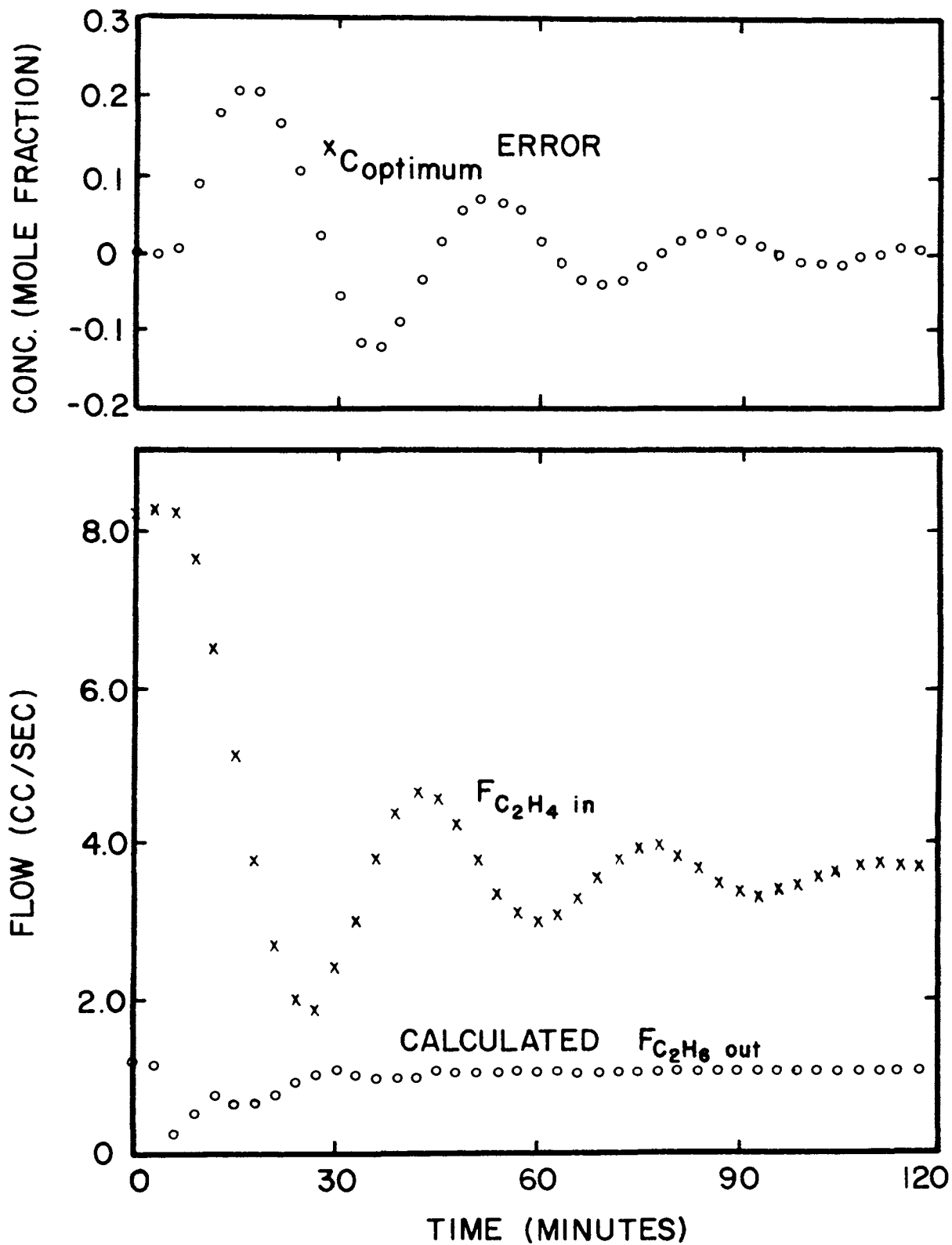


Figure 31. Flow Rate Response to a Step Down in the Feed of Hydrogen.

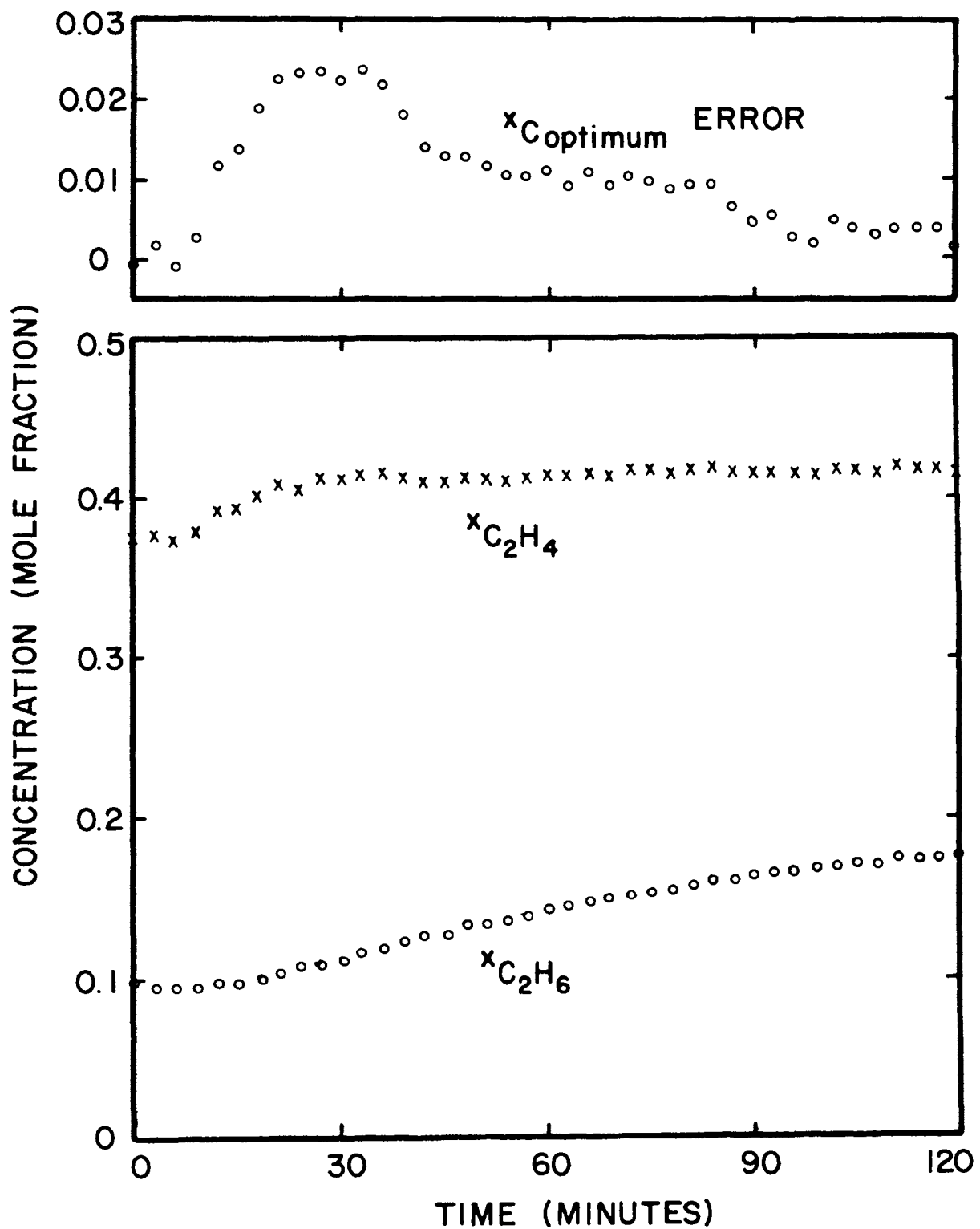


Figure 32. Composition Response to a Step Down in the Production Set Point.

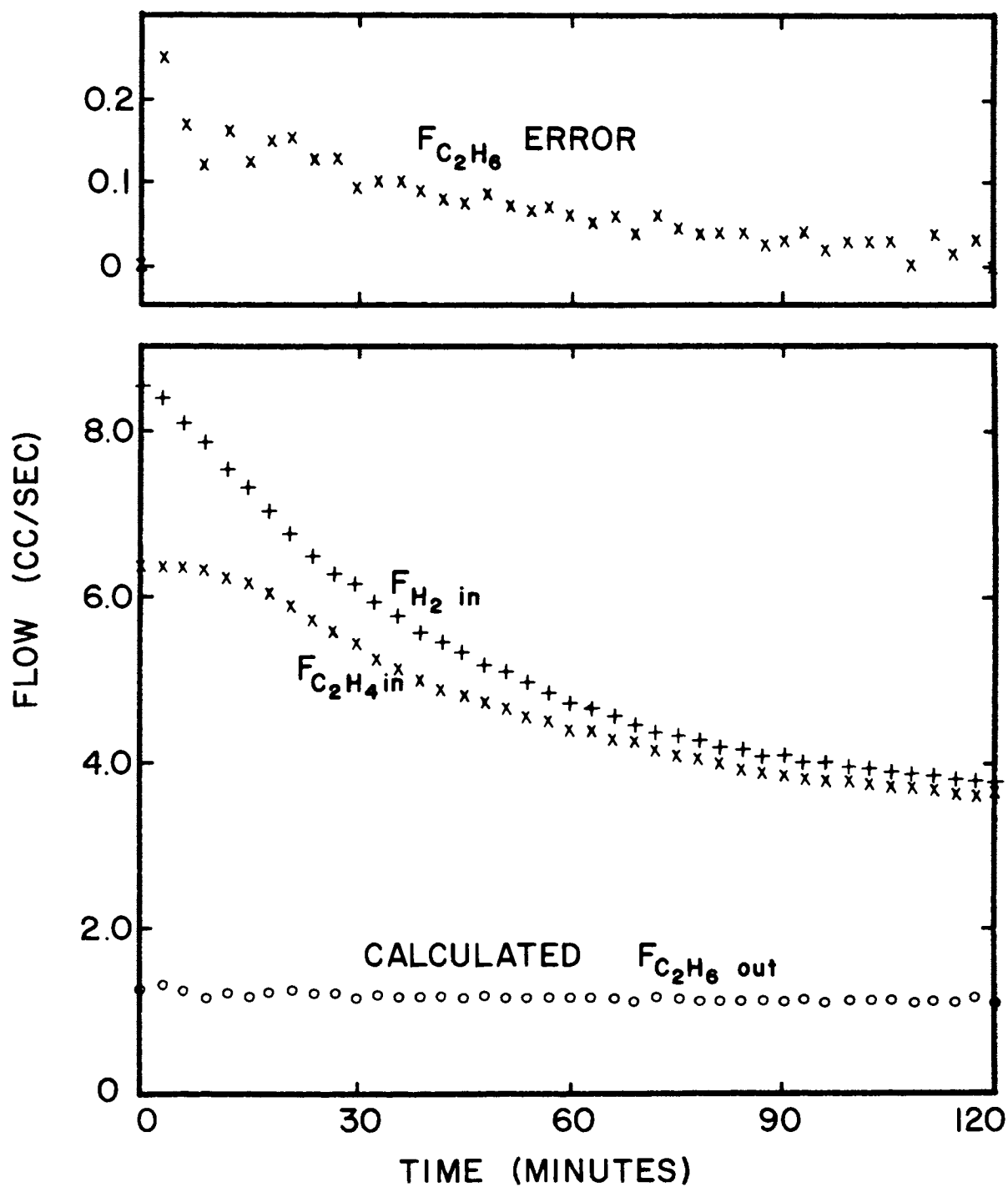


Figure 33. Flow Rate Response to a Step Down in the Production Set Point.

The reactor is operating in a region along the optimum curve in which production is fairly insensitive to the flow of hydrogen. A change in the hydrogen rate from 8.57 (cc)/(second) to 3.74 (cc)/(second), a change of 55 percent is required to change the production, flow rate of ethane, from 1.28 (cc)/(second) to 1.07 (cc)/(second), a change of 16 percent.

Figure 34 illustrates the composition response to a step up in the production set point from 1.07 (cc)/(second) to 1.23 (cc)/(second). Figure 35, page 93, shows the flow rate responses of the same experimental run. Again the lag in the optimizing loop is apparent.

Although only one crossover is shown in figures 35 and 34, the system did settle to the new set point. As discussed in the simulation, page 73, a higher optimizing loop gain could be employed in this case but would be unacceptable when the reactor time constant became longer.

C. Discussion of Results

1. Simulation: The simulation demonstrates that the optimizing scheme will function satisfactorily in an ideal situation.

If continuous analysis is employed a wide range of controller parameters may be employed with acceptable response of both the optimizing and production control loops.

Operation of the scheme utilizing sampled analysis with the sampled controller requires somewhat greater care in

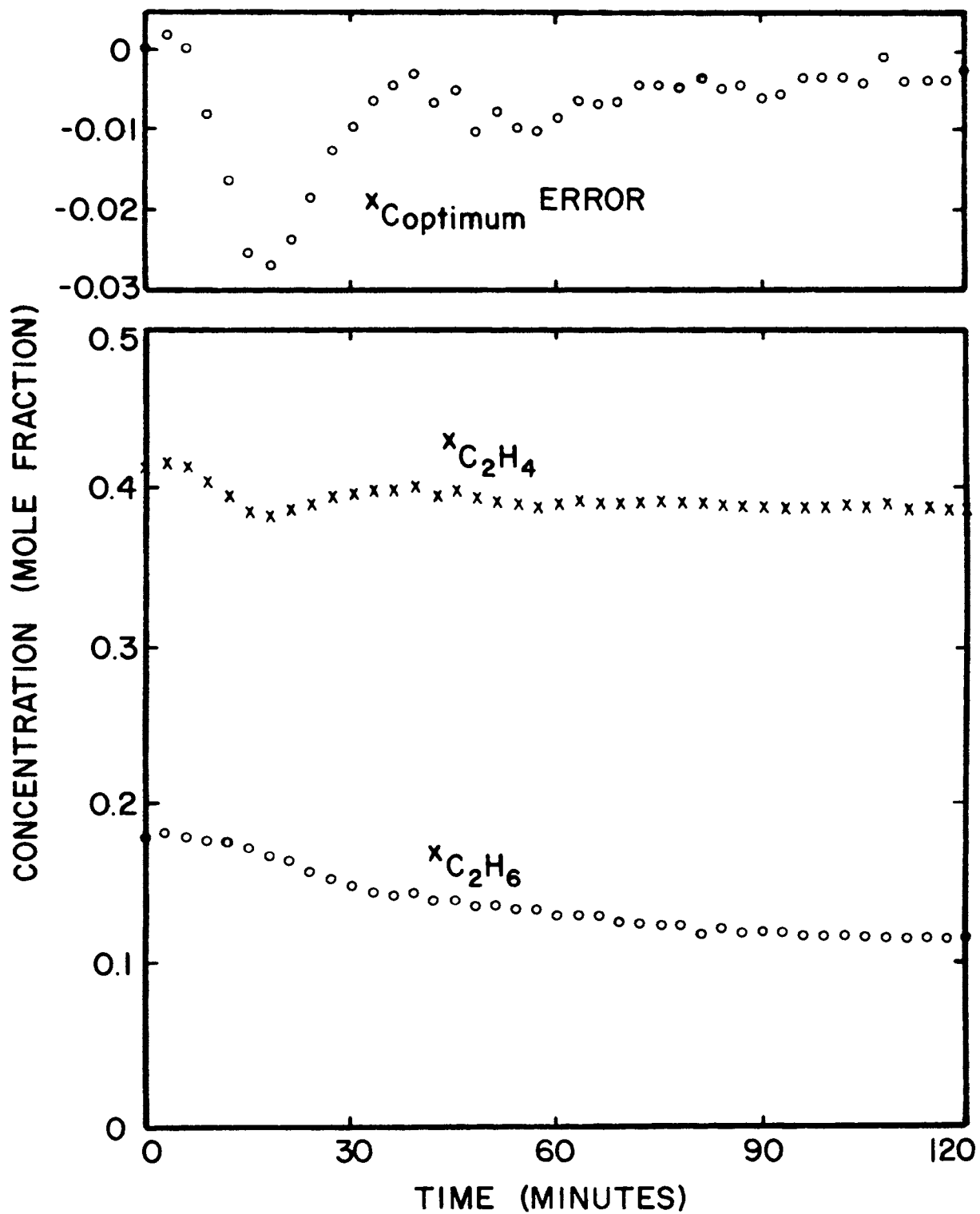


Figure 34. Composition Response to a Step Up in the Production Set Point.

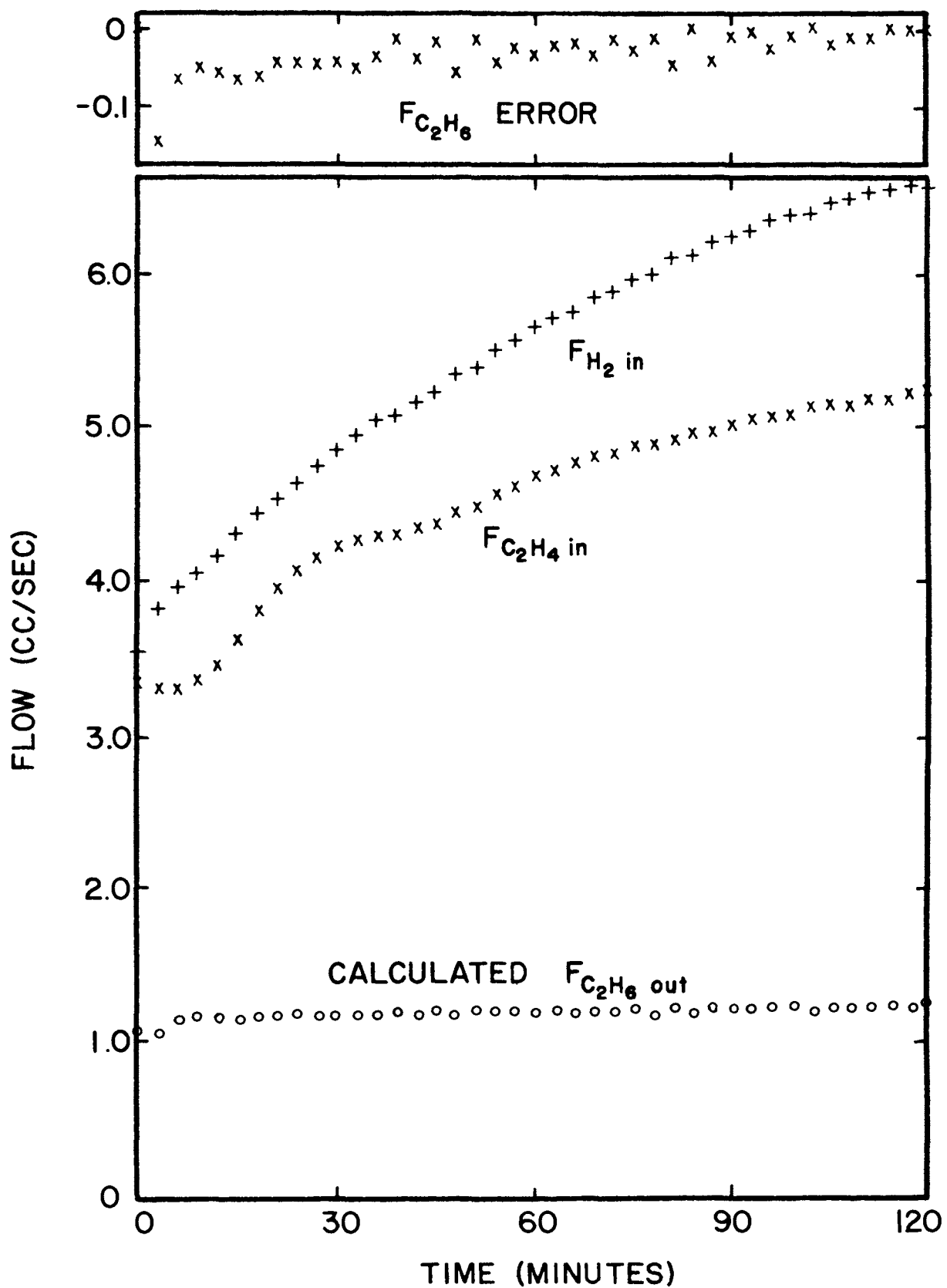


Figure 35. Flow Rate Response to a Step Up in the Production Set Point.

selecting the controller parameters. A single sample time, 3 minutes, was used in conjunction with reactor time constants of from 0.76 to 2.9 minutes with satisfactory operation of both the optimizing and production loops.

2. Experimental: The response of the pilot scale reactor system resembled closely that of the sampled analysis simulation.

The same sample time used in the simulation, 3 minutes, was employed with reactor time constants of from 1.05 to 3.76 minutes. For the most satisfactory operation the two gains, optimizing loop and production loop, should be adjusted whenever the system time constant makes a drastic change.

The prediction of the optimum is accurate, the loss in income because of not operating on the true optimum is less than 1 percent of that income.

VII. CONCLUSIONS

Operating conditions for a process may be adjusted to obtain a maximum income from a project. The existence of these conditions for a reactor is shown in Chapter IV. Values for these conditions can be computed on the basis of economic parameters and measurable operating variables. Further, the reactor conditions can be manipulated on-line to achieve this optimum return.

A reactor parameter, F_{Ain}/kV , has been identified in Chapter IV. It is measurable and completely specifies the position of the optimum condition, page 30, and thus is the key factor in establishing optimizing control. This reactor parameter can be used as the input to an optimizing control scheme, page 50. The output of this optimizing control scheme is an estimate of the actual position of the optimum condition, correct at steady state. This optimizing scheme may be implemented as a control loop on the reactor inputs, page 52.

As developed in Chapter IV, the optimizing scheme requires the application of a model of the reactor and reaction to an objective function which defines the economic performance criterion. The limitations of the scheme depend directly on the degree that the model deviates from the real system; however, inaccuracies in the model cannot cause

catastrophic affects, system shutdown, etc., because all possible outputs of the optimizing scheme are known before it is implemented, page 31. Severe inaccuracies in the model will produce a large economic reduction below that obtained at the maximum value of the performance criterion, page 45, but the economic loss when the scheme was applied to a pilot scale reactor was less than 1 percent of the maximum value of the performance criterion.

The optimizing scheme functions both in an ideal situation, page 53, and in a real application to a pilot scale reactor, page 82. Measurement of the slope of the performance is not required and therefore perturbations are not necessary.

The objective function which defines the performance criterion is incorporated into the optimizing scheme in order to predict the position of the optimum condition; therefore, measurement of the performance criterion is not necessary.

The optimizing control scheme can be applied when the feed of one reactant is specified or when the production rate is specified. Specification of the production rate requires the addition of a production controller which always interacts with the optimizing controller, page 28.

The reactor parameter can be measured through a non-linear function of the exit composition, page 42. When continuous analysis can be employed a conventional controller

may be used to manipulate the optimized variable. This system is stable for narrow proportional band but integral mode must be added to remove offset.

When sampled-delayed analysis is employed a sampled data controller is used to manipulate the optimized variable, page 65. The design of this controller is such that steady state offset is eliminated. This single parameter controller is more sensitive to changes in the reactor time constant and controller tuning becomes more important.

The production rate is controlled by manipulating the feed rate of one reactant. The change in the production rate with respect to the feed of this reactant changes sign at one point when the second reactant concentration is held at the optimum curve, page 41. In order to prevent positive feedback, operation must be restricted to a region in which this slope has a single sign. Because of the interaction of the optimizing and production controllers and the necessity of maintaining negative feedback, the optimizing controller speed must be high with respect to the speed of the production controller when it is desired to operate close to the production maximum, page 62.

BIBLIOGRAPHY

1. Draper, C.S., and Li, Y.T., "Principles of Optimizing Control Systems and an Application to the Internal Combustion Engine," The American Society of Mechanical Engineers Publication, (September, 1951).
2. Li, Y.T., "Optimizing System for Process Control," Instruments, 25 (January, 1952), 72-77, (February, 1952), 190-193, 228, (March, 1952) 350-352.
3. White, B., "The Quare Optimal Controller," Instruments and Automation, 29, 2 (1956), 2212-2216.
4. Tsien, H.S. and Serdengecti, S., "Analysis of Peak-Holding Optimizing Control," Journal Aeronautical Science, 22 (1955), 561-570.
5. Genthe, W.K., "Optimizing Control-Design of a Fully Automatic Cruise Control System for Turbojet Aircraft," 1957 WESCON Convention, 4 (1957), 47-57.
6. Hoffman, M.A., "Cruise Control Instrumentation Requirements for Turbojet Powered Aircraft," Report number ARG T-2, Aerophysics Research Group, MIT (May 16, 1955), 141-205.
7. Hoffman, M.A., Li, Y.T., and Navoy, A.J., "Programmed Cruise Control for Turbojet Aircraft, Part II," Sherman M. Fairchild Publication Fund Preprint Number 603, Institute of Aeronautical Sciences, (1956), 1-19.
8. Farber, B., "Computer Circuit Finds Peaks Automatically," Control Engineering, 1 (1954), 70-75.
9. Young, N.H., "An Automatic Control System with Provision for Scanning and Memory," Transactions American Institute of Electrical Engineers, 72, 1 (September, 1953), 392-395.
10. Whitaker, H.P., Yamron, J., and Kezer, A., "Reference Adaptive Control Systems for Aircraft," Report R-164, Instrument Laboratory, MIT (September, 1958).

11. Aseltine, J.A., Mancini, A.R., and Sarture, C.W., "A Survey of Adaptive Control Systems," Institute of Radio Engineers Transactions on Automatic Control, PGAC-6 (1958), 102-108.
12. Stromer, P.R., "Adaptive or Self-Optimizing Control Systems--A Bibliography," Institute of Radio Engineers Transactions on Automatic Control, AC-4, 1 (1959), 65-68.
13. Gibson, J.E., "Making Sense out of the Adaptive Principle," Control Engineering, 7, 8 (August, 1960), 113-119.
14. Gibson, J.E., "Mechanizing the Adaptive Principle," Control Engineering, 7, 10 (October, 1960), 109-114.
15. Truxal, J.G., "Trends in Adaptive Control Systems," Proceedings of the National Electronic Conference, 15 (1959), 1-16.
16. Hurley, J.R., Control of Chemical Processes by Parameter Perturbation. A Dissertation, The University of Wisconsin, 1963.
17. Deem, W.B., A System Engineering Study of Two-Variable Extremum Adaptive Control of a Gas Furnace. A Dissertation, The University of Wisconsin, 1965.
18. Schindler, R.N. Questing Control of a Continuous Flow Stirred Tank Reactor. A Dissertation, The University of Minnesota, 1966.
19. Wiley, Robert J., Optimization of a Batch Reacting Distillate System by Means of the Maximum Principle. A Dissertation, Stevens Institute of Technology, Castle Point, Hoboken, New Jersey, 1967.
20. Hoyer, G.G., Multivariable Adaptive Optimal Control of a Catalytic Reaction System. A Dissertation, The University of Wisconsin, 1967.
21. Chao, H.H., The Optimization of a Tubular Chemical Reactor: A Study of the Pseudo-Optimum Search Method. A Dissertation, The University of Oklahoma, 1967.
22. Foley, G.J., Analysis and Design of Input Perturbation Extremum Seeking Systems. A Dissertation, The University of Wisconsin, 1968.
23. Newberger, M.R., Optimal Operation of a Tubular Chemical Reactor. A Dissertation, The University of Michigan, 1968.

24. White, J.W., Univariable Input Perturbation Adaptive Optimization of Systems with Time Delay. A Dissertation, The University of Wisconsin, 1968.
25. Olmsted, J.M.H., Advanced Calculus. New York: Appleton-Century-Crofts, Inc., 1959, 85.
26. Eley, D.D., Catalysis. New York: Reinhold, 1955, 3, 49.
27. Jenkins, G.I. and Rideal, E., "The Catalytic Hydrogenation of Ethylene at a Nickel Surface," Journal of the Chemical Society (London), 158 (1955), 2490-2500.
28. Eyring, H., Colburn, C.B., and Zwolinski, B.J., "The Activated Complex in Chemisorption and Catalysis," Discussions Faraday Society, 8 (1950), 39-46.
29. Coughanowr, D.R. and Koppel, L.B., Process Systems Analysis and Control. New York: McGraw-Hill Book Company, 1965, 454.

VITA

Jesse Daniel Bennett was born on October 19, 1944, in Bloomfield, Missouri. He received his primary and secondary education in Bloomfield, Missouri. He has received his college education from the University of Missouri-Rolla, in Rolla, Missouri. He received a Bachelor of Science degree in Chemical Engineering in June 1966 and the Master of Science degree in Chemical Engineering in June 1968 from the University of Missouri-Rolla, in Rolla, Missouri.

His industrial experience has been with Shell Oil and Shell Chemical Company where he was employed as a petro-physical engineer, a process design engineer, and an instrumentation and control engineer.

His initial enrollment in the Graduate School of the University of Missouri-Rolla was in September 1966 and he held the NDEA Fellowship for the period September 1966 to June 1969.

APPENDIX A
LIST OF SYMBOLS

Symbol	Description	Units
A	Reactant	Unit Mole
B	Product	Unit Mole
C	Reactant or Catalyst	Unit Mole
C_A	Cost of Reactant A	(Monetary Units)/ (Mole A)
C_B	Credit for B, the Product	(Monetary Units)/ (Mole B)
C_C	Cost of Reactant C	(Monetary Units)/ (Mole C)
D_m	Molar Density of the Reaction Mass	(Moles)/(Volume)
e_o	Optimum Error	Mole Fraction
e_p	Production Error	Minute ⁻¹
F	Total Exit Flow from the Reactor	(Moles)/(Time)
F_{Ain}	Feed Rate of Reactant A	(Moles A)/(Time)
F_B	Production Rate	(Moles B)/(Time)
F_{Cin}	Feed Rate of Reactant C	(Moles C)/(Time)
G	Performance Criterion, Income	(Monetary Units)/ (Time)
k	Reaction Rate Constant	(Moles)/(Mole Fraction C ⁿ , Mole Fraction A, Time, Volume)

List of Symbols (continued)

Symbol	Description	Units
k_o	Continuous Analysis Optimizing Control Proportional Gain	(Flow Units C)/ (Mole Fraction C)
K_o	Sampled Analysis Optimizing Control Gain	(Flow Units C)/ (Mole Fraction C)
k_p	Continuous Analysis Production Control Proportional Gain	(Flow Units A)/ (Flow Units B)
K_p	Sampled Analysis Production Control Gain	(Flow Units A)/ (Flow Units B)
n	Order of the Reaction with Respect to Reactant C	Unitless
r_A	Rate of Reaction	(Moles A)/(Time, Volume)
T_o	Continuous Analysis Optimizing Control Integral Time Constant	(Time)
T_p	Continuous Analysis Production Control Integral Time Constant	(Time)
V	Reactor Volume	(Volume Units)
x_A	Mole Fraction Reactant A	(Moles A)/(Total Moles)
x_B	Mole Fraction Product, B	(Moles B)/(Total Moles)
x_C	Mole Fraction Reactant C	(Moles C)/(Total Moles)

APPENDIX B
SIMULATION DEVELOPMENT

1. Dynamic Equations

An analog simulation was chosen and was programmed to operate on a general purpose electronic analog computer, the Applied Dynamics 40, with an Applied Dynamics 24 slaved to it. The first step in a simulation is the derivation of the dynamic equations which describe the behavior of the pertinent variables of the reactor. The simulation work is limited to reaction systems which may be approximated by incompressible flow. Liquid systems exhibit little deviation from incompressible flow but gaseous systems are limited to cases in which the temperatures and pressures do not vary with time. A component mass balance is performed on each reactant. The component balance for reactant A is equation 26, page 43.

$$VD_m dx_A/dt = -kVx_Ax_C^n - Fx_A + F_{Ain} \quad 26.$$

The first order reaction rate law with respect to reactant C is used for the simulation. For the first order rate law equation 26 becomes the following:

$$VD_m dx_A/dt = -kVx_Ax_C - Fx_A + F_{Ain} \quad 1B.$$

In an exactly analogous manner the component mass balance for reactant C is performed to obtain the following:

$$VD_m dx_C/dt = -kVx_Ax_C - Fx_C + F_{Cin} \quad 2B.$$

As described on page 20 the rate law and the assumption of perfect mixing provide a relationship of production rate and reactant concentrations, equation 3. In the case of the first order rate law with respect to reactant C equation 3 may be expressed:

$$F_B = Fx_B = kVx_Ax_C \quad 3B.$$

Equation 3B is valid during dynamic changes for incompressible flow. The total flow out of the reactor can be written:

$$F = Fx_A + Fx_C + Fx_B \quad 4B.$$

Substitution of equations 5, 6, and 3B into equation 4B produces the following expression:

$$F = F_{Ain} + F_{Cin} - kVx_Ax_C \quad 5B.$$

Equations 1B, 2B, and 5B are rearranged for analog programming:

$$\begin{aligned} dx_A/dt = & -(k/D_m)x_Ax_C - (F/VD_m)x_A \\ & + F_{Ain}/VD_m \end{aligned} \quad 6B.$$

$$\begin{aligned} dx_C/dt = & -(k/D_m)x_Ax_C - (F/VD_m)x_C \\ & + F_{Cin}/VD_m \end{aligned} \quad 7B.$$

$$\begin{aligned} F/VD_m = & F_{Ain}/VD_m + F_{Cin}/VD_m \\ & - (k/D_m)x_Ax_C \end{aligned} \quad 8B.$$

The dependent variables are chosen as x_A and x_C . The parameters F_{Ain}/VD_m , F_{Cin}/VD_m , and k/D_m are used instead of F_{Ain} , F_{Cin} , and kV . This variable alteration is acceptable since for constant temperature and pressure D_m and V

are constants.

2. Time Scaling

The dimensions of the various terms must be investigated. The dimensions of the differential and each term on the right hand side of the differential equations, 6B and 7B, page 105 are (moles)/(time). The dimensions of the molar flows, F , F_{Ain} , and F_{Cin} , are (moles)/(time) and the dimensions of the group, VD_m , is moles; therefore, the dimension of the flow groups F/VD_m , F_{Ain}/VD_m , and F_{Cin}/VD_m is (time)⁻¹. The magnitude of these groups can then be defined as the reciprocal of the time constant of the reactor based on that particular component alone, i.e., the magnitude of F_{Ain}/VD would be the reciprocal of the time constant of the reactor if A were the only flow and no reaction occurred.

The use of the molar flow group reduces the requirement for time scaling since one minute of real time can be set equal to one second computer time.

3. Magnitude Scaling

The Applied Dynamics 40 and 24 are 100 volt computers capable of automatic mode control and other logical operations which may be accomplished through patching a control logic patchboard. The use of a 100 volt computer and mole fractions for the dependent variables allows a direct procedure for magnitude scaling. All voltages on the computer are made 100 times the variable they represent. In this

way a range of 0-100 volts on the computer represents the 0-1.0 range for mole fractions and in most cases the actual value of a parameter or constant may be placed directly on a potentiometer.

4. Analog Program

a. Process: The process consists of a bimolecular reaction which is first order with respect to each reactant. The reaction is carried out in a continuous stirred-tank reactor at constant temperature and pressure. This process is described by the differential equations 6B, 7B, and 8B. The analog program used to solve these equations and thereby simulate the process is presented in figure 1B, page 108. Table I-B, page 109, describes the function of each component presented in figure 1B.

Integrator A1 is used to generate the mole fraction of A and integrator A2 is used to generate the mole fraction of C. Equation 8B is solved with summer B3. The other amplifiers and multipliers are used to generate necessary terms of equations 6B, 7B, and 8B. For example, multiplier A5-6 produces the product of the two reactant mole fractions, $x_A x_C(100)$, which is attenuated and used to provide the rate of production of B, $(k/D_m)x_A x_C(100)$, at D4.

Switch 2A2 is used to impose upsets in the reaction rate constant. Amplifier D3 is used to generate a time base and comparator 1A10 is used to coordinate the step or pulse upset with this time base.

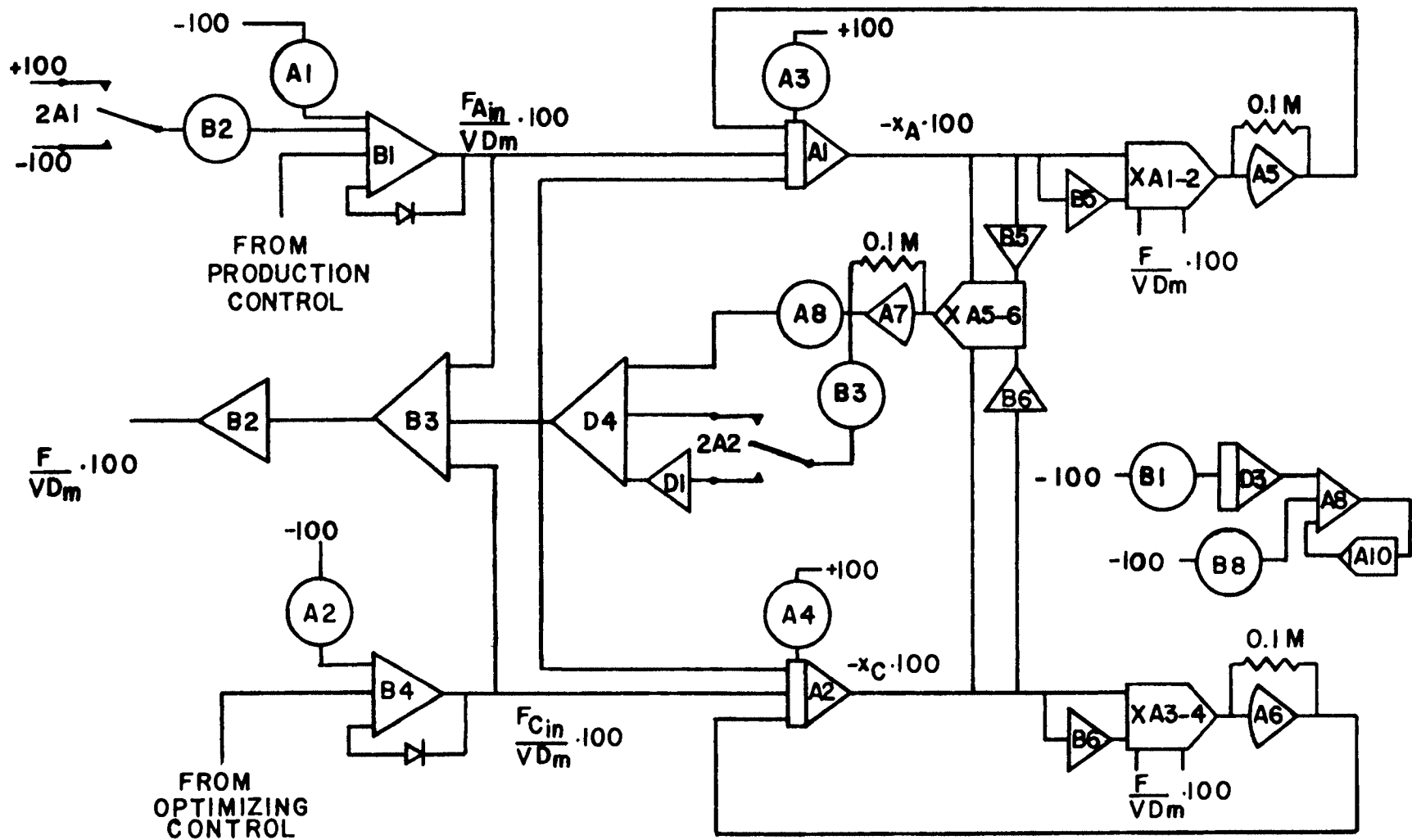


Figure 1B. Analog Program for Reactor Simulation.

TABLE I-B
COMPONENT LIST FOR REACTOR SIMULATION, FIGURE 1B

Element	Type	Output or Setting	Units
A1	Integrator	Conc. of A, $-(x_A)100$	Mole Fraction
A2	Integrator	Conc. of C, $-(x_C)100$	Mole Fraction
A5	Unloading Amplifier	Exit Flow of A, $-(Fx_A/VD_m)100$	Minute ⁻¹
A6	Unloading Amplifier	Exit Flow of C, $-(Fx_C/VD_m)100$	Minute ⁻¹
A7	Unloading Amplifier	Product of Reactant Conc., $(x_A x_C)100$	(Mole Fraction) ²
A8	Comparator Driver		
B1	Summer	Feed of A, $(F_{Ain}/VD_m)100$	Minute ⁻¹
B2	Inverter	Exit Flow, $(F/VD_m)100$	Minute ⁻¹
B3	Summer	Exit Flow, $-(F/VD_m)100$	Minute ⁻¹
B4	Summer	Feed of C, $(F_{Cin}/VD_m)100$	Minute ⁻¹
B5	Inverter	Conc. of A, $(x_A)100$	Mole Fraction
B6	Inverter	Conc. of C, $(x_C)100$	Mole Fraction
D1	Inverter	Production Change from Upset in Rate Constant, $(\Delta k x_A x_C / D_m)100$	Minute ⁻¹
D3	Integrator	Time Base, t (scaled)	Minutes
D4	Summer	Production, $(F_B/VD_m)100$	Minute ⁻¹
A1	Potentiometer	Feed of A, F_{Ain}/VD_m	Minute ⁻¹

Table I-B (continued)

Element	Type	Output or Setting	Units
A2	Potentiometer	Feed of C, F_{Cin}/VD_m	Minute ⁻¹
A3	Potentiometer	Initial Conc. A, x_{Ao}	Mole Fraction
A4	Potentiometer	Initial Conc. C, x_{Co}	Mole Fraction
A8	Potentiometer	Rate Constant, k/D_m	(Mole Fraction ² , Minute) ⁻¹
B1	Potentiometer	Time Base Driver	
B2	Potentiometer	Upset in Feed of A, $\Delta F_{Ain}/VD_m$	Minute ⁻¹
A1-2	Multiplier	Current Signal for Exit Flow of A	
A3-4	Multiplier	Current Signal for Exit Flow of C	
A5-6	Multiplier	Current Signal for Production Rate	
2A1	SPDT Switch	Step Function for Upset in Feed of A	
2A2	SPDT Switch	Step Function for Upset in Rate Constant	

The outputs of summers B1 and B2 are the signals representing the feed rates for reactants A and C, F_{Ain}/VD_m and F_{Cin}/VD_m . The inputs to these two summers are provided by potentiometers for constants and the control sections when the control loops are closed. Note that diodes are placed around these summers to limit their output to positive polarity during closed loop control since negative flow is not possible.

b. Non-Linear Calculations: In order to predict an optimum concentration of reactant C the parameter group, F_{Ain}/kV , must be estimated. This group is known by the analog programmer since the parameter is made up of the quotient of two potentiometer settings. In an on-line situation the parameter would have to be estimated from on-line data. The value of the group, F_{Ain}/kV , is obtained from analysis of the product stream. The signals are introduced into the non-linear function, equation 30, page 43. For the first order rate law equation 30 becomes:

$$F_{Ain}/kV = x_A^2 x_C / x_B + x_A x_C \quad 9B.$$

The introduction of equation 21 which describes the relationship of the optimum mole fraction of reactant C to the parameter group, F_{Ain}/kV , requires scaling. The cost ratio must be specified and the range of the parameter group must be considered. For the simulation a cost ratio, C_B/C_C , of 20.0 was employed and the range of F_{Ain}/kV was restricted to 0-2.5 (because of the position of the production maximum

for a cost ratio of 20.0, $F_{Ain}/kV \approx 2.0$). The scaled signal which represents F_{Ain}/kV on the computer is then $(F_{Ain}/kV)40$ and the signal which represents the optimum mole fraction of C is $(x_C \text{ optimum})250$.

If production control is required a measure of the actual production would have to be made. This measure of the production might be a flow meter on separated product. In the simulation the production rate is calculated from the analyzer output and the molar feed of reactant A. If equation 8, page 24, is multiplied by x_B , the mole fraction of B, the production is obtained.

$$F_B = Fx_B = F_{Ain}(x_B/(1 - x_C)) \quad 10B.$$

Figure 2B, page 113 is the analog program used for the solution of equations 9B and 10B. A component function list is presented in table II-B, page 114.

c. Continuous Analysis Control Schemes: The simulation is used to investigate situations in which continuous chemical analyzers are employed.

Figure 3B, page 116, is a block diagram of a continuous feedback control scheme used to maintain an optimum mole fraction of reactant C. This diagram is similar to figure 8, page 52, but uses a conventional feedback layout. This system requires that the composition of the exit stream be determined continuously. Figure 4B, page 116, is the analog program for simulation of the continuous feedback control system. When continuous analysis is possible the

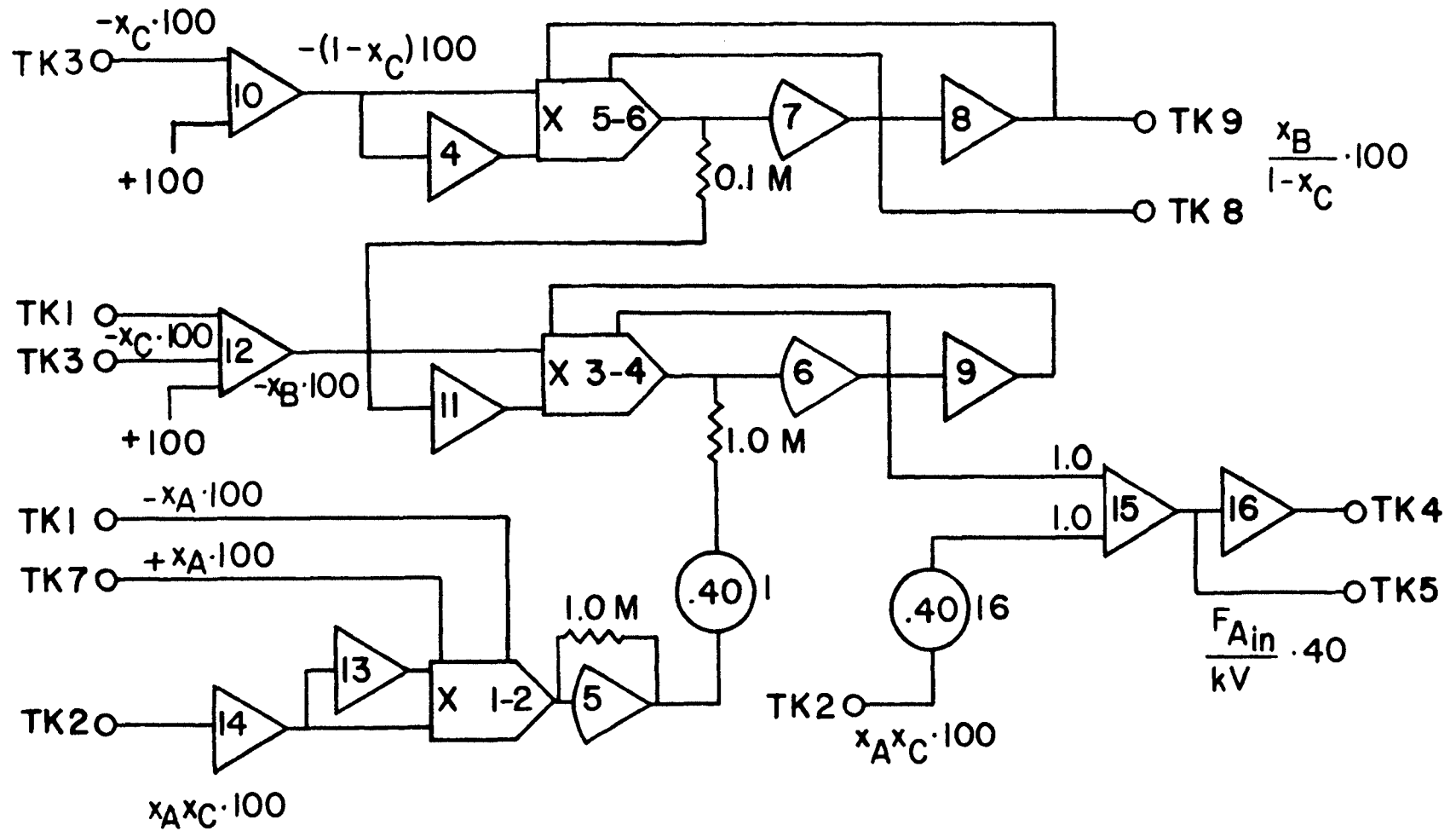


Figure 2B. Analog Program for Calculation of the Non-Linear Functions of Composition for use with the Simulation.

TABLE II-B
COMPONENT LIST FOR SIMULATION NON-LINEAR
CALCULATIONS, FIGURE 2B

Element	Type	Output or Setting	Units
4	Inverter	$(1 - x_C)100$	Mole Fraction
5	Unloading Amplifier	$(x_A^2 x_C)1000$	(Mole Fraction) ³
6	Unloading Amplifier	$(x_A^2 x_C/x_B)40$	(Mole Fraction) ²
7	Unloading Amplifier	$(x_B/(1 - x_C))100$	Unitless
8	Inverter	$-(x_B/(1 - x_C))100$	Unitless
9	Inverter	$-(x_A^2 x_C/x_B)40$	(Mole Fraction) ²
10	Summer	$-(1 - x_C)100$	Mole Fraction
11	Inverter	$(x_B)100$	Mole Fraction
12	Summer	$-(x_B)100$	Mole Fraction
13	Inverter	$(x_A x_C)100$	(Mole Fraction) ²
14	Inverter	$-(x_A x_C)100$	(Mole Fraction) ²
15	Summer	$-((x_A^2 x_C/x_B) + x_A x_C)40$	(Mole Fraction) ²
16	Inverter	$((x_A^2 x_C/x_B) + x_A x_C)40$	(Mole Fraction) ²
1	Potentiometer	Scaling Factor, .40	

Table II-B (continued)

Element	Type	Output or Setting	Units
16	Potentiometer	Scaling Factor, .40	
1-2	Multiplier	Current Signal for $x_A^2 x_C$	
3-4	Multiplier	Current Signal for $x_A^2 x_C / x_B$	
5-6	Multiplier	Current Signal for $x_B / (1 - x_C)$	

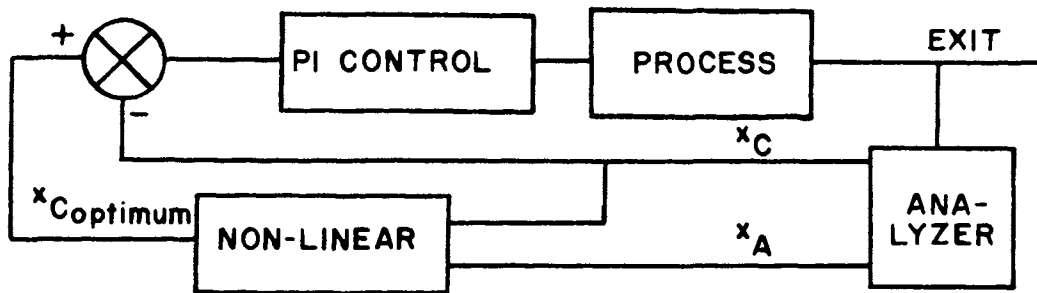


Figure 3B. Continuous Analysis Optimizing Control Scheme.

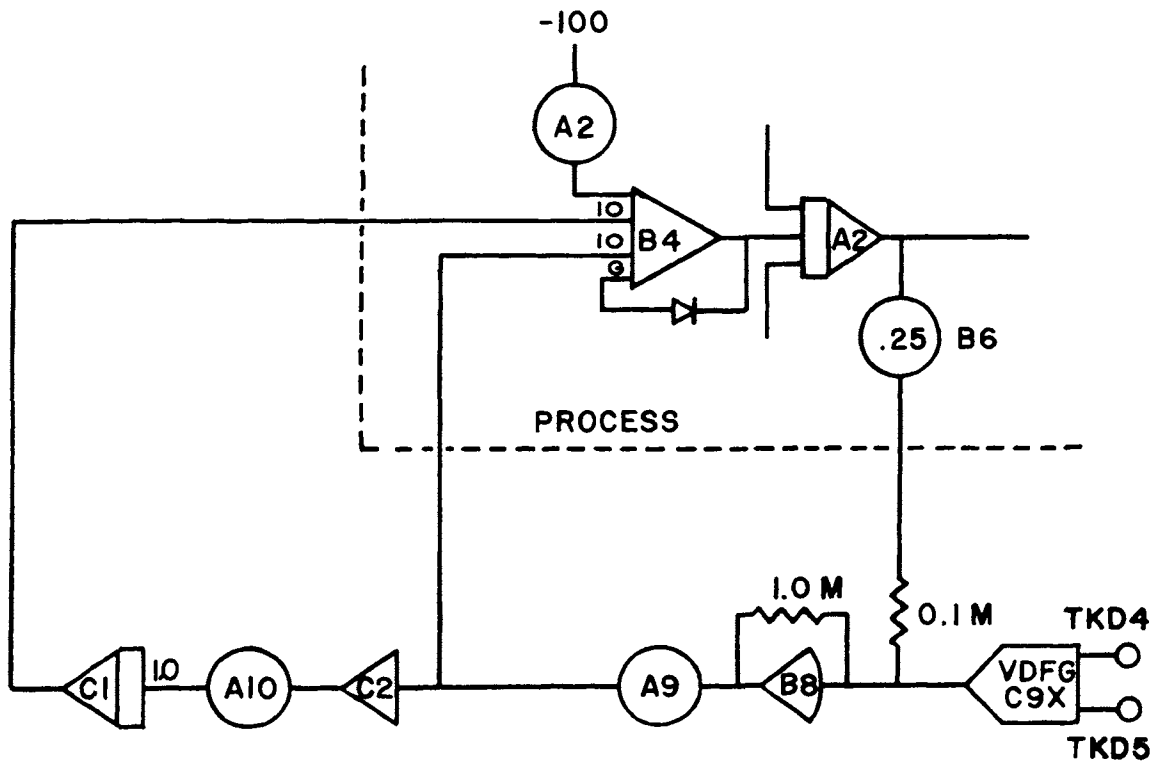


Figure 4B. Analog Program for Simulation of the Continuous Analysis Optimizing Control Scheme.

estimate of the parameter group, F_{Ain}/kV , accomplished by the solution of equation 9B on the AD-24 is provided at all times. An estimate of the optimum mole fraction of reactant C is obtained from a plot such as one presented in figure 1, page 33. As mentioned above the cost ratio, C_B/C_C , used for the simulation was 20.0 and the range of F_{Ain}/kV restricted to 0-2.5. Figure 5B is the plot of the optimum concentration of reactant C vs. F_{Ain}/kV for a cost ratio of 20.0 over the specified range. For automatic operation the function described by this plot must be incorporated into the control system which was done by transferring figure 5B to a variable diode function generator.

The plot from figure 5B is then contained in VDFG C9X and the estimate of the scaled optimum mole fraction of reactant C, correct at steady state, is supplied continuously. The negative of the actual value of the mole fraction of reactant C (scaled) is supplied from integrator A2, attenuated to obtain the same scaling as the optimum estimate by pot B6, and an error from the optimum generated in B8. This error then drives a conventional P-I controller constructed with summer C2, integrator C1, and one potentiometer for each of the two control parameters used in such a controller, the proportional gain and the integral time constant. The output of this P-I controller is an input to summer B4 which as mentioned above supplies the signal which represents the feed rate of reactant C.

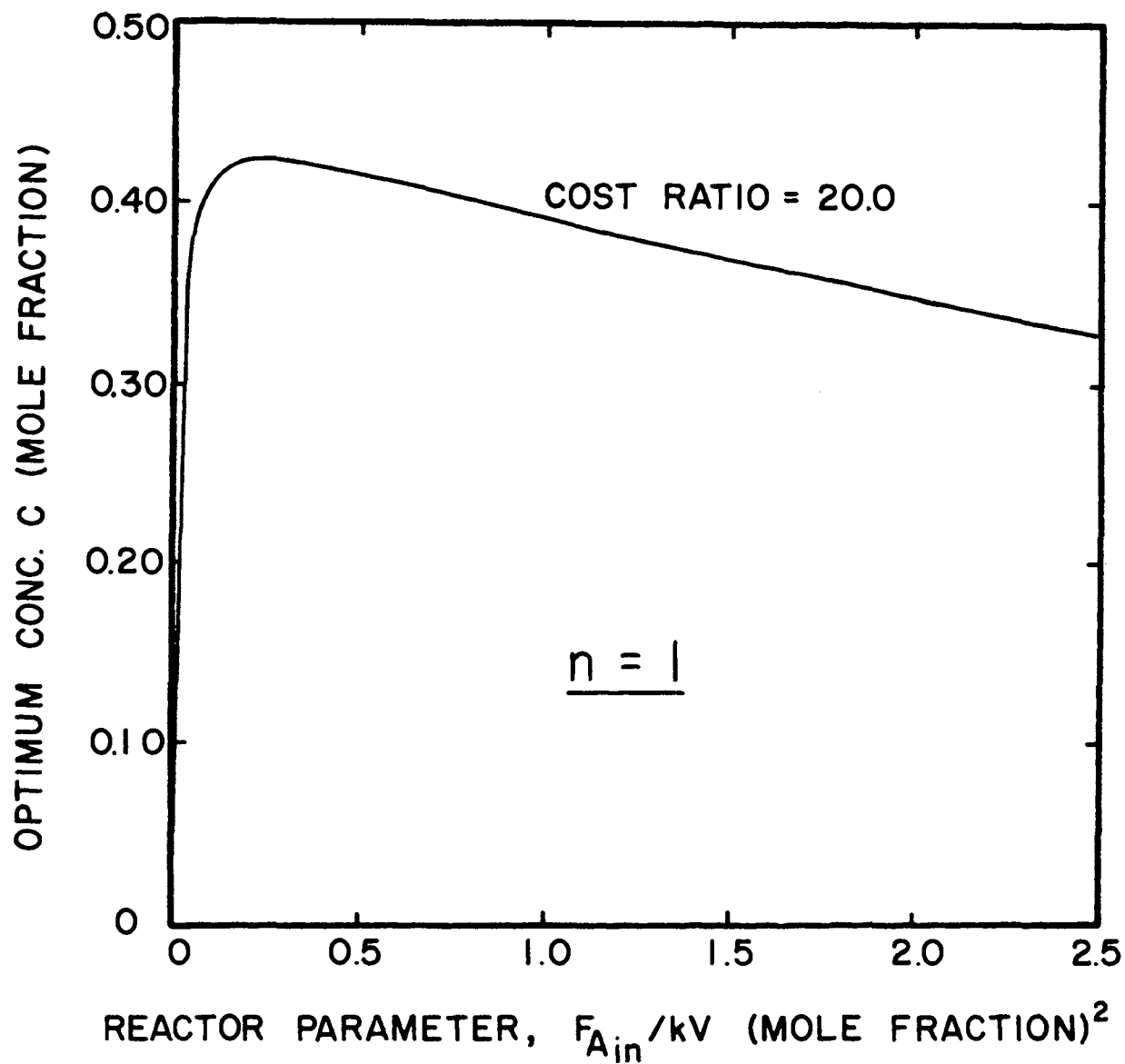


Figure 5B. Optimum Curve for $n = 1$, Cost Ratio = 20.0, used in the Simulation and Experimental Test.

The continuous control system to maintain the optimum concentration of reactant C was studied for upsets in the reaction rate constant and the feed rate of reactant A. If the production rate of B is specified an additional control system must be implemented.

Figure 6B is a block diagram of a production controller and figure 7B is the analog program used for the simulation of this production controller.

Equation 10B, page 112, is solved with multiplier A7-8 and the production set point obtained from potentiometer A5. For continuous analysis the production could also have been obtained directly from amplifier D4 (see figure 1B, page 108). An error from the production set point is generated in summer B7. This error then drives a second conventional P-I controller represented by summer C4, integrator C3, and a potentiometer for each of the two control parameters applicable to the loop. The output of this controller is an input to summer B1 which supplies the signal which represents the feed rate of reactant A. When both control loops are closed the feed rate of A is manipulated by the production rate controller; therefore, the only upsets that can be considered are those that effectively change the reaction rate constant or change the production set point. It should be noted that in order to control production in this manner operation must be restricted to the region in which an increase in F_{Ain}/kV increases the production. If F_{Ain}/kV

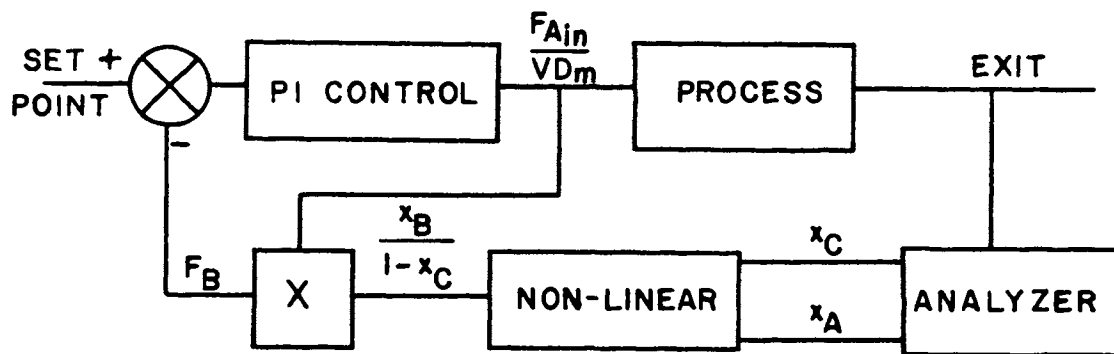


Figure 6B. Continuous Analysis Production Control Scheme.

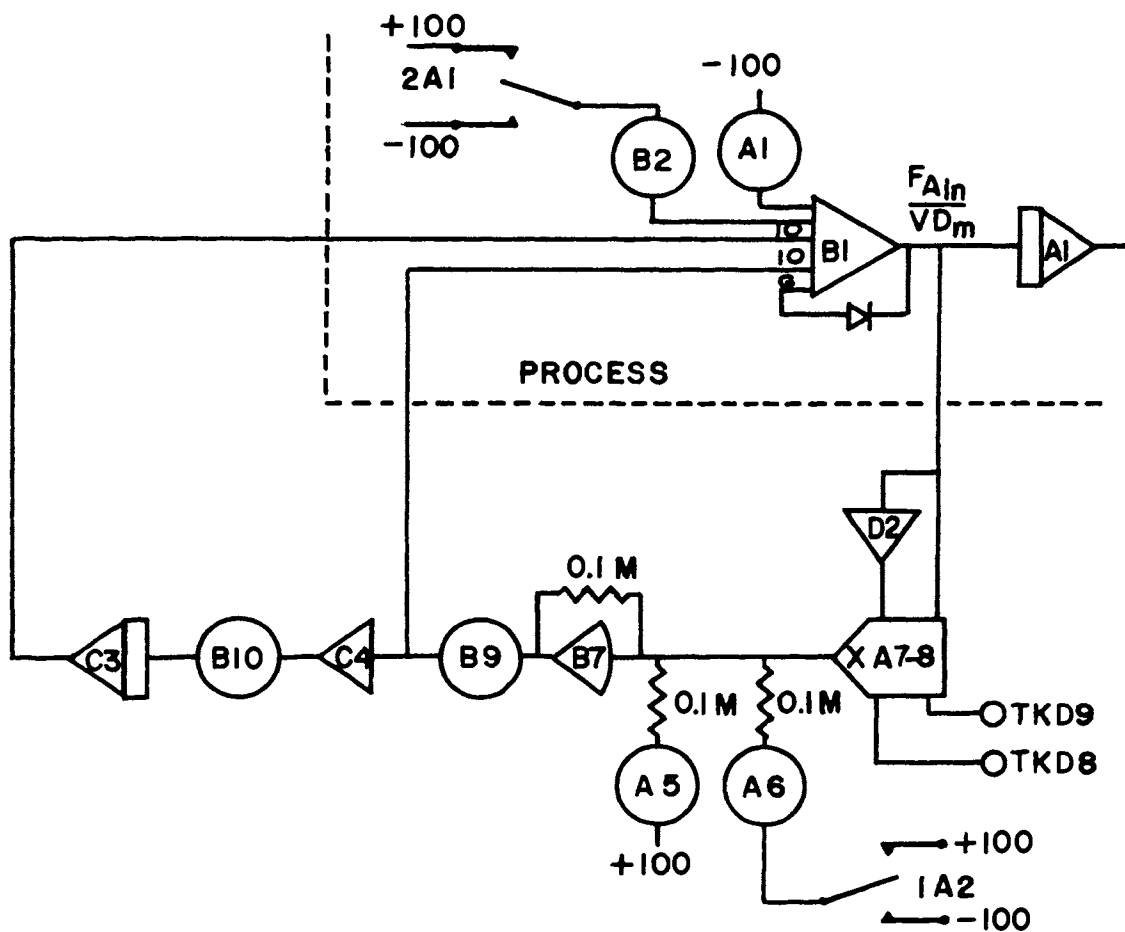


Figure 7B. Analog Program for Simulation of the Continuous Analysis Production Control Scheme.

is driven out of this region positive feedback and corresponding instability will occur.

Operation of both control loops introduces interaction into the system since any change in the feed rate of A can potentially change the reactor parameter and thereby upset the optimizing loop. Likewise, any change in the feed rate of C can potentially change the production of B and upset the production controller.

Table III-B is a component function list for the analog diagrams presented in figures 4B and 7B.

The mode control of the integrators, track-holds, switches and other devices on the Applied Dynamics computers is accomplished by patching a "Control Logic" board. For the continuous analysis simulation the control logic is used only for actuating upsets on the process. All integrators are controlled manually by the main computer control switch.

For step changes the inverse of comparator 1A10 is generated in a gate and drives one of the switches which places a step change on the reaction rate constant or the feed rate of reactant A. For pulse upsets the comparator 1A10 actuates a pulser which drives these switches. The pulser timer is set so that it resets at a point when the process is under fast dynamic change.

d. Sampled Analysis Control Schemes: If the composition of the product stream cannot be determined continuously

TABLE III-B
COMPONENT LIST FOR SIMULATION OF THE CONTINUOUS
ANALYSIS CONTROLLERS, FIGURES 4B AND 7B

Element	Type	Output or Setting	Units
B8	Unloading Amplifier and Summer	Optimum Error, $(e_o)250$	Mole Fraction
C1	Integrator	Integral Component of Optimizing P-I Controller	Minute ⁻¹
C2	Inverter	Optimum Error Times the Proportional Gain	Minute ⁻¹
A9	Potentiometer	Proportional Gain, $k_o(0.04)$	(Minute ⁻¹ C)/ (Mole Fraction C)
A10	Potentiometer	Reciprocal of Optimizing Integral Time Constant, T_o^{-1}	Minute ⁻¹
C9X	VDFG	Current Signal for Optimum Conc. C	
B7	Unloading Amplifier and Summer	Production Error, $(e_p)100$	Minute ⁻¹
C3	Integrator	Integral Component of Production P-I Controller	Minute ⁻¹
C4	Inverter	Production Error Times the Proportional Gain	Minute ⁻¹
D2	Inverter	Feed of A, $-(F_{Ain}/VD_m)$	Minute ⁻¹
A5	Potentiometer	Production Set Point, $(F_B/VD_m)_{SP}$	Minute ⁻¹

Table III-B

Element	Type	Output or Setting	Units
A6	Potentiometer	Upset in Production Set Point, $(\Delta F_B / VD_m)_{SP}$	Minute ⁻¹
B9	Potentiometer	Proportional Gain, $k_p(0.10)$	(Minute ⁻¹ A) / (Minute ⁻¹ B)
B10	Potentiometer	Reciprocal of Production Integral Time Constant, T_p^{-1}	Minute ⁻¹
1A2	SPDT Switch	Step Function for Upset in Production Set Point	

then a sampled approach must be considered. This situation is encountered when a gas chromatograph is used.

Figure 8B is a block diagram for a feedback control system which maintains the optimum concentration of reactant C when a chromatograph is used for the analysis. When a chromatograph is used the output, composition, is sampled and delayed by a time equal to the sample time. The system presented in figure 9B exhibits the same characteristics as the system in figure 8B but requires less equipment to simulate.

The controller section uses the following equation to determine the feed rate of reactant C:

$$F_{Cin}/VD_m(i) = F_{Cin}/VD_m(1) + K_o(e_o(i-1) + e_o(i-2) + \dots + e_o(3) + e_o(2) + e_o(1)) \quad 11B.$$

where: i = time increments

K_o = controller gain; $(\text{time}^{-1})/(\text{mole fraction})$

$e_o(i)$ = optimum error at time i ; mole fraction

This control scheme, in which the successive errors are summed, eliminates steady state offset. Figure 10B is an analog diagram for the simulation of the scheme outlined by figure 9B and equation 11B.

The control of production can also be accomplished with the use of a sampling analyzer. Figure 11B, page 127, is a block diagram for a feedback control system to control the production. A new value of production is determined each sample period by solving equation 10B, page 112. The

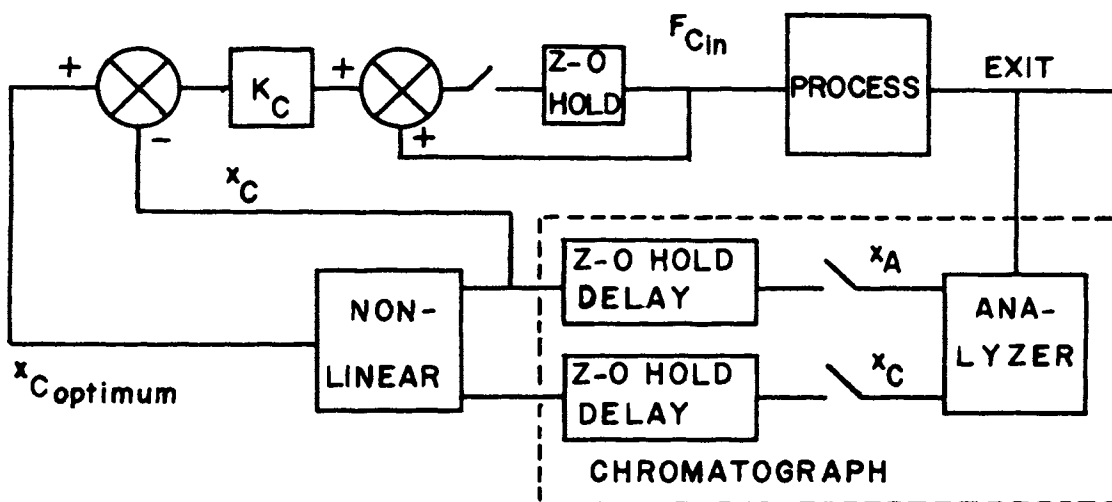


Figure 8B. Sampled Analysis Optimizing Control Scheme.

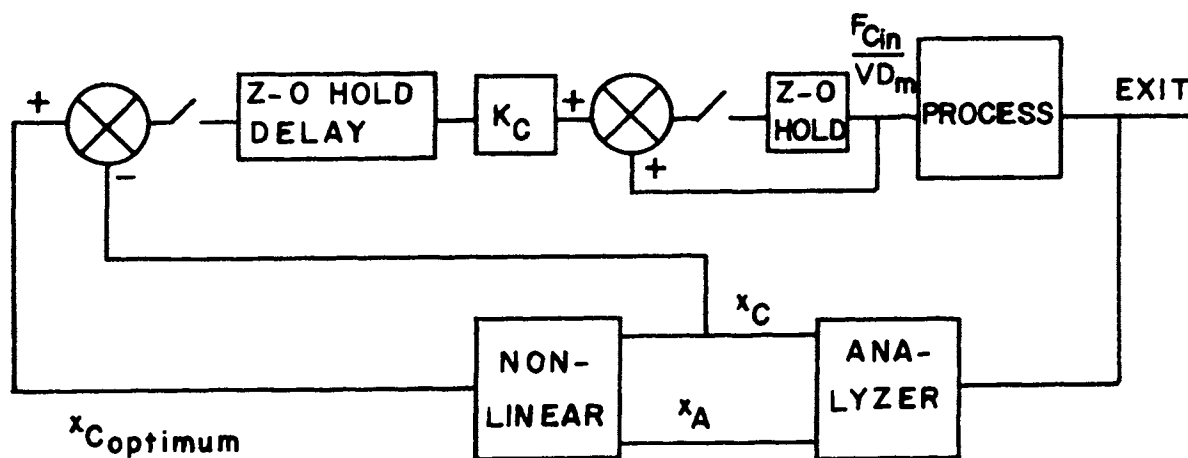


Figure 9B. Sampled Analysis Optimizing Control Scheme for Simulation Purposes.

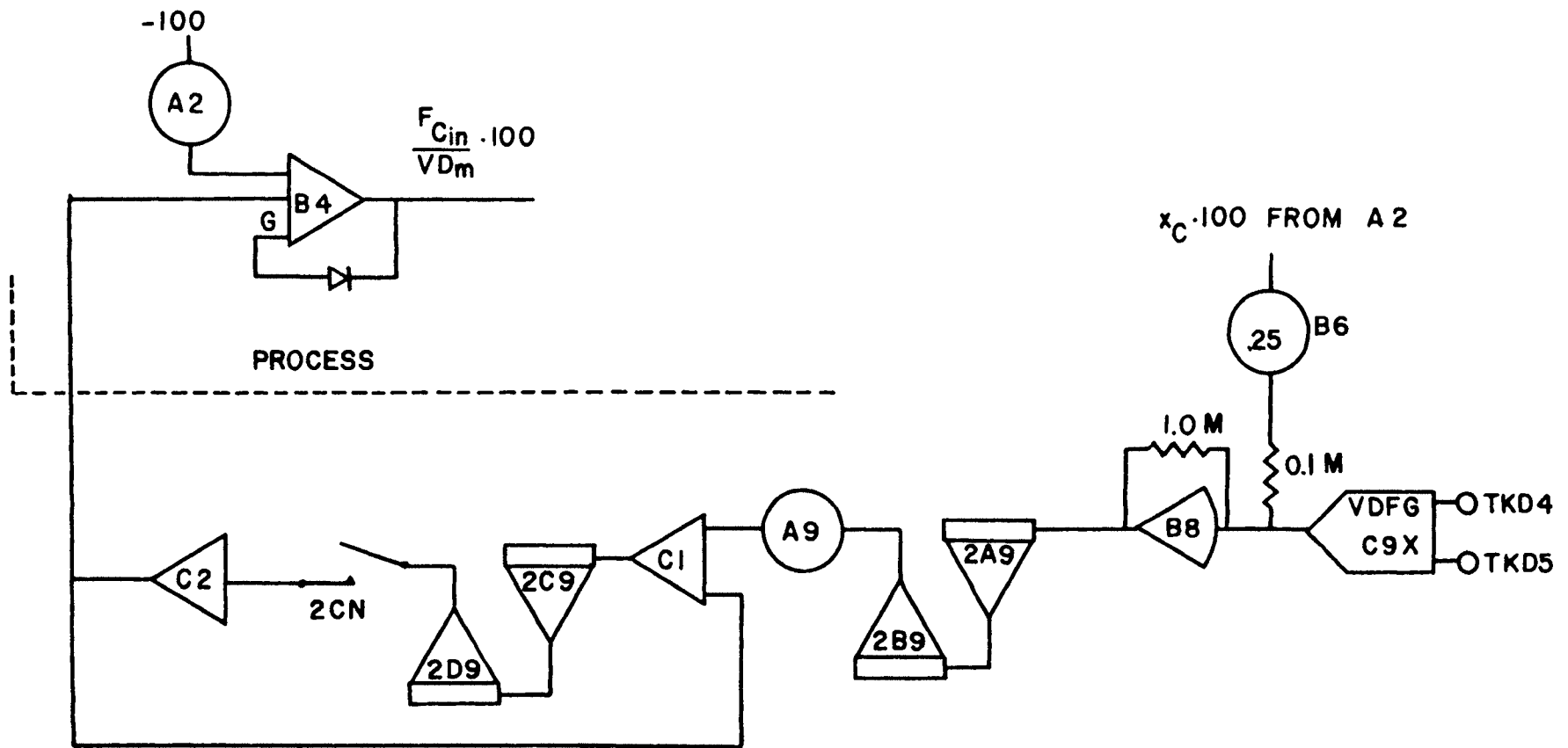


Figure 10B. Analog Program for Simulation of the Sampled Analysis Optimizing Control Scheme.

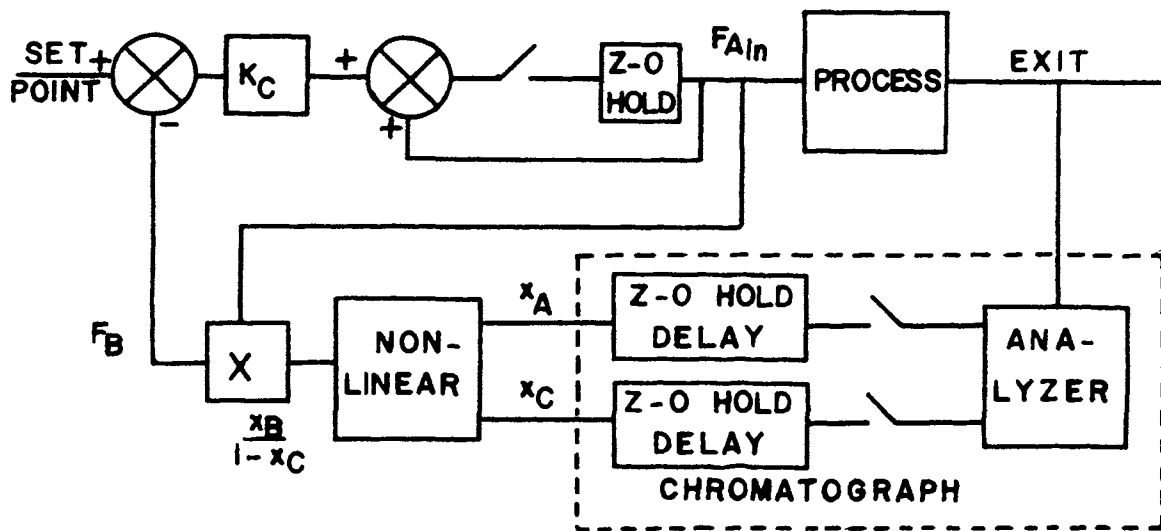


Figure 11B. Sampled Analysis Production Control Scheme.

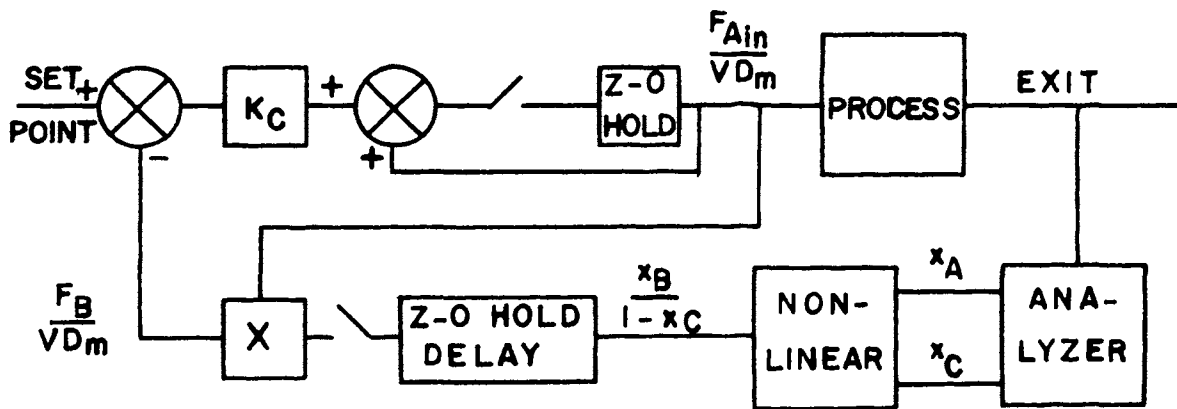


Figure 12B. Sampled Analysis Production Control Scheme for Simulation Purposes.

product of the delayed value of $x_B/(1 - x_C)$ and the current value of F_{Ain}/VD_m is computed. This computed value of production is compared with the set point and a correction made in the feed rate of A.

The system presented in figure 12B exhibits the same characteristics as the system in figure 11B but requires less equipment to simulate. The controller section uses the following equation, similar to 11B, to determine the feed rate of reactant A:

$$F_{Ain}/VD_m(i) = F_{Ain}/VD_m(1) + K_p(e_p(i-1) + e_p(i-2) + \dots + e_p(3) + e_p(2) + e_p(1)) \quad 12B.$$

where: i = time increments

K_p = controller gain; $(\text{time}^{-1})/(\text{time}^{-1} \text{ B})$

$e_p(i)$ = production error at time i ; $\text{time}^{-1} \text{ B}$

Figure 13B, page 129, is the section of the analog program used to simulate the sampled analysis production control. Table IV-B is the component function list for the analog diagrams presented in figures 10B and 13B.

Two track-hold amplifiers are sufficient to simulate both a zero-order hold and a delay. Three pulsers instead of a pulser pair are required to time the sampler. Figure 14B is a patching diagram of the control logic board which contains the pulsers and controls the analog simulation. Figure 15B demonstrates graphically the sample-delay order of operation. If the pulse times for pulsers P1 and P3 are made very small compared to that for P2, the output

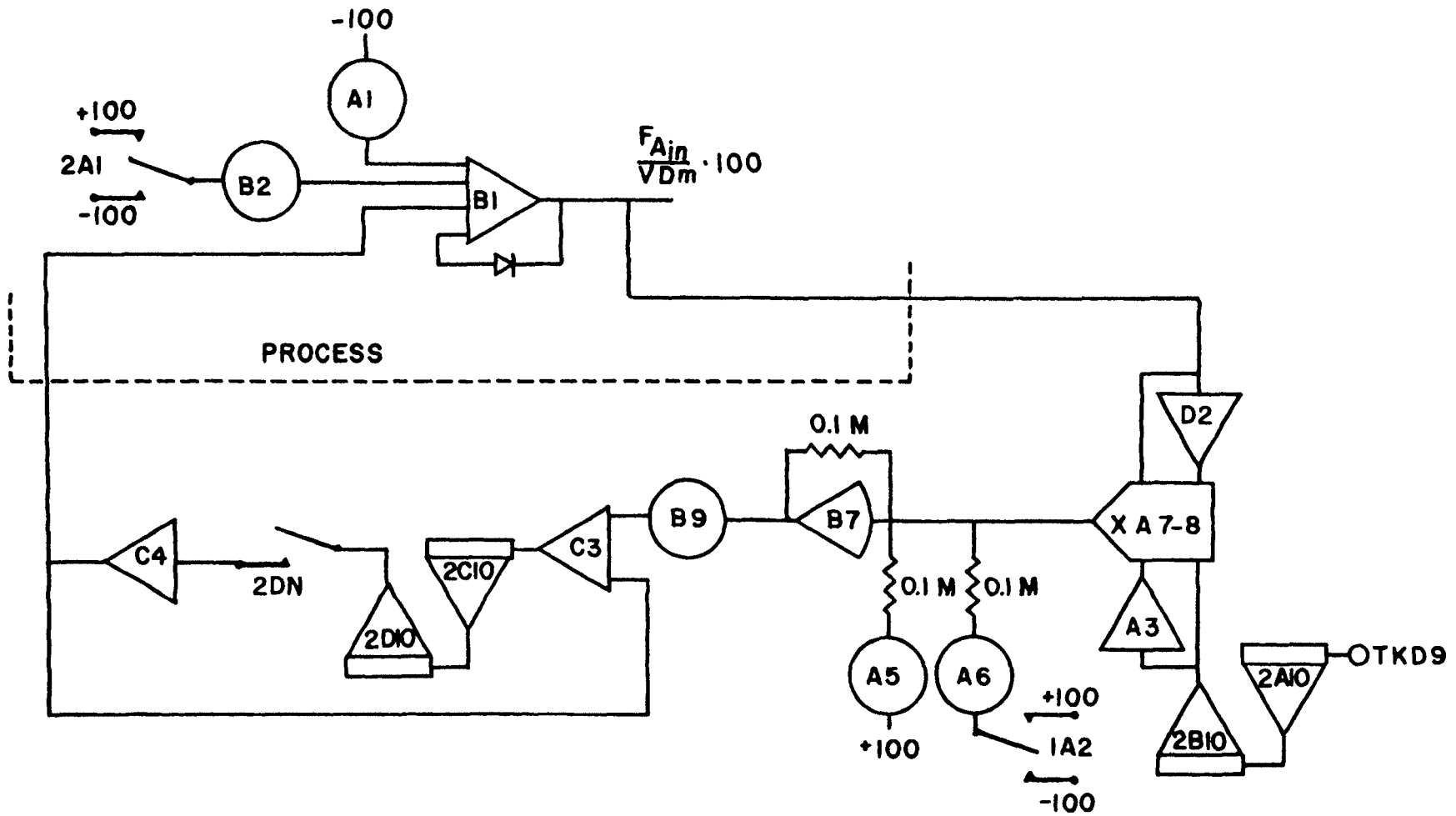


Figure 13B. Analog Program for Simulation of Sampled Analysis Production Control Scheme.

TABLE IV-B
COMPONENT LIST FOR SIMULATION OF THE SAMPLED
ANALYSIS CONTROLLERS, FIGURES 10B AND 13B

Element	Type	Output or Setting	Units
B8	Unloading Amplifier and Summer	Optimum Error, $(e_o)_{250}$	Mole Fraction
C1	Summer	New Controller Output, $(F_{Cin}/VD_m)_{100}$	Minute ⁻¹
C2	Inverter	Controller Output C, $-(F_{Cin}/VD_m)_{100}$	Minute ⁻¹
2A9-2B9	Track-Hold Pair	Optimum Error Z-0 Hold and Delay	Mole Fraction
2C9-2D9	Track-Hold Pair	Controller Output Z-0 Hold, $(F_{Cin}/VD_m)_{100}$	Minute ⁻¹
A9	Potentiometer	Optimizing Loop Gain, $K_o(0.4)$	(Minute ⁻¹ C) / (Mole Fraction C)
C9X	VDFG	Current Signal for Optimum Conc. C, $(x_C \text{ optimum})_{250}$	
2CN	SPST Switch	Closes Optimizing Control Loop	
A3	Inverter	$(x_B/(1 - x_C))_{100}$	Unitless
B7	Unloading Amplifier and Summer	Production Error, $(e_p)_{100}$	Minute ⁻¹
C3	Summer	New Controller Output, $(F_{Ain}/VD_m)_{100}$	Minute ⁻¹

Table IV-B (continued)

Element	Type	Output or Setting	Units
C4	Inverter	Controller Output, $(F_{Ain}/VD_m)100$	Minute ⁻¹
D2	Inverter	Feed of A, $-(F_{Ain}/VD_m)100$	Minute ⁻¹
2A10- 2B10	Track- Hold Pair	$(x_B/(1 - x_C))100$ Z-0 Hold and Delay	Unitless
2C10- 2D10	Track- Hold Pair	Controller Output, Z-0 Hold, $(F_{Ain}/VD_m)100$	Minute ⁻¹
A5	Potenti- ometer	Production Set Point, $(F_B/VD_m)_{SP}$	Minute ⁻¹
A6	Potenti- ometer	Upset in Production Set Point, $(\Delta F_B/VD_m)_{SP}$	Minute ⁻¹
B9	Potenti- ometer	Production Loop Gain, K_p	$(\text{Minute}^{-1} A)/$ $(\text{Minute}^{-1} B)$
A7-8	Multiplier	Current Signal for Production, $(F_B/VD_m)100$	
1A2	SPDT Switch	Step Function for Upset in Production Set Point	
2DN	SPST Switch	Closes Production Control Loop	

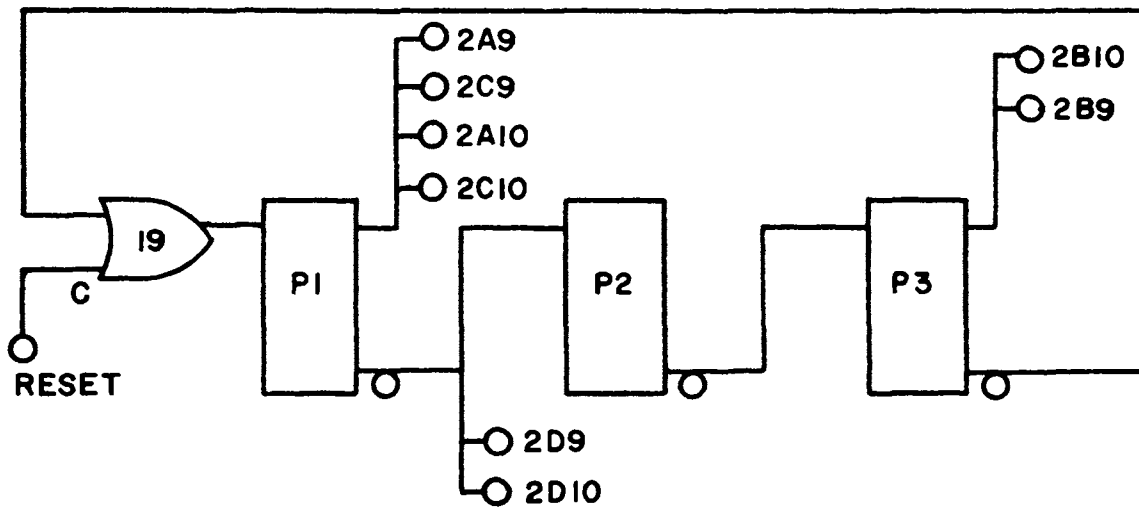


Figure 14B. Control Logic for Generation of Zero-Order Hold and Delay.

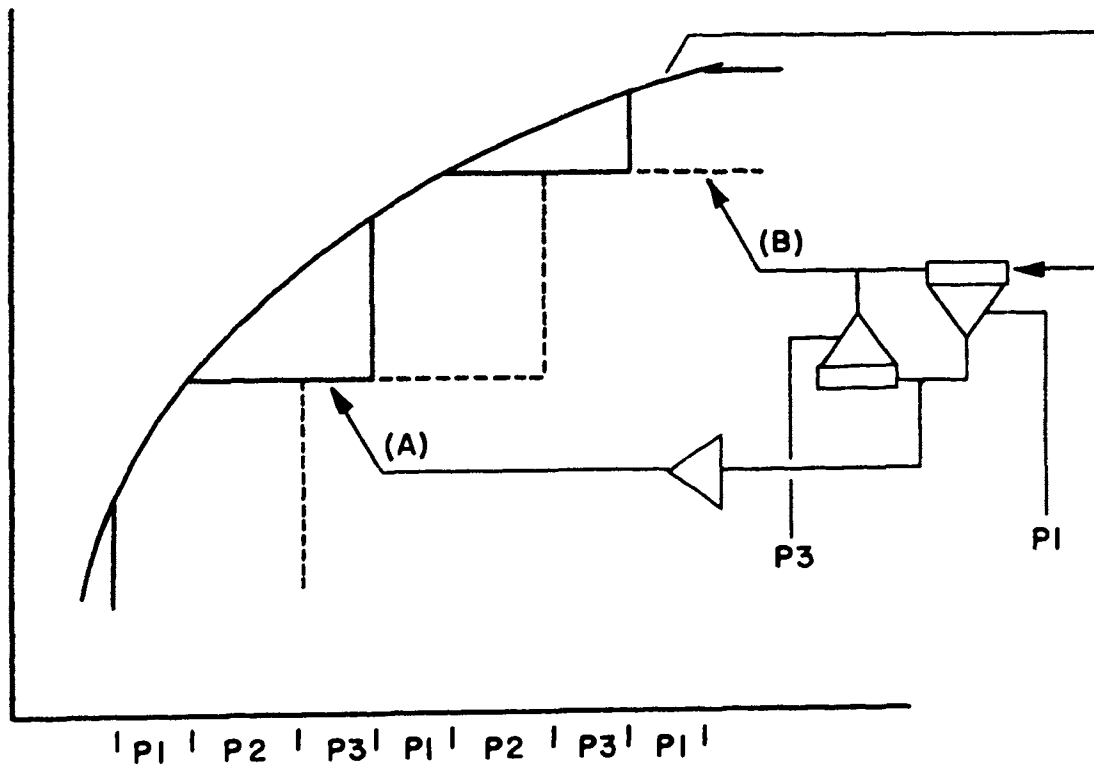


Figure 15B. Action of Zero-Order Hold and Delay from One Track-Hold Pair.

will be sampled and delayed by an amount approximately equal to the P2 pulser time. This characteristic is demonstrated for a ramp input to the sample-delay simulator in figure 16B.

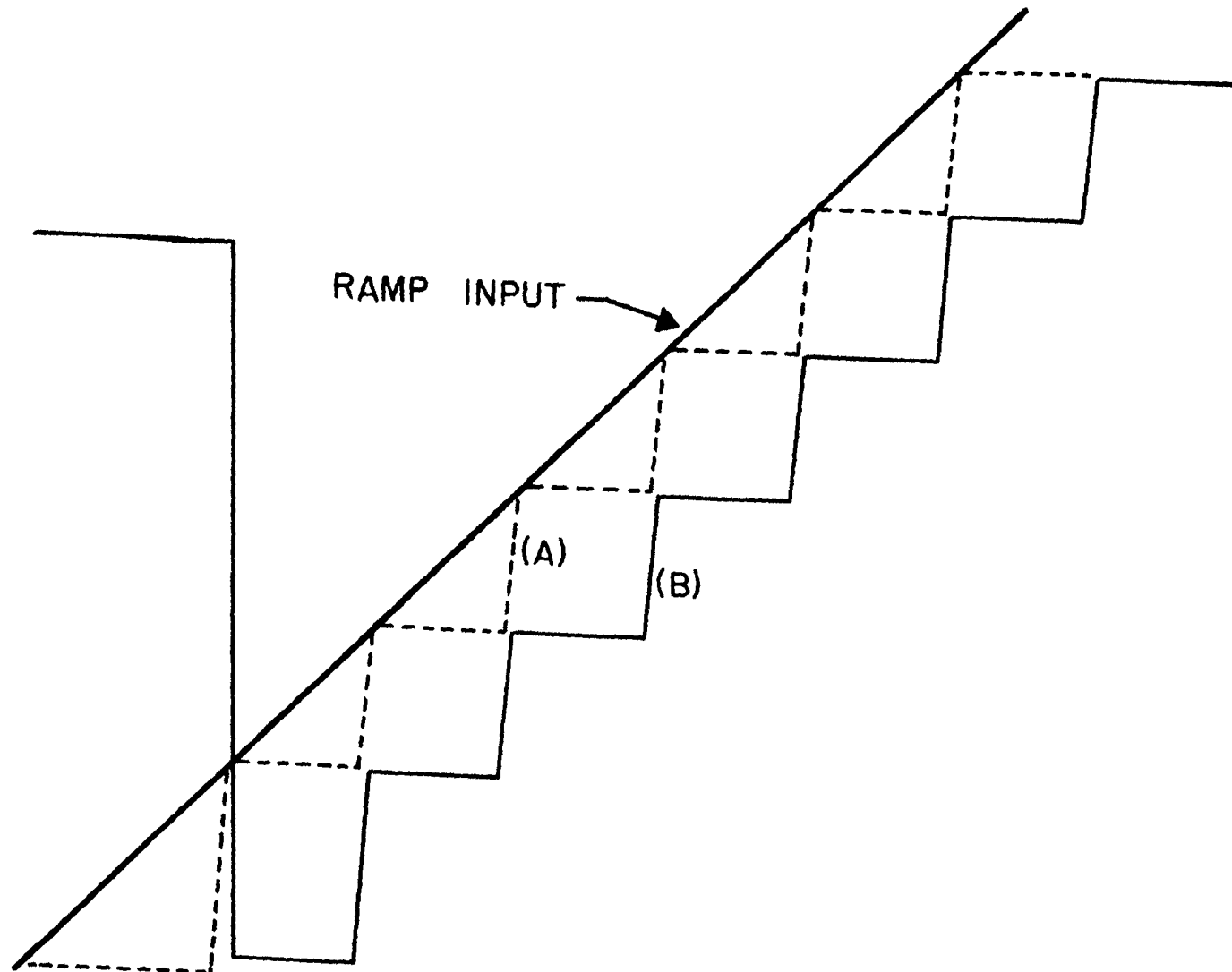


Figure 16B. Output of Track-Hold Pair Generating Both Zero-Order Hold and Delay for Ramp Input.

APPENDIX C
EXPERIMENTAL SYSTEM CONSTRUCTION

1. Reaction

The reaction chosen for this experimental test was the hydrogenation of ethylene to ethane on a nickel catalyst. The reaction has the following stoichiometry:



2. Reactor Design

The reactor was designed to approximate a stirred tank from a dynamic viewpoint. Figure 1C is a simplified drawing of the reaction chamber. The reactor actually consists of a small chamber, 1/8 inch pipe tee, which holds the catalyst particles and a larger chamber to simulate a stirred tank and dampen high frequency composition changes. Eight 1/8 inch by 1/8 inch cylindrical catalyst particles are held in place in the small chamber by four machine screws so that they are directly in the reactant flow stream.

In an attempt to obtain essentially complete mixing a diaphragm pump was installed in a recycle line around the reactor. If this recycle flow could have been maintained at a very high rate, at least a factor of 10 higher than the throughput, the reactor conditions would approach those of complete mixing. However, the rebuilt surplus pump did not meet the manufacturer's original flow rate specifications

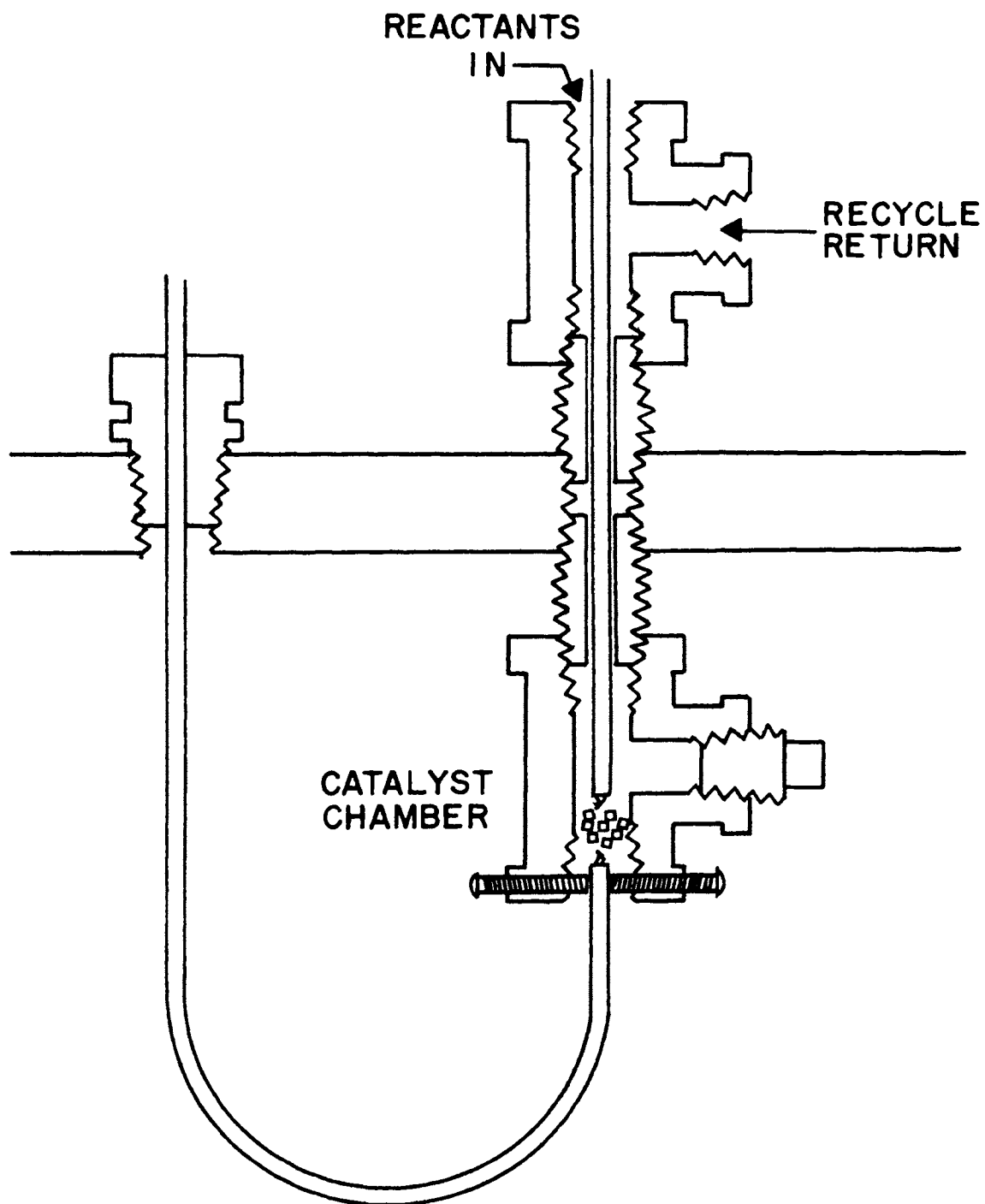


Figure 1C. Reaction Chamber.

and this high flow could not be obtained. The addition of the recycle pump contributes to better mixing and lowers the concentration gradient along the catalyst bed; therefore, it was installed in the system.

The maximum throughput possible without reaction is the sum of the maximum flow rate of hydrogen and ethylene. The maximum flow of hydrogen is 19.2 (cc)/(second) and the maximum flow of ethylene is 13.2 (cc)/(second). Therefore the maximum total flow possible occurs without reaction and is equal to 32.4 (cc)/(second) when the recycle pump is not used. The volume of the reactor section containing the eight 1/8 inch by 1/8 inch cylindrical catalyst particles is approximately 0.47 cc. The void volume and weighted viscosities and densities are calculated at 150^o C. The maximum Reynold's number in the catalyst bed without using the recycle pump is then found to be approximately 300. The recycle pump was attached to the bubble flow meter and the maximum flow found to be approximately 10 (cc)/(second). Therefore, the addition of recycle will not raise the flow out of the laminar region and the catalyst bed is always operated in laminar flow.

Photographs of the reactor appear in figures 2C and 3C, pages 138 and 139.

3. Process Description

Figure 4C, page 140, is a schematic of the reactant feed system. Figure 5C, page 141, is a schematic of the reactor-analyzer system. Instruments are represented by

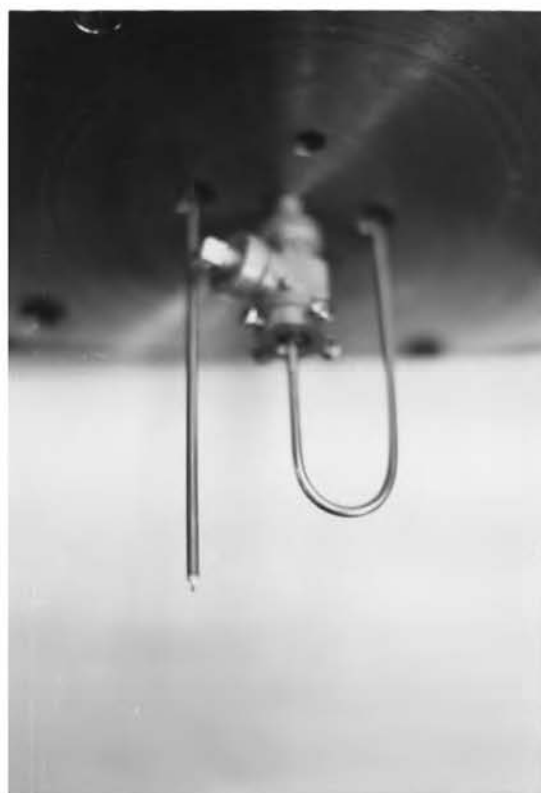
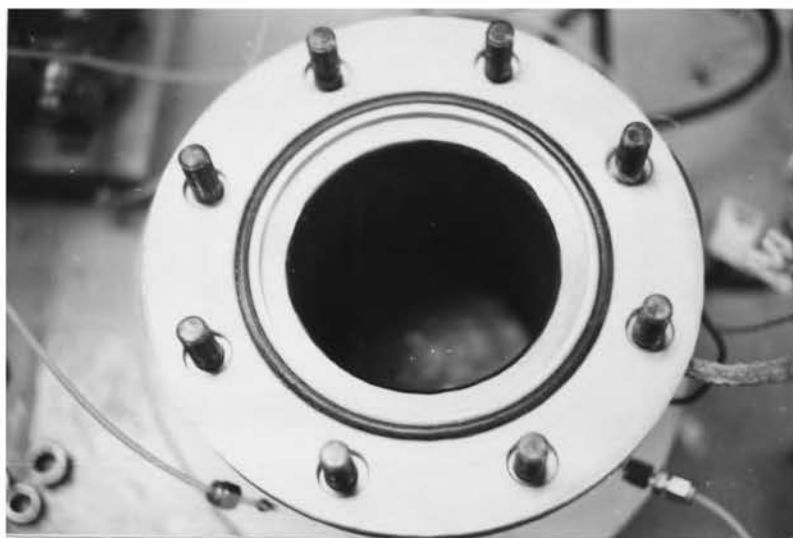


Figure 2C. Main Reaction Chamber and Top Plate.

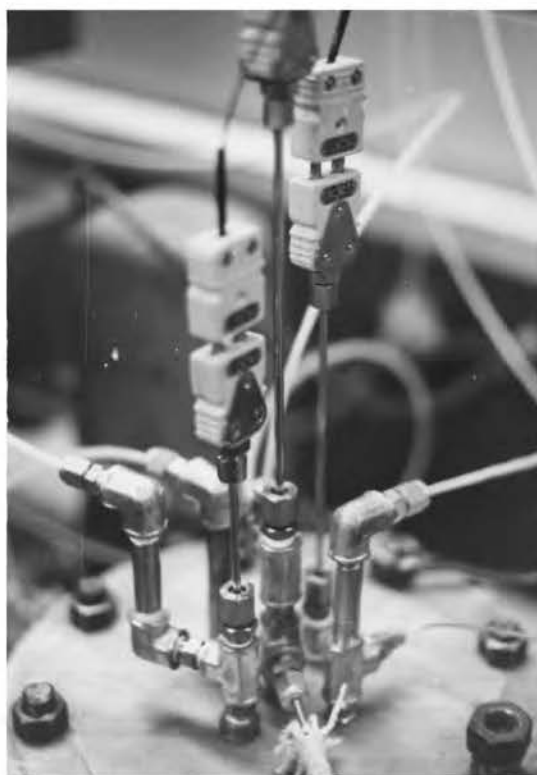
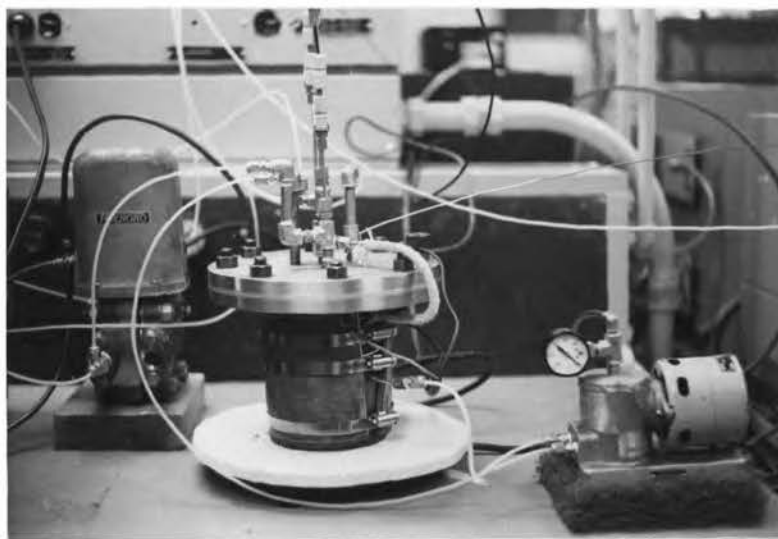


Figure 3C. Main Reactor in System.

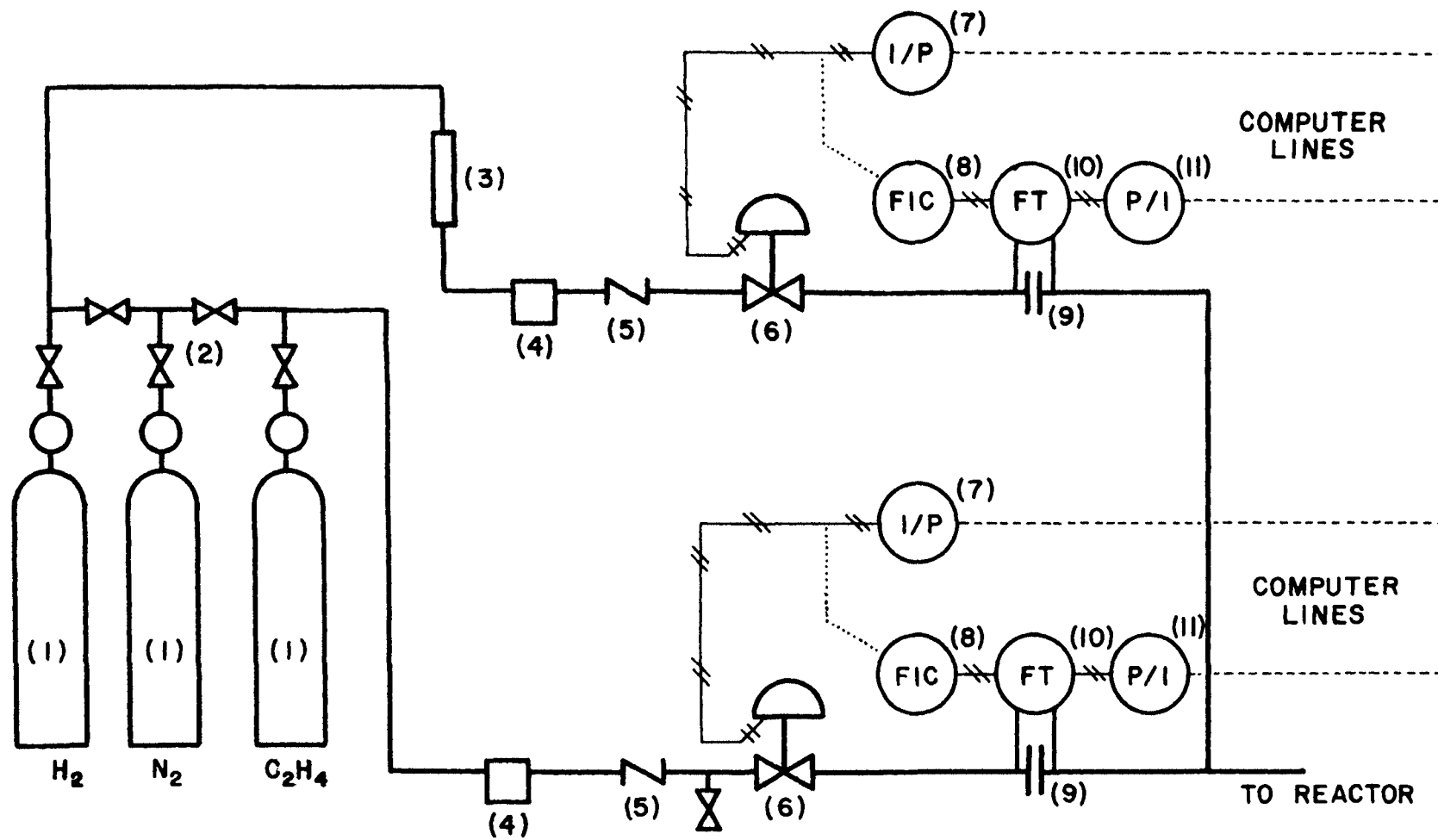


Figure 4C. Reactant Feed Control System.

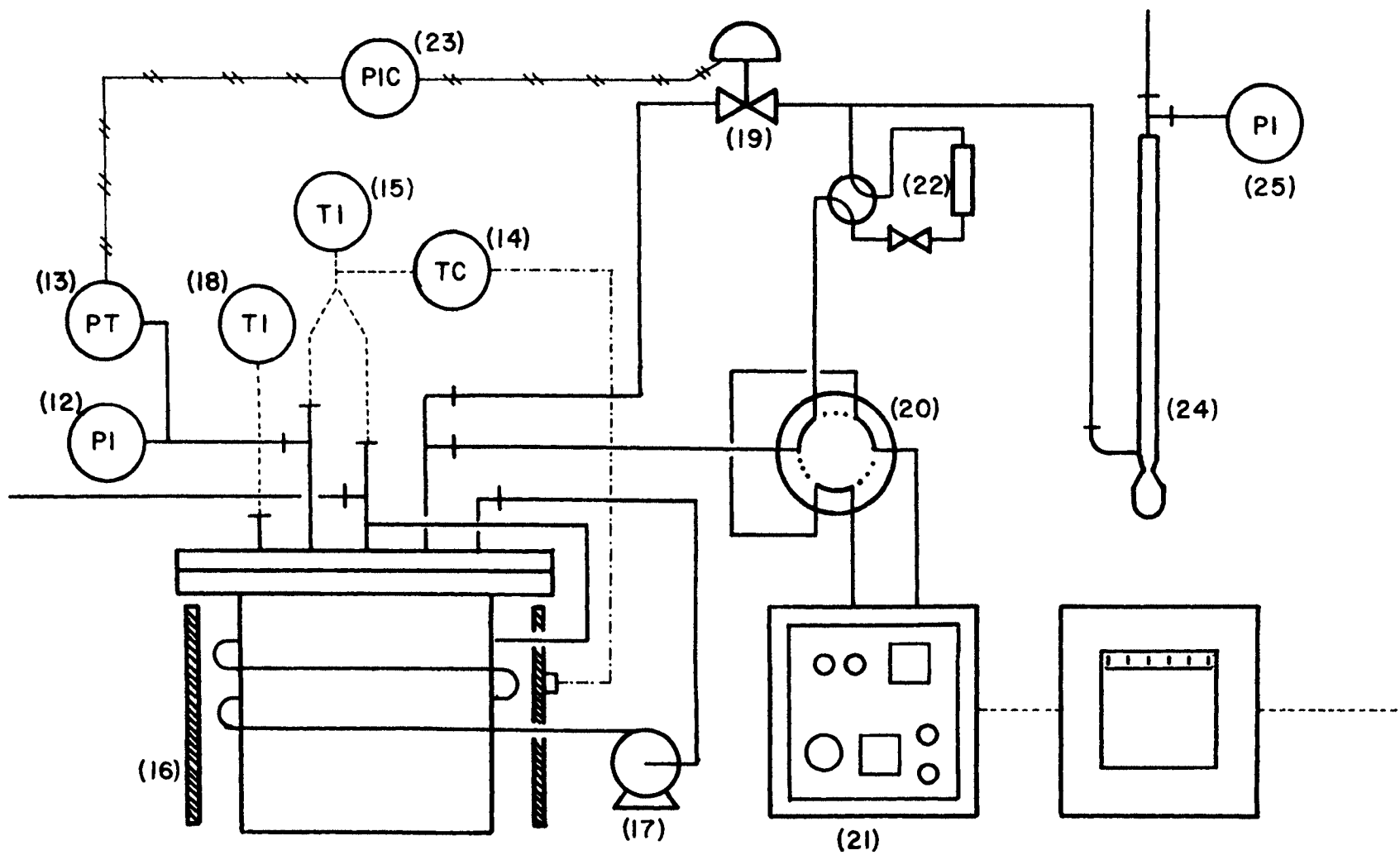


Figure 5C. Reactor - Chromatograph System.

standard ISA symbols and table I-C, page 143, lists all equipment and instruments in these two figures.

The reactants, ethylene and hydrogen, are supplied from high pressure cylinders (1) equipped with two stage regulators. A third cylinder equipped with a single stage regulator is used to supply nitrogen in order to purge the system of oxygen prior to admitting hydrogen. These three cylinders are also equipped with a number of on-off valves (2) which are used to route the reactants and purge gas to different sections of the process. The hydrogen line is equipped with a packed bed catalytic reactor (3), Engelhard Type D, used to react any oxygen in the hydrogen to water which is removed in the desiccant type dryer (4). The ethylene line is connected to a second desiccant type dryer. Both reactant streams pass through check valves (5) and enter air to open diaphragm type motor control valves (6). The pneumatic signal for these valves is obtained from two current to pressure transducers (7) which receive their current inputs from the Applied Dynamics analog computer. The control valves may be switched to receive their power from two standby pneumatic controllers (8).

A photograph of the flow control valves, differential pressure transmitters and instrument pressure to current transducers is presented in figure 6C, page 145.

Orifice meters (9) are employed to measure the two reactant flows. The orifices were intentionally placed

TABLE I-C
EXPERIMENTAL EQUIPMENT LIST

Reference Number	Description
1	Size 1A high pressure cylinders of ethylene, hydrogen and nitrogen
2	On-off valves
3	Hydrogen purifier
4	Desiccant dryers
5	Check valves
6	Reactant motor control valves
7	Current to pressure transducers
8	Standby pneumatic reactant flow controllers
9	Orifice meters
10	Reactant differential pressure transmitters
11	Pressure to current transmitters
12	Reactor pressure indicator
13	Reactor pressure transmitter
14	Temperature controller
15	Catalyst chamber temperature indicator
16	Band heater
17	Recycle pump
18	Main reactor temperature indicator

Table I-C (continued)

Reference Number	Description
21	Gas chromatograph
22	Sample flow control equipment
23	Reactor pressure controller
24	Bubble flow meter
25	Bubble meter pressure indicator

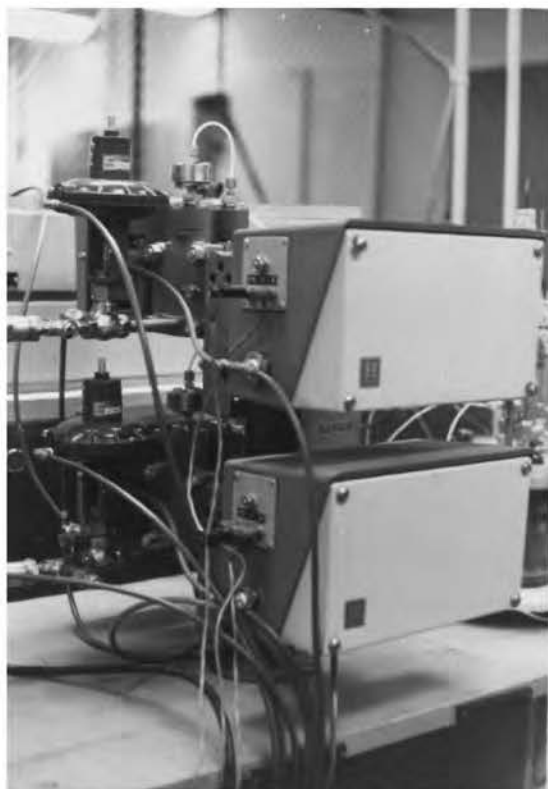


Figure 6C. Reactant Control Valves, dp Transmitters, and P/I Transducers.

downstream of the control valves because the accurate pressure control of the reactor should produce better flow reproducibility. The differential pressures across the orifices are measured by two differential pressure to instrument pressure transmitters (10). The signal from these differential pressure transmitters is converted to one acceptable to the computer by the pressure to current transducers (11). The two reactants then pass into a pipe tee placed directly over the catalyst bed.

As shown in figure 5C, page 141, there are a total of five pipe threaded ports in the top plate of the main reactor. A tee is connected to one port which then feeds a pressure indicator (12) and a pressure transmitter (13). A relatively low reactor pressure is required since it is used to force a stream of product through the sampling valve. Because of the low pressure required the pressure transmitter used is a differential pressure transmitter with the low pressure port open to the atmosphere.

A bare chromel alumel thermocouple is connected to the pressure port and as shown in figure 1C, page 136, makes a 180° bend and is inserted into the bottom of the catalyst bed. The reactants enter the reactor through the center port. Another bare chromel alumel thermocouple is also connected to this center port and is inserted into the top of the catalyst bed. These two thermocouples are connected in parallel to a temperature controller (14) and a null

balance digital millivoltmeter (15). The controller supplies power to a band heater (16) wrapped around the reactor. In this manner the measured temperature, being controlled, is the average of the temperature at the top of the bed and that at the bottom of the bed.

The return line from the recycle pump (17) also enters the center port, in another tee just below the reactant feed. This recycle return line is a length of 1/8 inch stainless steel tubing, approximately 4 feet long, which is coiled between the reactor and the band heater.

A third port contains a third chromel alumel thermocouple which extends into the main reactor to within about 1 inch of the bottom. This thermocouple is monitored with another null balance digital voltmeter (18). The fourth port is the supply point for the recycle pump.

The last port used is the exit of the reactor for the two parallel product streams. As shown in figure 5C, page 141, the main stream goes directly to the upstream side of the exit control valve (19). The sampled stream passes through a gas sampling valve (20) attached to the gas chromatograph (21) and exits through a constant differential type flow controller, a valve and rotameter (22) to the downstream side of the exit control valve.

Since normalization is not utilized in the calculation of the product composition from the chromatograph signal the number of moles in the sampling loop must be held constant

for each sample. The sample pressure is controlled by holding both the reactor pressure and the flow through the sampling valve constant. The sample is passed through a relatively long length of 1/16 inch chromatograph type tubing so that it comes to ambient temperature.

The output of the reactor pressure transmitter (13) is the input to a conventional proportional-integral pneumatic controller (23). The output of the P-I controller drives the exit control valve (19). This system then controls the reactor pressure.

The total exit flow passes through a 100 cc graduated cylinder (24) used as a bubble flow meter and then to an external vent. The pressure in the bubble flow meter is monitored with a pressure indicator (25). The bubble flow meter is used to calibrate the orifice meters. A photograph of the bubble flow meter, the exit control valve and the pressure indicators is presented in figure 7C.

Detailed descriptions of the transducer connections and the analog computer--gas chromatograph interface are presented in Appendices D and E respectively.

4. Analog Program

Figure 8C, page 150, is the analog program used to control the pilot scale reactor system. This analog program contains two cascade control loops--one controlling the hydrogen flow with the set point used to control production and the second controlling the ethylene flow with the set point used to maintain the economic optimum.

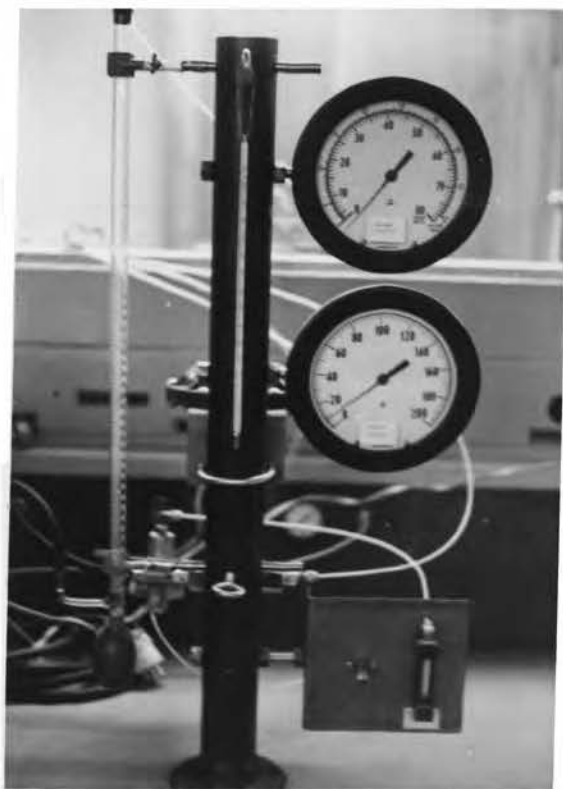


Figure 7C. Bubble Flow Meter, Exit Flow Control Equipment, and Pressure Indicators.

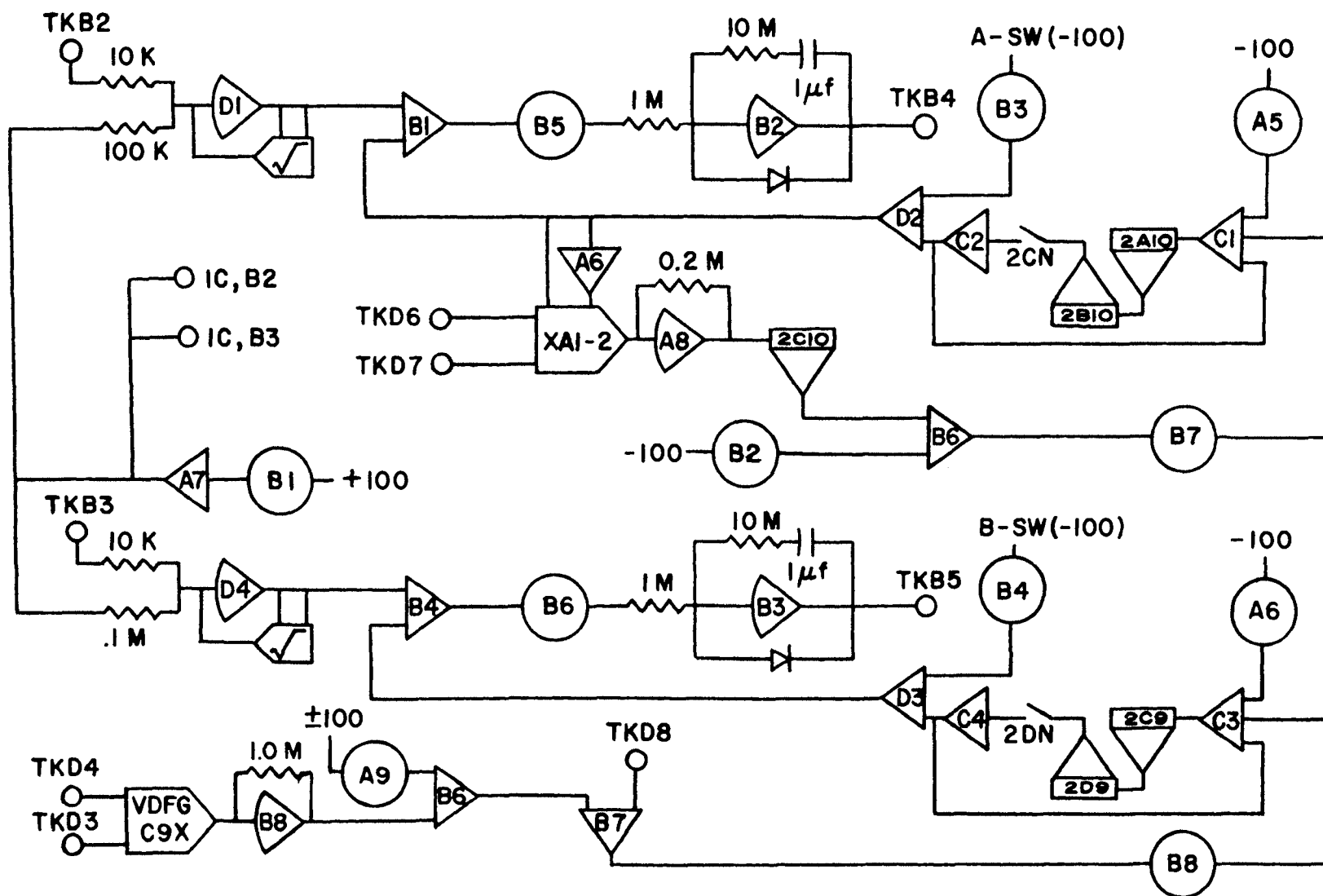


Figure 8C. Analog Program for Pilot Scale Reactor Control.

TABLE II-C
COMPONENT LIST FOR PILOT SCALE
REACTOR CONTROL, FIGURE 8C

Element	Type	Output or Setting	Units
A6	Inverter	Hydrogen Feed Rate Set Point	% Maximum
A7	Inverter	Zeroing Voltage, (25.0 volts)	
A8	Unloading Amplifier	Ethane Flow Rate	% Maximum Hydrogen
B1	Summer	Hydrogen Feed Rate Error	% Maximum
B2	High Gain Amplifier	Hydrogen Control Valve Position	% Maximum
B3	High Gain Amplifier	Ethylene Control Valve Position	% Maximum
B4	Summer	Ethylene Feed Rate Error	% Maximum
B6	Summer	Optimum Conc. Ethylene (250) with Optional Offset	Mole Fraction
B7	Summer	Optimum Error (250)	Mole Fraction
B8	Unloading Amplifier	Optimum Conc. Ethylene (250)	Mole Fraction
C1	Summer	New Hydrogen Set Point Correction	% Maximum
C2	Inverter	Hydrogen Set Point Correction	% Maximum

Table II-C (continued)

Element	Type	Output or Setting	Units
C3	Summer	New Ethylene Set Point Correction	% Maximum
C4	Inverter	Ethylene Set Point Correction	% Maximum
D1	Unloading Amplifier and Summer	Hydrogen Feed Rate (Linear)	% Maximum
D2	Summer	Hydrogen Feed Rate Set Point	% Maximum
D3	Summer	Ethylene Feed Rate Set Point	% Maximum
D4	Unloading Amplifier and Summer	Ethylene Feed Rate (Linear)	% Maximum
A5	Potentiometer	Hydrogen T-H Drift Correction	% Maximum
A6	Potentiometer	Ethylene T-H Drift Correction	% Maximum
A9	Potentiometer	Optional Offset in Optimum Conc. Ethylene	Mole Fraction
B1	Potentiometer	Zeroing Voltage, .25	
B2	Potentiometer	Ethane Flow Rate Set Point	% Maximum Hydrogen
B3	Potentiometer	Manual Hydrogen Flow Set Point	% Maximum
B4	Potentiometer	Manual Ethylene Flow Set Point	% Maximum
B5	Potentiometer	Hydrogen Flow Control Parameter	

Table II-C (continued)

Element	Type	Output or Setting	Units
B6	Potentiometer	Ethylene Flow Control Parameter	
B7	Potentiometer	Production Control Loop Gain, K_p	Unitless
B8	Potentiometer	Optimizing Control Loop Gain, K_o	(% Ethylene)/ (Mole Fraction)
2A10- 2B10	Track- Hold Pair	Hydrogen Set Point Correction, Z-0 Hold	% Maximum
2C9- 2D9	Track- Hold Pair	Ethylene Set Point Correction, Z-0 Hold	% Maximum
A1-2	Multiplier	Current Signal for Ethane Flow Rate	
C9X	VDFG	Current Signal for Optimum Conc. Ethylene	
2CN	SPST Switch	Closes Production Loop	
2DN	SPST Switch	Closes Optimizing Loop	

The signal obtained from an orifice flow meter is proportional to the square of the flow. To obtain a signal which is linear with respect to flow the square root of this signal must be taken. The "zero" voltage of the instrument pressure to current transducer, 2.5 volts for this calibration, must be subtracted from the signal prior to taking the square root. Amplifier D1 accomplishes the above operations for the hydrogen flow signal and D4 for the ethylene flow signal.

The voltage representing a signal proportional to the square of the hydrogen flow, 2.5 to 12.5 volts, enters in trunk B2. This signal passes through a 10K ohm resistor to the summing junction of D1. The "zero" voltage $\times 10$, 25.0 volts, passes through a 100K ohm resistor to the summing junction of D1. A fixed diode function generator forms the feedback loop for amplifier D1 thereby generating the square root and a signal proportional to the flow of hydrogen. The ethylene flow signal is obtained in the same manner using amplifier D4.

The summing point for the hydrogen flow controller is amplifier B1. The set point is obtained from amplifier D2 in the outer loop and the feedback is of course obtained from amplifier D1 described above. Amplifier B4 is the summing point for the ethylene flow controller.

The errors obtained from amplifier B1 for hydrogen and B4 for ethylene are fed to proportional-integral controllers

constructed by placing a resistor and capacitor in series in the feedback of amplifiers B2 and B3. This circuit for constructing a P-I controller with a single amplifier is presented by Coughanowr and Koppel (29).

The output of these P-I controllers feed thru current to pressure transducers and adjust instrument pressure to the reactant flow motor control valves. The "zero" voltage of these current to pressure transducers is 25.0 volts. This "zero" voltage is placed on the amplifiers used as P-I controllers as an initial condition.

The outside loops which place the set points for the reactant flow controllers are identical to those used in the simulation. The production rate is calculated again from equation 10B, page 112.

$$F_B = F_{Ain}(x_B/(1 - x_C)) \quad 10B.$$

which may be written:

$$F_{C_2H_6} = F_{H_2in}(x_{C_2H_6}/(1 - x_{C_2H_4})) \quad 2C.$$

The composition group, $x_{C_2H_6}/(1 - x_{C_2H_4})$, is calculated in the non-linear section described later. The product of this composition group and the feed rate of reactant A, the hydrogen, is generated at amplifier A8, figure 8C, to give a voltage proportional to production rate at steady state. The production rate set point is placed on potentiometer B2 and the deviation from this set point generated in amplifier B6. The actual production rate used to generate this error is the product of the current feed rate of hydrogen and the

value of the composition group, $x_{C_2H_6}/(1 - x_{C_2H_4})$, delayed by the chromatograph. The value of the composition group changes when the control pulse goes on and the value of the feed rate of hydrogen changes when the control pulse goes off; therefore, the actual production used to generate the production error appears only during the control pulse. Track-hold amplifier 2C10, figure 8C, is used to hold this error for the recorder.

The sampling time for experimental operation is relatively long, 3 minutes, and the track-hold amplifiers are found to drift slightly, less than one percent, over this period. The drift rate was found to be very constant, invariant with changes in the actual voltage. Potentiometers A5 and A6 were then added to compensate for this drift. In this manner the drift remains during the sample period but is corrected at the end of each sample period.

The program for calculation of the exit concentration from the chromatograph signal is presented in Appendix E, page 171.

The patching diagram for the analog program used to perform the necessary non-linear calculations is shown as figure 9C. Equation 30, page 43, is solved to provide an estimate of the reactor parameter, F_{Ain}/kV . For the experimental system equation 30 may be written:

$$F_{H_2in}/kV - x_{H_2} x_{C_2H_4} (1 - x_{C_2H_4})/x_{C_2H_6} \quad 3C.$$

The voltage representing the exit concentrations are

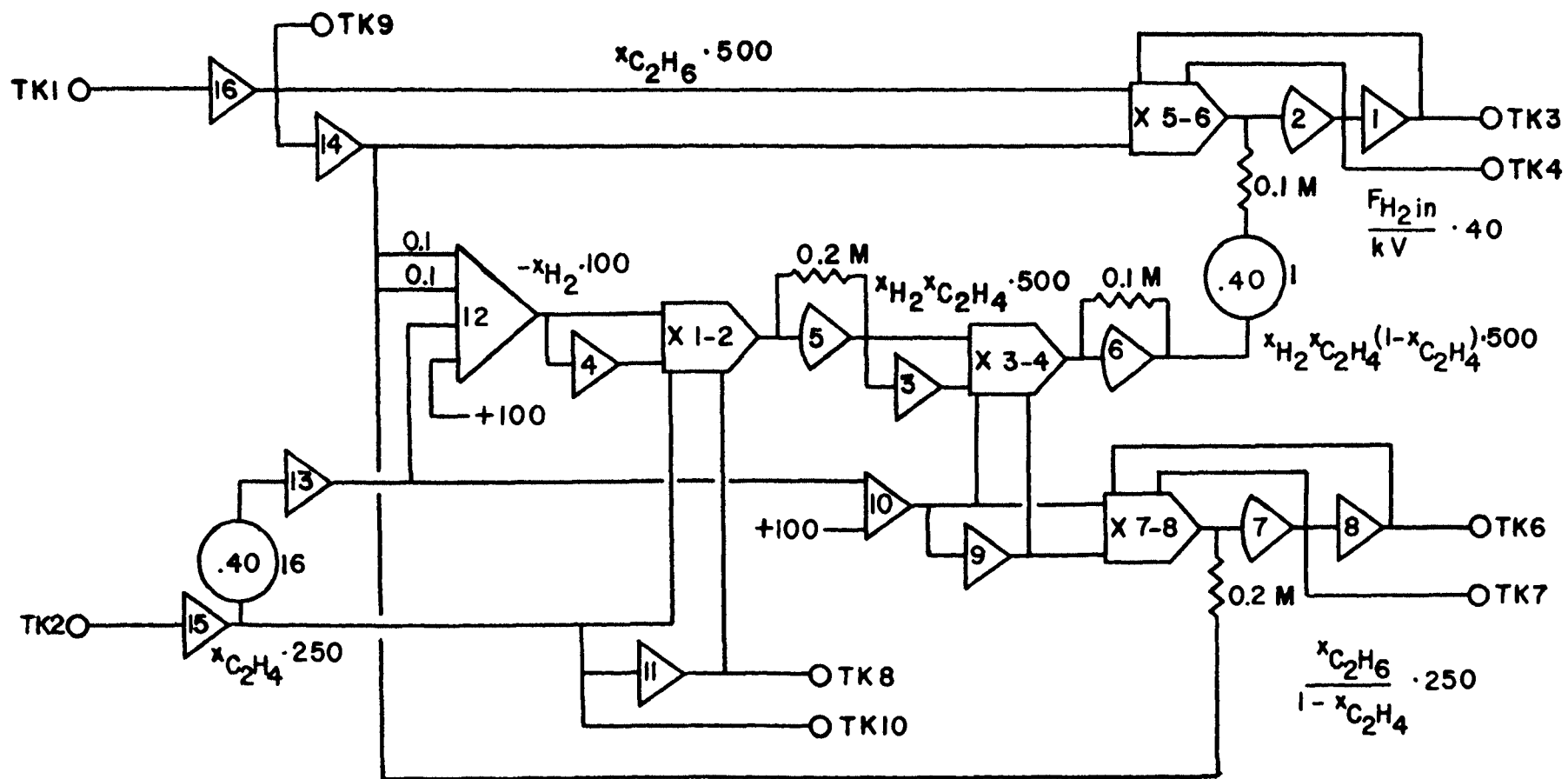


Figure 9C. Analog Program for Calculation of Non-Linear Functions of Composition for use with the Experimental Reactor.

$(x_{\text{C}_2\text{H}_4})250$ for ethylene, $(x_{\text{C}_2\text{H}_6})500$ for ethane, and $(x_{\text{H}_2})100$ for hydrogen. The scaled value of the reactor parameter is $(F_{\text{H}_2\text{in}}/\text{kV})40$.

Basically this program, figure 9C, differs from the one used in the simulation in the scaling employed and the chemical analysis of one reactant, ethylene, and the product, ethane, instead of both reactants. The concentration of hydrogen is obtained by difference in the experimental system.

A motor driven cam timer controls the sampling sequence. The cams control the position of single pole, double throw switches which are supplied with logic one and logic zero from the control logic system of the Applied Dynamics 40. They return logic signals to control the computer components. The control logic program used to control the sampled data control sequence is presented in figure 10C, page 159. Gate 3 receives a pulse from trunk 1 during each sample injection. Gate 3 then triggers a pulser inserted to prevent a relay bounce from causing a multiple sequence. The output of the pulser then activates the track-hold amplifiers to effect one control step. Push-button 1 can also be used to activate a single control step.

Gates 12 and 13, actuated by latching switches 3 and 4 close the inner loops of the flow control system by placing amplifiers B2 and B3 in the operate mode. Latching switches 1 and 2 are used to close the outer loops of the

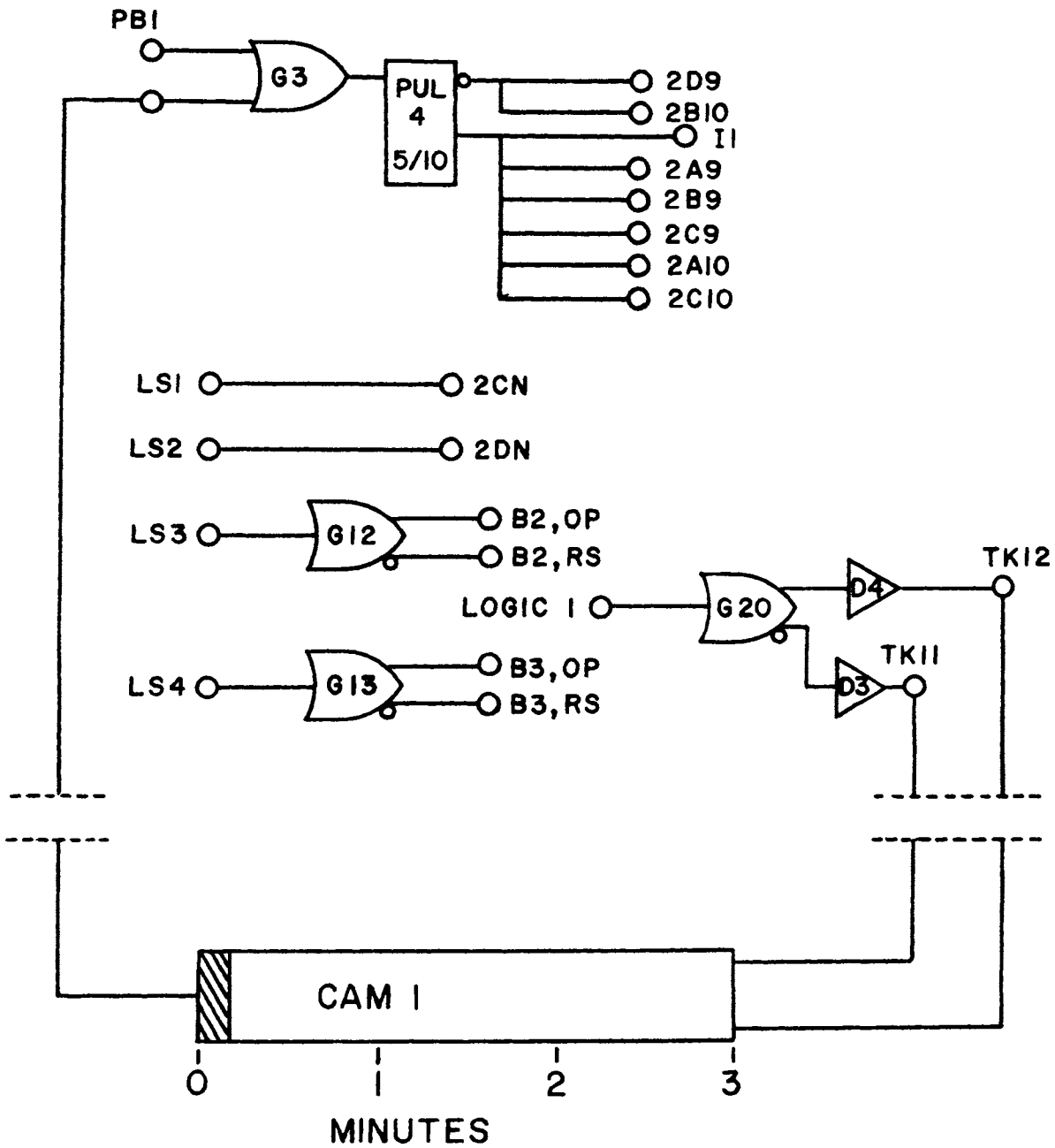


Figure 10C. Logic Program for Activation of Sampled Data Control Sequence.

flow control system activating the production and optimizing controllers respectively.

Specifications for the instruments and equipment used in this experimental reactor system are presented in Appendix F, page 178.

APPENDIX DPROCESS - ANALOG COMPUTER INTERFACE

The current to pressure transducers, figure 4C, page 140, are used to convert a voltage signal from the analog computer to an instrument pressure which powers a motor control valve. A resistor and potentiometer is built into the rear cover plate of each transducer to scale the analog voltage signal to the current range of the transducer. Figure 1D is the electrical circuit used.

The pressure to current transducers, figure 4C, page 140, are used to convert the output instrument pressure of the differential pressure transmitters to a voltage signal which can be accepted by the analog computer. A 48 volt D.C. power supply is used to supply the power for these transducers. A resistor and potentiometer is built into the cover plate of each pressure to current transducer to scale the output current to a voltage range convenient for use with the analog computer. Figure 2D is the electrical circuit used.

A surplus helical feedback potentiometer is attached to the chromatograph recorder pen drive cable, figure 5C, page 141. This potentiometer serves as a transmitting potentiometer and supplies the computer with a voltage

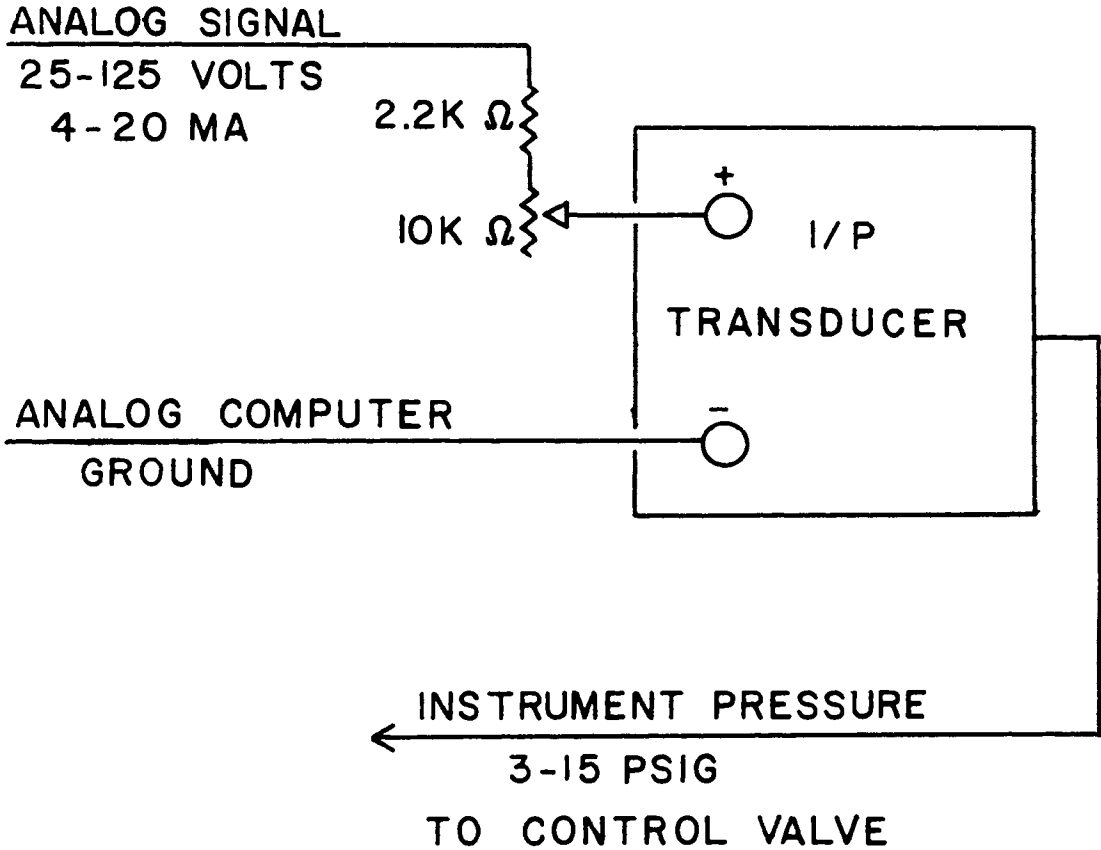


Figure 1D. Current to Pressure Transducer Wiring.

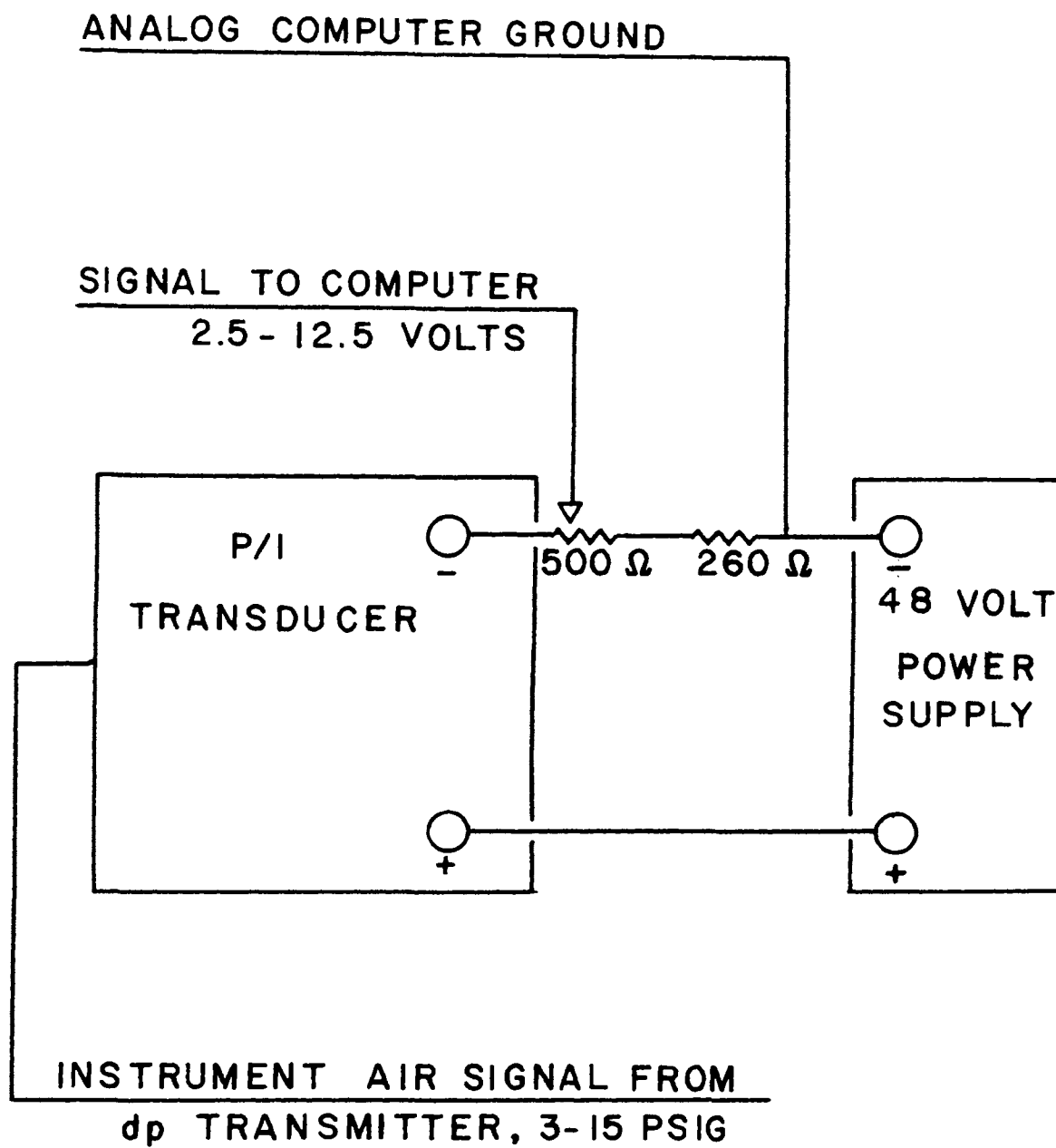


Figure 2D. Pressure to Current Transducer Wiring.

proportional to the pen position of the strip chart recorder. The wiring diagram for the transmitting potentiometer is presented in figure 3D, page 165.

The process - computer interface wiring for the analog instruments is listed in table I-D, page 166.

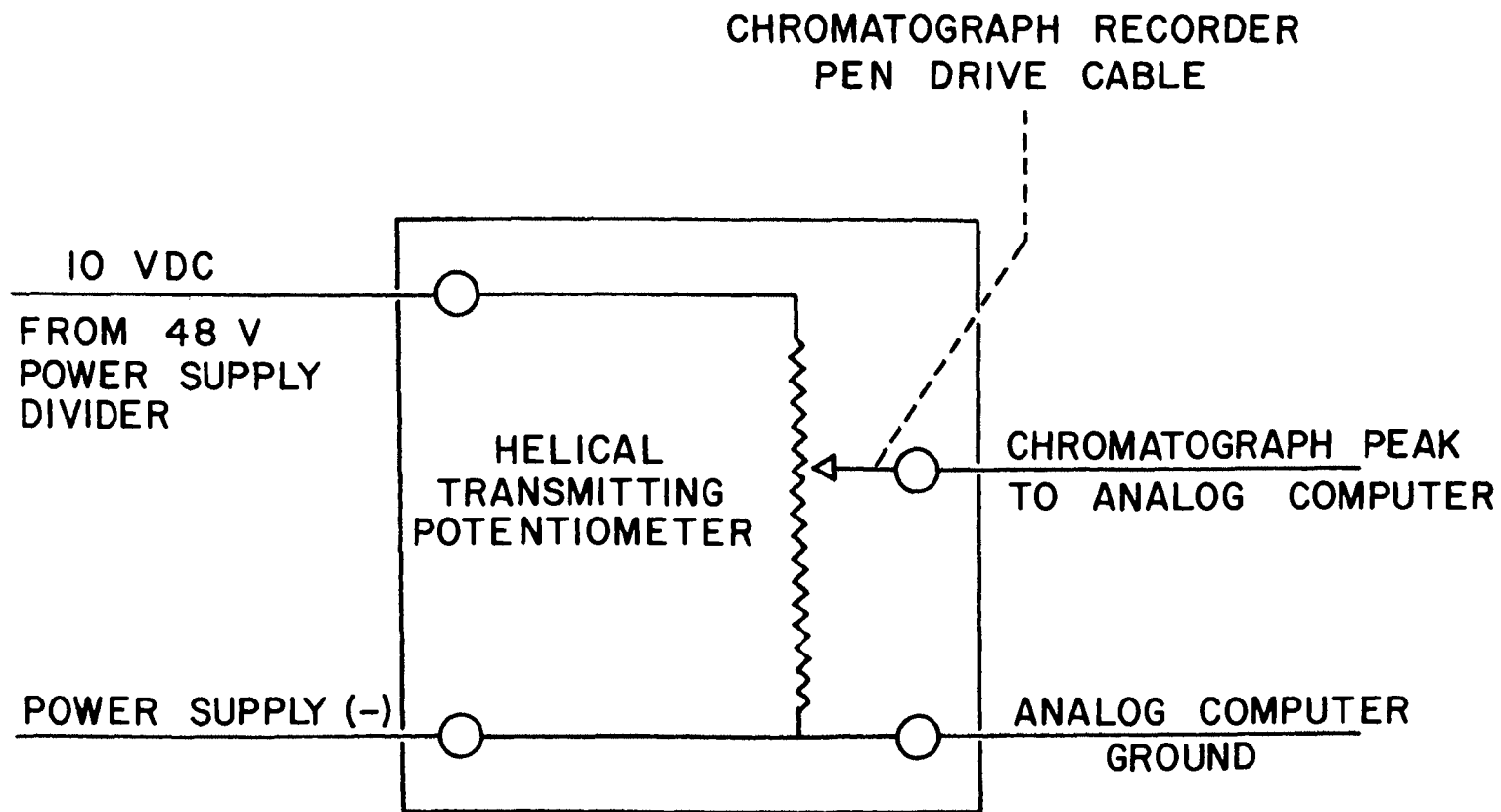


Figure 3D. Transmitting Potentiometer Wiring.

TABLE I-D
PROCESS - COMPUTER INTERFACE WIRING

Analog Trunk	Selector Position	Color	Equipment
B1	1	Black	Computer Gnd.
B2	2	Red	Hydrogen P/I
B3	3	Black	Ethylene P/I
B4	4	Green	Hydrogen I/P
B5	5	White	Ethylene I/P
A1		Black	Computer Gnd.
A2		Red	Transmitting Potentiometer

APPENDIX E
CHROMATOGRAPH - COMPUTER INTERFACE

The gas chromatograph operates on the principle of selective absorption to separate the components of a gaseous or vaporized mixture. Samples for analysis are carried through the column packed with a particulate material. The components of the mixture are selectively absorbed and leave the column separated into bands. The carrier gas used in this case is helium and the column is 1/4 inch copper, 3 feet long packed with 100/120 mesh Poropak R, a porous polymer bead.

The Varian 90-P3 chromatograph used is a thermoconductivity type instrument. It contains a bridge circuit composed of resistance elements which have high temperature sensitivity. These elements are contacted by the column eluent and a reference gas. When the thermoconductivity of a separated component differs from that of the reference gas the temperature sensitive elements are cooled at different rates and the bridge becomes unbalanced. The bridge thus generates a signal for each component in the mv range which is recorded on the chromatograph strip chart recorder. Photographs of the chromatograph and strip chart recorder are presented in figures 1E and 2E.

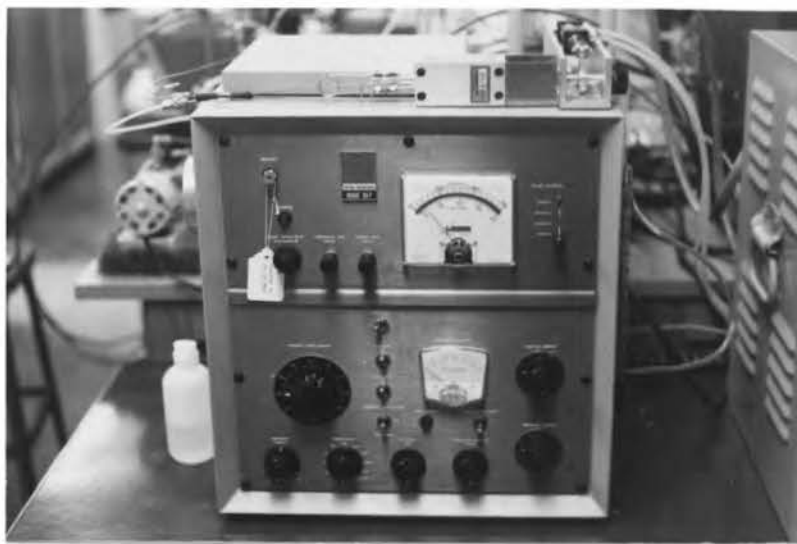


Figure 1E. Varian 90-P3 Gas Chromatograph.



Figure 2E. Chromatograph Strip Chart Recorder.

The analog computer is used to integrate the peaks generated by the chromatograph and thus calculates the sample composition. Each analysis has a reproducibility of ± 0.2 percent of the composition. If steady state data is taken and averaging may be used it is found that a group of analyses are repeatable to ± 0.1 percent.

The analog program used to integrate the peaks is presented in figure 3E, page 171. Amplifier A1 is used to amplify the voltage obtained from the transmitting slide-wire and correct for base line drift. Integrator A2 generates the base line drift correction voltage during a period when it is known that no peak is present. Integrator A3 is used to integrate the ethylene peak and A4 used to integrate the ethane peak. The value of the pot settings on potentiometers A1, A2, A3 and A4 are obtained through a chromatograph calibration.

The chromatograph is calibrated by sampling known compositions obtained from various flow rates of hydrogen and ethylene with no reaction. The slope and y-intercept of the resulting plot of voltage vs. known composition in the operating range is used to calculate the potentiometer settings. Once the calibration is accomplished the chromatograph settings, column temperature, detector temperature, carrier flow rate, etc. are not altered. The output voltage of integrator A3 is calibrated to be the mole fraction of ethylene $\times 250$ and the output voltage of integrator A4 is

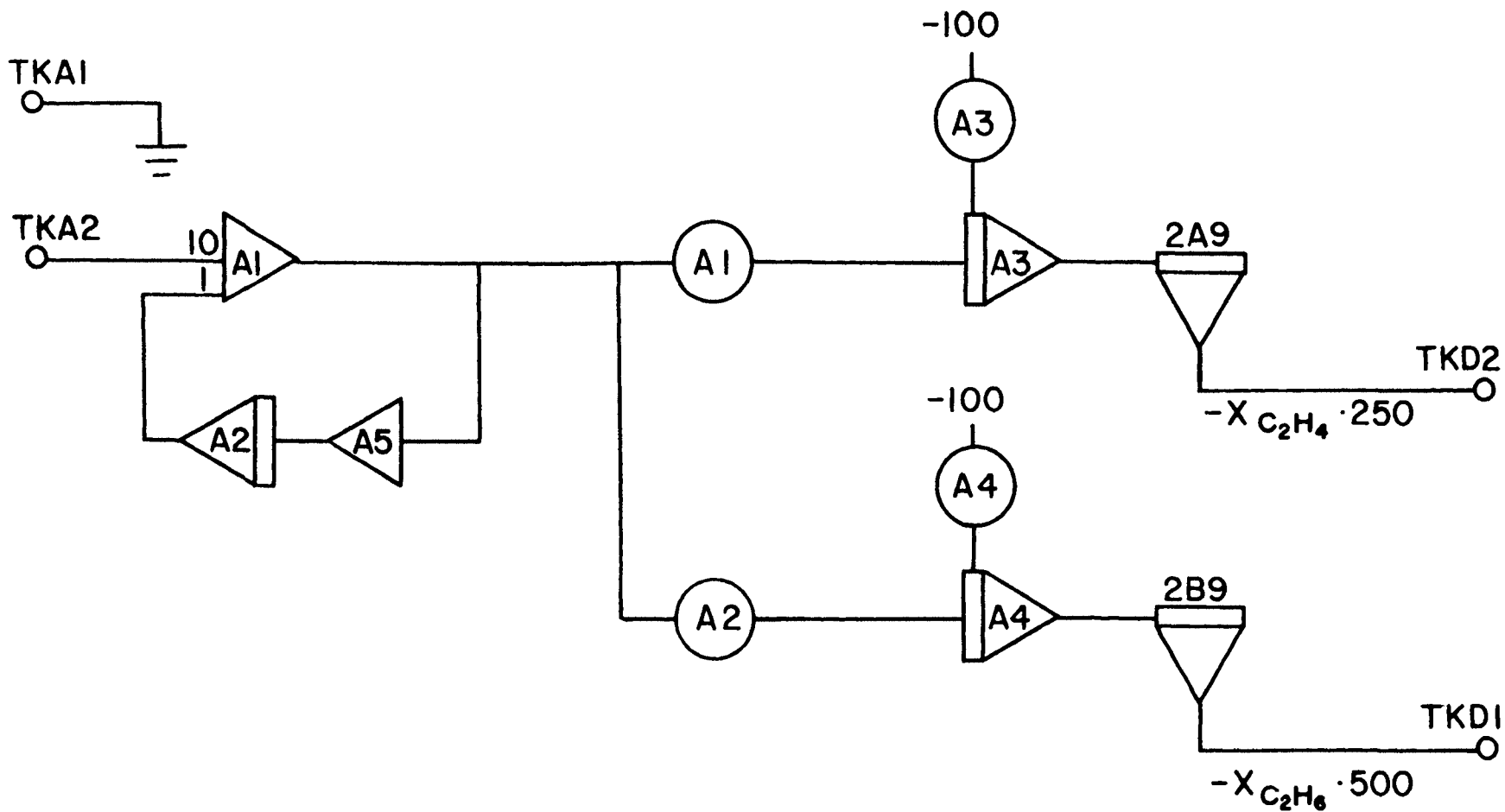


Figure 3E. Analog Program for Calculation of Sample Composition from Chromatograph Output.

calibrated to be the mole fraction of ethane x500.

The following is a list of typical chromatograph operating parameters:

Ambient Temperature: 81^o F
Column Temperature: 119^o F, Column Power: 20%
Detector Temperature: 213^o F, Detector Power: 25%
Injector Temperature: 182^o F, Injector Power: 25%
Carrier Flow Rate: 0.855 (cc)/(second) He
Reference Flow Rate: 0.486 (cc)/(second) He
Filament Current: 200 ma
Sample Flow Rate: 0.2 SCFH indicated
Reactor Pressure: 169 inches water gauge
Potentiometer Settings:

A1 = 0.0955 A3 = 0.0425
A2 = 0.2045 A4 = 0.0100

As mentioned before, page 158, a cam timer made up of a set of motor driven cams which actuate SPDT switches supplied with logic signals controls the entire system. A diagram showing the cam positions and the control logic program used in conjunction with the timer is presented in figure 4E. A logic one signal is applied to the logic trunk during the shaded period. One cam is used to actuate the sampled control schemes described in the experimental section, figure 10C, page 159. The timer - computer wiring is presented in table I-E, page 174.

Two additional cams are used to control the position

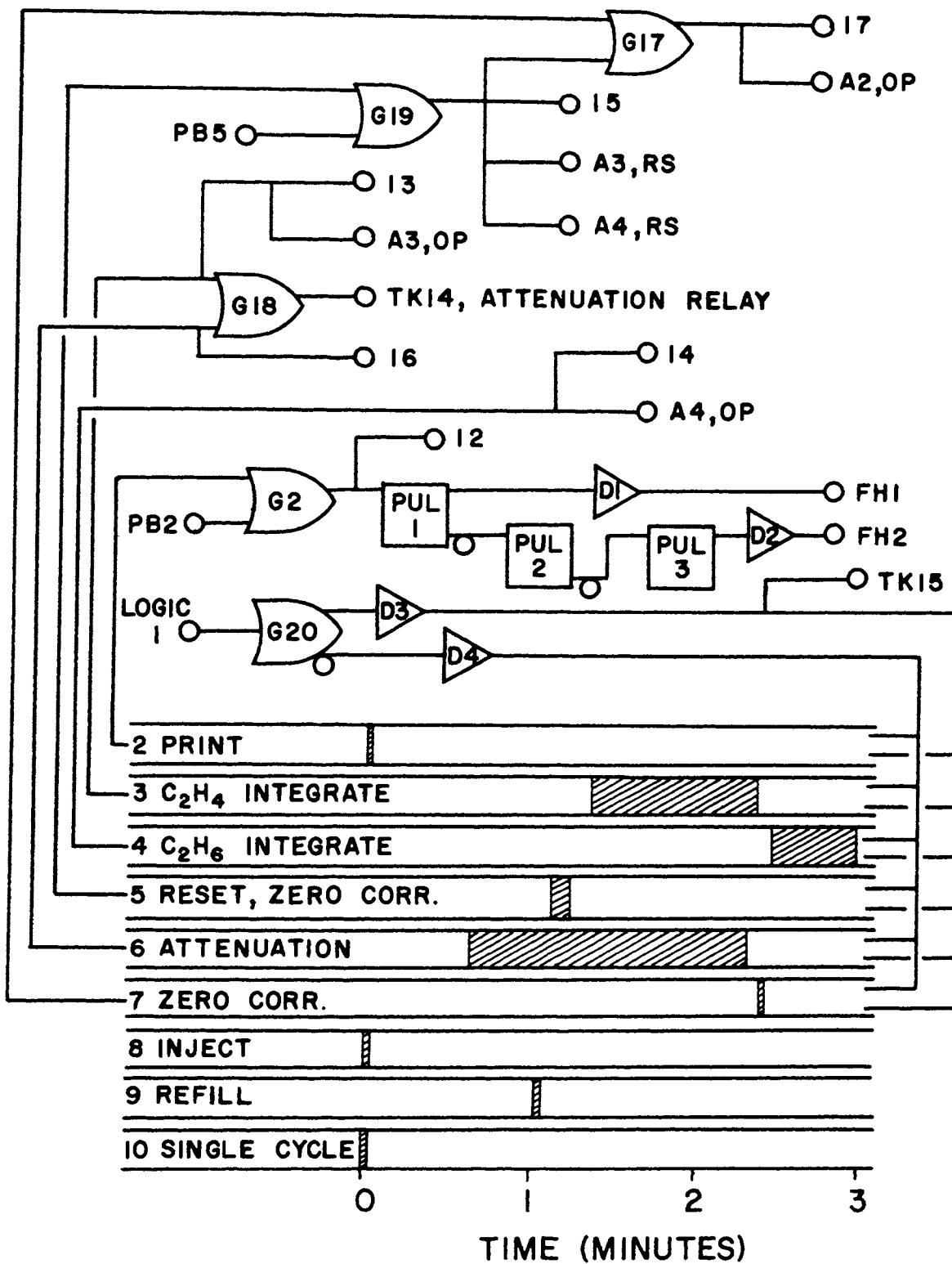


Figure 4E. Logic Program and Cam Timer Settings for Controlling the Analog Computation of Sample Composition.

TABLE I-E
CHROMATOGRAPH TIMER - COMPUTER WIRING

Timer Cam Connection	Color	Computer Logic Trunk
NC of 1,2,3,4,5,6 & 7	Red	11
NO of 1,2,3,4,5,6 & 7	Black	12
Common 1	White	1
Common 2	Orange	2
Common 3	Red	3
Common 4	Black	4
Common 5	Green	5
Common 6	Yellow	6
Common 7	Blue	7

of the gas sampling valve and another used to allow single cycle operation of the timer. The sampling valve is controlled by activating either of the two coils of a solenoid valve supplying air to the piston actuator of the sampling valve. The wiring diagram for these operations is presented in figure 5E, page 176. A photograph of the cam timer and the solenoid valve appear in figure 6E, page 177.

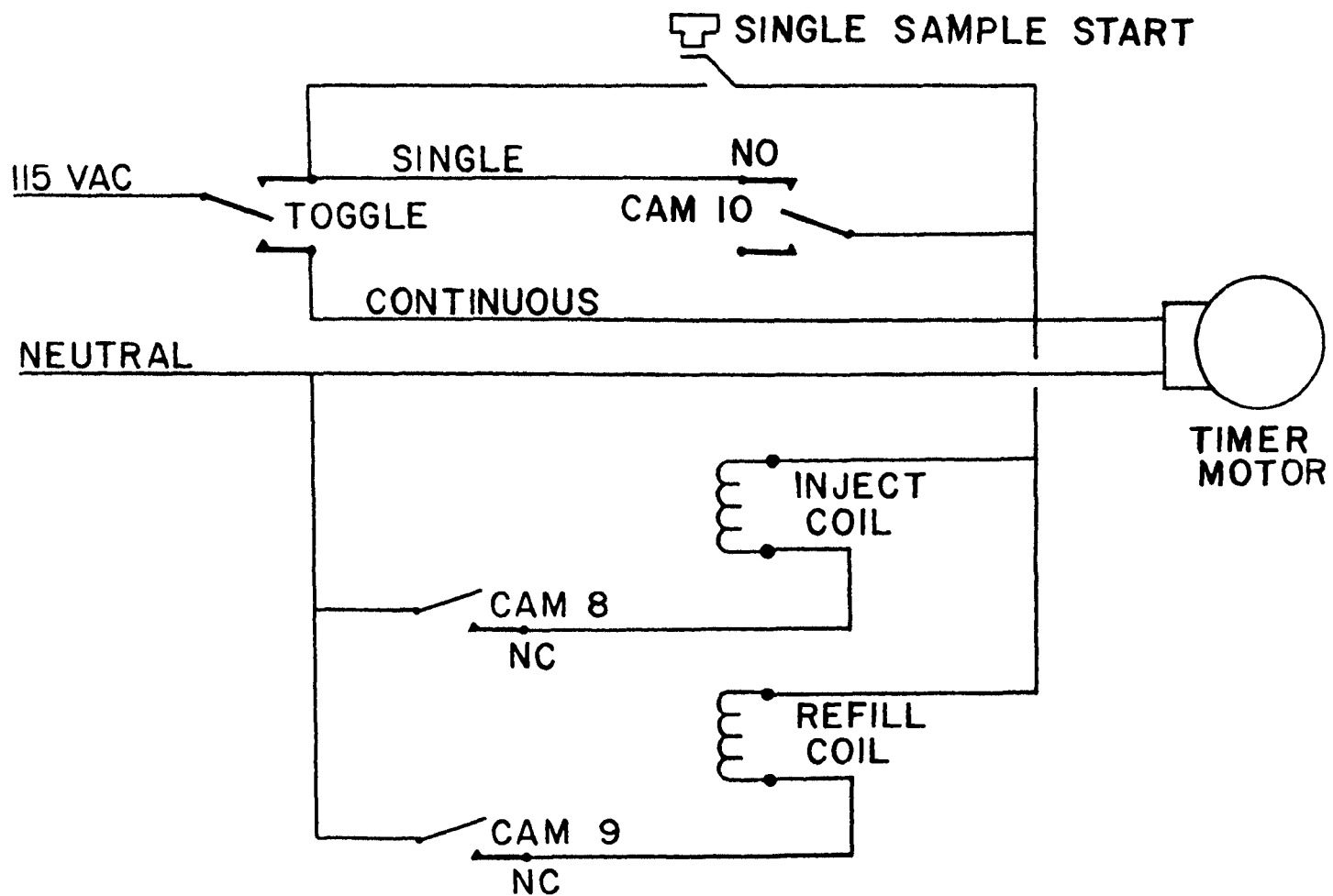


Figure 5E. Wiring for the Control of the Cam Timer and Sampling Actuation Valve.

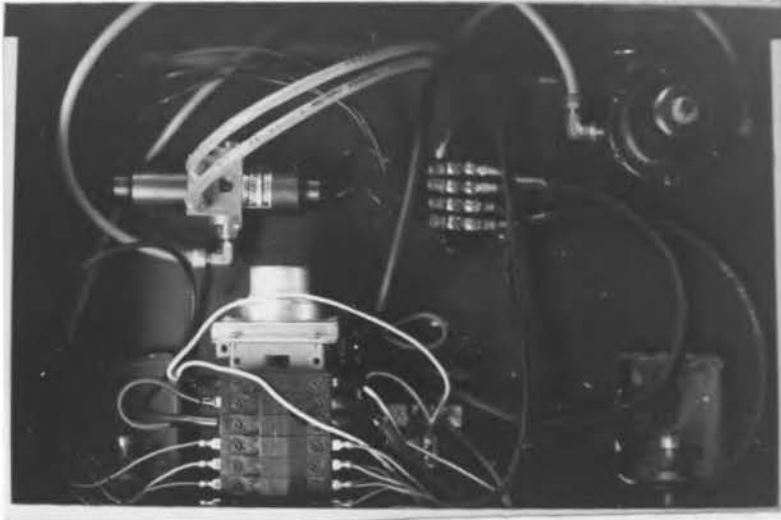


Figure 6E. Cam Timer and Solenoid Valve.

APPENDIX F
PILOT SCALE PROCESS SPECIFICATIONS

Analog Computer: The computer appears in figure 1F and has the following specifications:

Manufacturer: Applied Dynamics Corporation

Model: AD-40, 24

Other: These two computers contain 20 integrator-summers, 20 summer-inverters, 8 track-hold amplifiers, 40 potentiometers, 8 hybrid comparators, 6 SPST reed switches, 4 SPDT reed switches, 10 electronic multipliers, 2 log devices, 2 squarers, 2 variable diode function generators, 24 logic gates, 8 flip-flops, 1 4-bit shift register, and 4 variable pulsers.

Output Devices: The various flows, concentrations and calculated data were recorded with a digital printer actuated by an electronic digital voltmeter with the following specifications:

Manufacturer: United Systems Corporation

Model: 691 Printer, 251 Digital Voltmeter

Hydrogen Purifier: The catalytic purifier used to eliminate any oxygen in the hydrogen supply has the following specifications:

Manufacturer: Englehard Industries, Inc.

Model: D-10-2500

Dryers: The desiccant type dryers used to remove any water in the reactant supply lines have the following specifications:

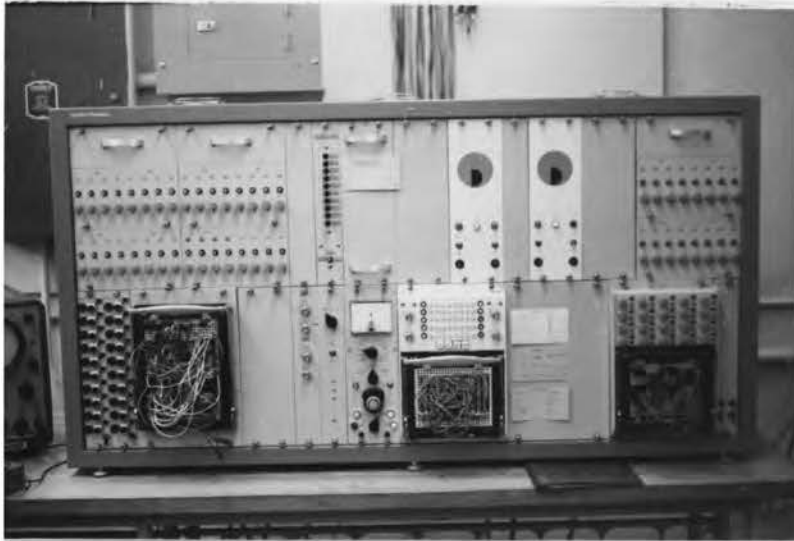


Figure 1F. Applied Dynamics 40, 24 Analog Computer.

Manufacturer: Wilkerson Corporation

Model: 6119-2

Other: These have a clear polycarbonate bowl so that the condition of the desiccant may be observed.

Control Valves: The two control valves used to regulate the flow of the reactants have the following specifications:

Manufacturer: Research Control Valves

Model: 78S

Other: These valves have instrument air to open, 3-15 psig actuators. The trim is Research Control Type P4 which has a C_v of 0.0006. The control valve controlling the exit v flow is similar to these but with Research Control Type N trim, C_v of 0.006.

Orifice Meters: The actual orifice flanges and plates were manufactured by Special Services Department of the University of Missouri-Rolla. The drawings for the flanges and plates are presented in figure 2F, page 181. The orifice plates are stainless steel, 0.003 inches thick and were drilled with a number 87, 0.010 inch, bit.

Differential Pressure Transmitters: The dp transmitters used in conjunction with the orifice meters have the following specifications:

Manufacturer: Honeywell, Inc.

Model: 29212-01-0-1

Other: The range of differential pressure spans available on these instruments is 20-250 inches water and the output is 3-15 psig instrument air. The reactants are routed through the dp transmitters as if they were equipped with integral orifices.

Pressure to Current Transducers: The pressure to current transducers used to obtain a voltage signal from the

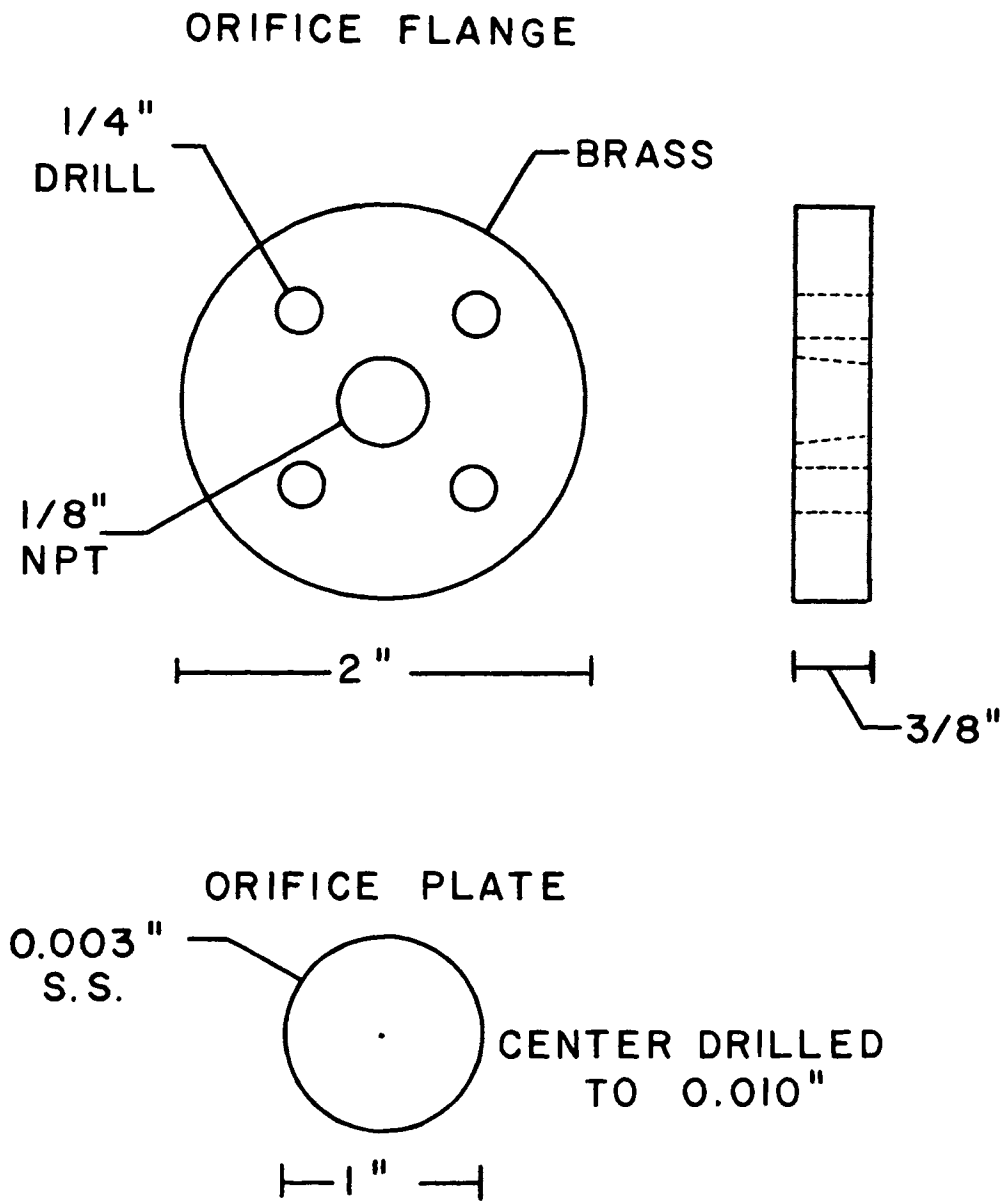


Figure 2F. Orifice Meter Specifications.

differential pressure transmitters pneumatic signal have the following specifications:

Manufacturer: Honeywell, Inc.

Model: 31300-03

Other: The input is 3-15 psig instrument air and the output is 4-20 ma current. The wiring is discussed in Appendix D.

Current to Pressure Transducers: The current to pressure transducers used to obtain an instrument air signal to power the motor control valves have the following specifications:

Manufacturer: Honeywell, Inc.

Model: 31200-1

Other: The input is 4-20 ma current and the output is 3-15 psig instrument air. The wiring is discussed in Appendix D.

D.C. Power Supply: The D.C. supply used to power the P/I transducers and the transmitting potentiometer on the chromatograph recorder has the following specifications:

Manufacturer: Sola Electric Company

Model: 281048

Other: The output of this power supply is 48 VDC with a maximum current of 4 amperes.

Reactor: The main reaction vessel is all stainless steel. It is shown in figure 2C and 3C pages 138 and 139. The manufacturer is unknown.

Recycle Pump: The reactor recycle pump has the following specifications:

Manufacturer: Fisher Scientific

Model: 18-309X

Other: This is a diaphragm type pump.

Band Heater: The band heater which is wrapped around the main reaction vessel has the following specifications:

Manufacturer: Ogden Sales Inc.

Model: B-45 ST 55

Other: The power rating is 1950 watts, 220 VAC.

Temperature Controller: The null balance temperature controller used to regulate the reaction temperature has the following specifications:

Manufacturer: Barber Coleman

Model: 357A

Other: This controller is equipped with cold junction compensation for chromel-alumel thermocouple. It has an output signal of 2-12 ma current used to control a Barber Coleman model 621 SCR power supply which powers the reactor band heater.

Thermocouples: The chromel-alumel thermocouples used to monitor the reactor temperature and serve as primary devices for the temperature controller have the following specifications:

Manufacturer: Conax

Model: 5512K-B-PJFC-MPG-125-T-12

Other: These are 1/8 inch stainless steel sheathed, bare chromel-alumel thermocouples equipped with 1/8 inch mpt fittings.

Reactor Pressure Transmitter: The reactor pressure transmitter is actually a differential pressure transmitter with

the low pressure port open to the atmosphere. It is the primary device for the reactor pressure controller and has the following specifications:

Manufacturer: Foxboro

Model: 13A

Other: The range of differential pressure spans is 50-250 inches water and the output is 3-15 psig instrument air.

Reactor Pressure Indicator: The pressure gauge used to monitor the reactor has the following specifications:

Manufacturer: Ashcroft

Other: This pressure gauge is a brass bellows type and has a range of 0-200 inches water.

Temperature Indicators: The two null balance mv indicators used to monitor the thermocouples have the following specifications:

Manufacturer: United Systems Corporation

Model: 211

Chromatograph: The gas chromatograph used for the analysis has the following specifications:

Manufacturer: Varian Aerograph

Model: 90-P3

Other: This is a single column, four element thermoconductivity detector instrument with on-off column temperature control, high mass detector oven, and constant differential type carrier flow control.

Sampling Valve: The gas sampling valve used to inject a product sample into the chromatograph has the following specifications:

Manufacturer: Carle Instruments Inc.

Model: 2018

Other: This is a single loop sampling valve and is powered by a pneumatic piston actuator, Carle model 2050. The control of the pneumatic actuator is described in Appendix E.

Chromatograph Recorder: The potentiometric recorder used to record and transmit the chromatograph peaks has the following specifications:

Manufacturer: Honeywell Inc.

Model: 153X17V-X-30

Other: The range of this recorder is 0-10 mv. A surplus feedback helical potentiometer is attached to the pen drive cable and acts as a transmitting potentiometer.

Cam Timer: The cam timer used to control the sampling valve and the analog program has the following specifications:

Manufacturer: Mallory

Model: 10T

Other: A three minute drive motor is used to power the timer.

Pneumatic Controllers: The pneumatic controllers used to control the reactor pressure and serve as standby controllers for the reactant flows have the following specifications:

Manufacturer: Foxboro

Model: 52

Other: These are 3-15 psig instrument air proportional integral controllers.

Sample Flow Controller: The sample flow controller is a constant differential type flow controller with the following specifications:

Manufacturer: Fischer and Porter

Model: R4

Sample Flow Rotameter: The sample flow rotameter appears in figure 7C, page 149.

Manufacturer: Fischer and Porter

Model: 130-G

Other: This has a full scale range of 2 SCFH air.

Bubble Flow Meter: The bubble flow meter is a graduated cylinder with the following specifications:

Manufacturer: Fisher Scientific

Model: Cat. No. 3-711C

Other: This is a 100 cc graduated cylinder with a side arm but without a stopcock. A squeeze bulb full of soap solution is attached to the bottom connection.

Bubble Meter Pressure Indicator: The pressure gauge used to monitor the bubble meter pressure has the following specifications:

Manufacturer: Ashcroft

Other: The pressure gauge is a brass bellows type and has a range of 0-80 inches of water.